Österreichische Beiträge zu
Meteorologie und Geophysik

Heft 15

PIDCAP [1)]
QUICK LOOK PRECIPITATION ATLAS

Franz Rubel [2)]

1) Pilot Study fo Intensive Data Collection and Analysis of Precipitation, August to November, 1995

2) Division for Biometeorology, Institute of Medical Physics, University of Veterinary Medicine Vienna, and
Division for Theoretical Meteorology, Institute for Meteorology and Geophysics, University of Vienna

Wien 1996

Zentralanstalt für Meteorologie und Geodynamik
Publ. Nr. 374
ISSN 1016-6254

CONTENTS

Preface

An essential element of the *World Climate Research Programme* (WCRP) is the *Global Energy and Water Cycle Experiment* (GEWEX). Within GEWEX five continental-scale experiments are being conducted of which the *Baltic Sea Experiment* (BALTEX) is one. Its scientific objectives include comprehensive determination of the energy and water budgets of the BALTEX area. The components of the atmospheric branch of the hydrological cycle are the key elements to be investigated. Special observing campaigns for gaining basic data sets are planned within BALTEX. The first of these is the *Pilot Study for Intensive Data Collection and Analysis of Precipitation* (PIDCAP) which covers the period from August through November 1995.

A description of the weather patterns during PIDCAP, including an overview of 26 selected precipitation records distributed over the area, has recently been published by the International BALTEX Secretariat (Isemer 1996). The present PIDCAP precipitation atlas based on 1 000 stations and interpolated to gridpoints compiled by Rubel gives an account of the spatial precipitation field during each day of PIDCAP. BALTEX users may wish to have a quicklook archive available for easy reference to the PIDCAP precipitation regime over their research area; Rubel's atlas may serve this purpose. It is the first contribution of the convection group at the University of Vienna that has joined the BALTEX community within the research project *Numerical Studies of the Energy and Water Cycle of the Baltic Region* (NEWBALTIC). Beginning January 1996, NEWBALTIC is being funded by the European Union.

Michael Hantel

Summary

PIDCAP is the *Baltic Sea Experiment* (BALTEX) pilot study for intensive data collection and analysis of precipitation in the Baltic Sea water catchment region. For the period of August to November 1995, the routine SYNOP precipitation over the BALTEX model domain is objectively analyzed twice daily. Additionally, both the areal distribution and the total amount of the monthly precipitation input into the Baltic drainage basin are calculated.

Approximately 1 000 SYNOP stations exist over the extended domain of the regional model REMO. The spatial resolution for the present analysis is 55 km ($41 \cdot 61$ grid points of the DWD *Europa-Modell*), and the time resolution is 12 hours. The precipitation fields are calculated on equidistant gridpoints by a statistical interpolation technique which is known in meteorology as *optimum averaging with normalized weights*, and in hydrology as *block kriging*. Prior to the analysis the data are checked for unrealistic values. The observation error is set at a constant 5 %. The autocorrelation function for the precipitation is characterized by the distance for which it decreases to $1/e$. The 12 closest stations within this distance are used for the calculation of each areal mean precipitation value. The decorrelation distance is 240 km for August, 260 km for September, 280 km for October, and 300 km for November 1995.

This analysis procedure yields two 12 hour-accumulated precipitation fields per day, for the synoptic times 06:00 and 18:00 UTC. For each precipitation field, the error field is available in the same format. The interpolation error is typically 15 % of the variance of the precipitation field over Central Europe; over parts of the Baltic Sea it reaches 30 %.

The analyzed precipitation fields give a quick-look view of events during PIDCAP, which allows for the selection of meteorologically interesting episodes in full REMO-model resolution. Further, they can directly be compared with the corresponding forecasts from numerical weather prediction models. Visual comparison with precipitation fields from the *European Centre for Medium Range Weather Forecasts* (ECMWF) shows fair agreement in both the pattern and the values between the forecast and the analyzed fields.

The climatological water balance of the Baltic drainage basin exhibits a strong seasonal dependence on the averaged monthly precipitation input. For example, the highest amount of precipitation can be expected in August and the lowest in February. This does not correspond to the presently analyzed monthly averages for the PIDCAP period which are generally lower than the climatological values. The monthly areally averaged estimates of precipitation are 53 mm for August, 71 mm for September, 41 mm for October, and 46 mm for November 1995.

Zusammenfassung

PIDCAP ist die Pilotstudie für intensive Datensammlung und Analyse von Niederschlag im Einzugsgebiet der Ostsee und Teil des BALTEX (*Baltic Sea Experiment*) Programmes. Für die Periode August bis November 1995 wurden die zweimal täglich routinemäßig gemessenen SYNOP-Niederschläge objektiv analysiert. Zusätzlich wurde die räumliche Verteilung sowie der gesamte monatliche Niederschlagseintrag in das Einzugsgebiet der Ostsee berechnet.

Über dem erweiterten Gebiet des regionalen Modells REMO sind Daten von ca. 1 000 SYNOP Stationen verfügbar. Die räumliche Auflösung der vorliegenden Analyse beträgt 55 km ($41 \cdot 61$ Gitterpunkte des DWD *Europa-Modells*), die zeitliche Auflösung beträgt 12 Stunden. Die Niederschlagsfelder auf diesem äquidistanten Gitter wurden mittels eines statistischen Interpolationsverfahrens berechnet, das in der Meteorologie als *Optimum Averaging with Normalized Weights* und in der Hydrologie als *Block Kriging* bezeichnet wird. Vor der Analyse wurden die Daten auf unrealistische Werte überprüft. Für den Beobachtungsfehler wurde ein konstanter Wert von 5 % angenommen. Die Autokorrelationsfunktion des Niederschlages wurde durch die Distanz, nach der sie auf 1/e abfällt, charakterisiert; die 12 nächstgelegenen Stationen innerhalb dieser Distanz wurden für die Analyse des Flächenniederschlages einer Gitterbox verwendet. Für August wurde eine Dekorrelationsdistanz von 240 km, für September von 260 km, für Oktober von 280 km und für November von 300 km ermittelt.

Mit dieser Analyse wurden zweimal täglich die 12-stündig akkumulierten Niederschlagsfelder zu den synoptischen Terminen 06:00 und 18:00 UTC berechnet. Zusätzlich zu jedem Niederschlagsfeld ist das entsprechende Fehlerfeld verfügbar. Der Interpolationsfehler, angegeben in Prozent der Varianz des Niederschlagsfeldes, hat eine typische Größenordnung von 15 % über Mitteleuropa und erreicht 30 % über Teilen der Ostsee.

Die analysierten Felder geben einen Überblick bezüglich der Niederschlagsereignisse während PIDCAP. Sie erleichtern somit die Auswahl meteorologisch interessanter Episoden für eine nachfolgende Analyse in der vollen REMO Auflösung. Weiters sind sie direkt mit Prognosen von numerischen Wettervorhersage-Modellen vergleichbar. Ein erster visueller Vergleich mit Niederschlagsfeldern vom *Europäischen Zentrum für Mittelfristige Wettervorhersage* (EZMW) zeigt eine gute Übereinstimmung im Muster und in den absoluten Werten vorhergesagter und analysierter Felder.

Aus der klimatologischen Wasserbilanz des Einzugsgebietes der Ostsee ist eine starke jahreszeitliche Abhängigkeit des monatlichen Niederschlagseintrages ersichtlich. Danach sind die höchsten Niederschlagsmengen im August und die geringsten im Februar zu erwarten. Eine diesbezügliche Übereinstimmung mit den analysierten Monatsmittel während der PIDCAP-Periode ist allerdings nicht gegeben. Die analysierten Niederschläge sind, verglichen mit den klimatologischen Werten, generell zu gering. Das Monatsmittel des Flächenniederschlages beträgt 53 mm im August, 71 mm im September, 41 mm im Oktober und 46 mm im November 1995.

Acronyms

BALTEX	**BALT**ic Sea **EX**periment
DIAMOD	**DIA**gnostic **MOD**el
DM	**D**eutschland **M**odell
DWD	**D**eutscher **W**etter**D**ienst
ECMWF	**E**uropean **C**entre for **M**edium Range **W**eather **F**orecasts
GEWEX	**G**lobal **E**nergy and **W**ater Cycle **EX**periment
GTS	**G**obal **T**elecommunication **S**ystem
HIRLAM	**HI**gh **R**esolution **L**imited **A**rea **M**odel
NEWBALTIC	**N**umerical Studies of the **E**nergy and **W**ater Cycle of the **BALTIC** Region
PIDCAP	**P**ilot Study for **I**ntensive **D**ata **C**ollection and **A**nalysis of **P**recipitation
REMO	**RE**gional **MO**del
SYNOP	**SYNOP**tic Observations
UTC	**U**niversal **T**ime **C**oordinated
WCRP	**W**orld **C**limate **R**esearch **P**rogramme

1 INTRODUCTION

A particularly important part of BALTEX (*Baltic Sea Experiment*) is the development of methods for the determination of precipitation and evaporation over large bodies of water. This atlas contains the synoptic scale precipitation fields of the PIDCAP (*Pilot Study for Intensive Data Collection and Analysis of Precipitation*), carried out from August to November 1995.

The synoptic scale precipitation fields are used to give a quick-look view of events during PIDCAP, which allows for the selection of meteorologically interesting episodes for further studies. The precipitation fields are analyzed on the grid of the DWD *Europa-Modell*, and are therefore directly comparable with the corresponding forecasts. Further, they are used as input for the thermodynamic diagnostic model η-DIAMOD (Dorninger et al. 1992, Hantel et al. 1993, and Haimberger et al. 1995). The aim of DIAMOD is to calculate the sub-gridscale fluxes of latent and sensible heat, and contribute to the study of energy exchange between the atmosphere and the surface of the earth. This is a further topic within BALTEX.

The presented precipitation fields are calculated from the routinely available 12-hourly accumulated observations of the synoptic network. They do not contain special PIDCAP data. The latter, together with high resolution radar data, will be used in the future for selected case studies. According to the density of the available data, the definition of the spatial resolution was set to 55 km, in approximate correspondence to the present time resolution of 12 hours. Because of the limited density of the synoptic network, a higher space resolution precipitation analysis over the whole BALTEX domain does not seem realistic. However, detailed case studies will be performed in the full resolution of the BALTEX model REMO (*Regional Model*) which was set to 18 km.

For the spatial analysis of the irregularly distributed precipitation data, many methods have been proposed and applied to rainfall fields. These are the *nearest neighbour method*, the *arithmetic mean*, *spline surface fitting*, *interpolation based on empirical orthogonal functions* and statistical interpolation techniques. The latter are the so-called *optimum interpolation* or *optimal averaging* (Gandin 1993) and the so-called *kriging methods* (Krige 1981, Rendu 1981). These methods have been developed since the early 60s in both meteorology (Gandin 1965) and hydrology (Krige 1962, Matheron 1963). Today, statistical interpolation methods are state of the art; objective comparisons have pointed out their advantage to other methods (Creutin and Obled 1982).

The *optimum interpolation* and *kriging* techniques require the knowledge of the statistical structure function (semivariogram), or the covariance function (Bacci and Kottegoda 1995). While in hydrology the semivariogram or variogram is generally used, in meteorology the autocorrelation function (normalized covariance function) is more common. With the analysis of PIDCAP precipitation data, it is assumed that the precipitation process is stationary of second order (homogeneity of mean, variance, and covariance). Under this assumption, it is possible to transform the semivariogram function into the autocorrelation function, and vice versa.

The autocorrelation function of precipitation depends on the considered space-time aggregation (Rubel 1994) and can be characterized by decorrelation distances (Zawadzki 1973). Further, it depends on the precipitation process itself, namely on the dominance of either the convective or the stratiform component. The spatial autocorrelation functions, estimated from the 12-hourly accumulated precipitation data during the PIDCAP period, are characterized by decorrelation distances of about 270 km. This guarantees the possibility of performing a synoptic scale statistical interpolation with sufficient accuracy.

The statistical interpolation methods are either linear or nonlinear, biased or unbiased, least-squares spatial interpolation techniques. They are advanced applications of *Gauss' Theory of*

Errors, and therefore optimal in a statistical sense. However, because of the necessary assumptions (e.g., homogeneity and isotropy) that have to be made for the practical implementation, they are sometimes too far off to yield optimal results. That is the reason why various alternative assumptions have been proposed, that lead to different, more or less expensive, interpolation methods. Different is also the terminology between meteorological and hydrological applications. The main difference between *optimum interpolation* and *kriging* is the hypothesis of ergodicity used in kriging. A process is said to be ergodic, if the estimates of its moments, obtained on the basis of the available realizations, converge in probability to the theoretical moments when the available sample increases. Thus, one can perform a precipitation analysis based on the knowledge of only a single realization. Further, for observations of precipitation accumulated over short times (e.g., hourly or daily means), it is not practical to use first guess (background) fields, as it is done in the classical *optimum interpolation*. The reason is that the accuracy of the precipitation forecast of today's meteorological models is not sufficient. Forecast errors could produce a completely unrealistic precipitation analysis, because precipitation is not a state variable. Further, a climatological background field is not appropriate because of the high variability of precipitation events for 12-hourly precipitation.

For that reason, the PIDCAP precipitation analysis is performed here with the analysis technique called *ordinary kriging* which is well-known in geosciences. This method is also known in the meteorological literature as *optimum interpolation with normalized weights*, although it is rarely used. This is due to of the availability of first guess fields from model forecasts for the atmospheric state variables through which the analysis is improved. Reversibly, the classical *optimum interpolation* method is known in hydrology as *simple kriging*.

Atmospheric values are generally analyzed on grid points. In the case of precipitation, not grid point values, but areally averaged values had to be analyzed. One can distinguish between *point kriging* and *block kriging*; the latter is the application of kriging to area and volume interpolation, and contains *point kriging* as special case. Based on this terminology, our present interpolation technique will be referred to as *ordinary block kriging*.

2 MODEL DOMAIN AND DATA

The *BALTEX model area* can be seen in *fig. 1*. The PIDCAP precipitation data are analyzed on the grid of the *Europa-Modell* of the DWD. It uses a rotated latitude/longitude grid, which can be calculated from the geographical system by rotation of a defined angle (DWD 1995). The new position of the north pole resulting from this rotation is 170° W and 32.5° N ($-170°/32.5°$), and was defined in a way such that the rotated equator is placed in the middle of the model domain. Models benefit from this rotated latitude/longitude grid, because it allows them to operate on larger time steps.

The lower left corner of the BALTEX grid has the rotated coordinates $-5°/-14°$; the upper right corner $15°/16°$. The grid spacing in zonal and meridional direction is set to 0.5°, which corresponds to a grid distance of about 55 km. Therefore, the dimension of the grid is set to $41 \cdot 61$ grid points.

For the precipitation analysis the 06:00 UTC and 18:00 UTC observational precipitation values of the synoptic network are used. The number of the available stations varies from realization to realization. In *fig. 1, right* the stations transmitted via GTS on 4 November 1995, 18:00 UTC, are shown. For the analysis, observations in the vicinity of the model domain are also used. Together with these observations, with no more than 5 grid distances (corresponding to the mean decorrelation distance of synoptic scale precipitation) outside the model domain, the number of the available stations is over 1 000. The station density is highest in Central

Europe, and lowest over Eastern Europe. Over the Baltic Sea the station density is relatively low, but it is guaranteed that for each grid point to be analyzed several observations are available within the decorrelation distance. A precipitation analysis is therefore possible, even over the data-poor region of the Baltic Sea.

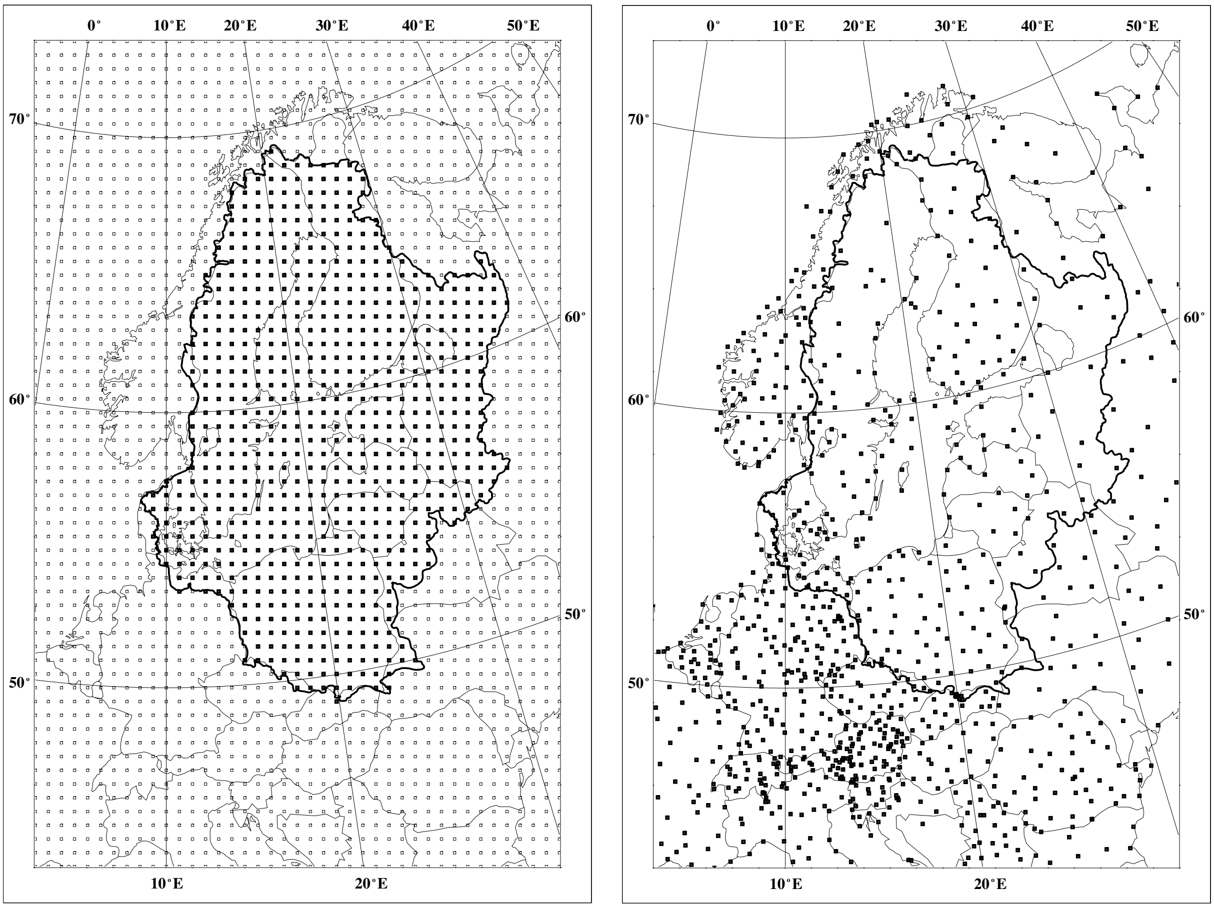

Figure 1 BALTEX model domain with the grid of the regional model REMO (left) and the location of the synoptical surface stations for 4 September 1995, 18:00 UTC (right). Bold grid points are within the boundary of the Baltic drainage basin, which is marked by a solid line.

3 STATISTICAL STRUCTURE OF PRECIPITATION

The statistical structure of precipitation is usually represented by spatial and temporal autocorrelation functions. However, this representation is not unique because precipitation is a complex physical phenomenon, it is not possible to fully describe precipitation processes with only one universal correlation model. Ideally, precipitation events should be separated by different criteria, e.g. stratiform or convective type precipitation. Each type of precipitation could then be assumed to be part of an ensemble of homogeneous realizations with defined statistical properties. The synoptic scale precipitation over Europe contains stratiform and convective components of different intensities and compositions at the same time. Moreover, it is hardly possible to separate them. For this reason, the analysis of the PIDCAP precipitation fields was performed with the use of only a single autocorrelation function for the whole model domain.

Empirical estimation of correlation functions

We assume that n contemporary observations of the precipitation process $Z(\mathbf{u})$ exist at the locations $\mathbf{u}_i \equiv (x_i, y_i)$, i=1,2,...,n. Further, if there are multiple realizations t=1,2,...,T of this process $Z(\mathbf{u})$, then the empirical estimation of the interstation correlation $\widehat{R}(\mathbf{u}_i, \mathbf{u}_j)$ can be performed as follows:

$$\widehat{R}\left(\mathbf{u}_i, \mathbf{u}_j\right) = \frac{\sum\limits_{t=1}^{T} \left[Z_t\left(\mathbf{u}_i\right) - \widehat{m}\left(\mathbf{u}_i\right)\right] \left[Z_t\left(\mathbf{u}_j\right) - \widehat{m}\left(\mathbf{u}_j\right)\right]}{\sqrt{\sum\limits_{t=1}^{T} \left[Z_t\left(\mathbf{u}_i\right) - \widehat{m}\left(\mathbf{u}_i\right)\right]^2 \sum\limits_{t=1}^{T} \left[Z_t\left(\mathbf{u}_j\right) - \widehat{m}\left(\mathbf{u}_j\right)\right]^2}} \tag{1}$$

where the mean $\widehat{m}(\mathbf{u}_i)$ is estimated from

$$\widehat{m}\left(\mathbf{u_i}\right) = \frac{1}{T} \sum_{t=1}^{T} Z_t\left(\mathbf{u}_i\right) \tag{2}$$

The correlations are then obviously bounded by

$$-1 \leq \widehat{R}\left(\overline{\rho}\right) \leq 1 \tag{3}$$

Assuming that the precipitation process is homogeneous and isotrop within the model domain, then the correlations $\widehat{R}(\mathbf{u}_i, \mathbf{u}_j)$ are dependent only on the interstation distance ρ_{ij}, and independent of the geographical locations of the stations.

$$\widehat{R}\left(\mathbf{u}_i, \mathbf{u}_j\right) = \widehat{R}\left(\left|\mathbf{u}_i - \mathbf{u}_j\right|\right) = \widehat{R}\left(\rho_{ij}\right) \tag{4}$$

The result of an interstation correlation analysis is usually presented in form of a scatter plot (Berndtsson 1987, Rubel 1994). A second way is to group the correlations based on their interstation distance ρ_{ij}. Then it is possible to describe the scattering of the correlation coefficients by the mean and standard deviation of each distance group.

To identify the structure of precipitation, a hypothesis about the theoretical model had to be formed. For the synoptic scale precipitation over Europe, the following nonlinear model with 3 coefficients c_1, c_2 and c_3 was chosen.

$$\widehat{R}\left(\rho\right) = c_1 \; exp\left(-c_2\, \rho^{c_3}\right) \quad , \tag{5}$$

The exponential autocorrelation function has the required property of being positive definite (Weber and Talkner 1993). In order to fit the parameters of the function to the empirically estimated data, the coefficients were determined according to the maximum likelihood hypothesis. For the practical runs the *Levenberg-Marquardt* algorithm (Press et al. 1987), which is a standard algorithm of the least square method, is used.

Autocorrelation functions for PIDCAP

Fig. 2 shows the correlations calculated from the synoptic precipitation observations, together with the fitted correlation functions. The dots are the mean and the vertical lines the standard deviations of the correlations in the distance group. For each month of the PIDCAP period, a separate correlation model was estimated.

All synoptic stations within the BALTEX model domain, including those which are outside the domain by no more than 5 grid distances, are used; this number may be n. This yields:

$$N_P(n) = \sum_{i=1}^{n-1} i = \frac{n(n-1)}{2} \tag{6}$$

interstation pairs. The total number of these stations can be estimated to be 1 000. For each of the N_p interstation pairs (here about 500 000) a correlation coefficient can be calculated provided an ensemble of observations is available. The number of realizations per month (60 dates) yields a reasonable basis for each correlation coefficient.

In practice, the theoretically possible number of correlations will be reduced by pairs of stations with interstation distances larger than 500 km, and pairs of stations which both have zero precipitation. The latter are excluded from the correlation analysis per definition (Bacchi and Kottegoda 1995). The high number of possible correlation coefficients is the reason why the mean correlation coefficients of the distance grouped pairs of stations are quite well fitted by the selected exponential correlation model (fig. 2). With a decreasing number of observations, the deviation of the mean correlation coefficients from the fitted correlation function increases.

month	**model parameter**			**decorrelation**
	c_1	c_2	c_3	**distance [km]**
August	0.95	0.039	0.590	≈ 240
September	0.95	0.008	0.859	≈ 260
October	0.95	0.012	0.770	≈ 280
November	0.95	0.011	0.762	≈ 300

Table 1 Autocorrelation models for the PIDCAP-period: coefficients c_1, c_2 and c_3 of the model $\widehat{R}(\rho) = c_1 exp(-c_2 \rho^{c_3})$ and decorrelation distances as function of the month. The coefficient c_1 is set to 0.95 and corresponds to an observational error (nugget effect) of Δ^2=0.05 (see *chapter 4*).

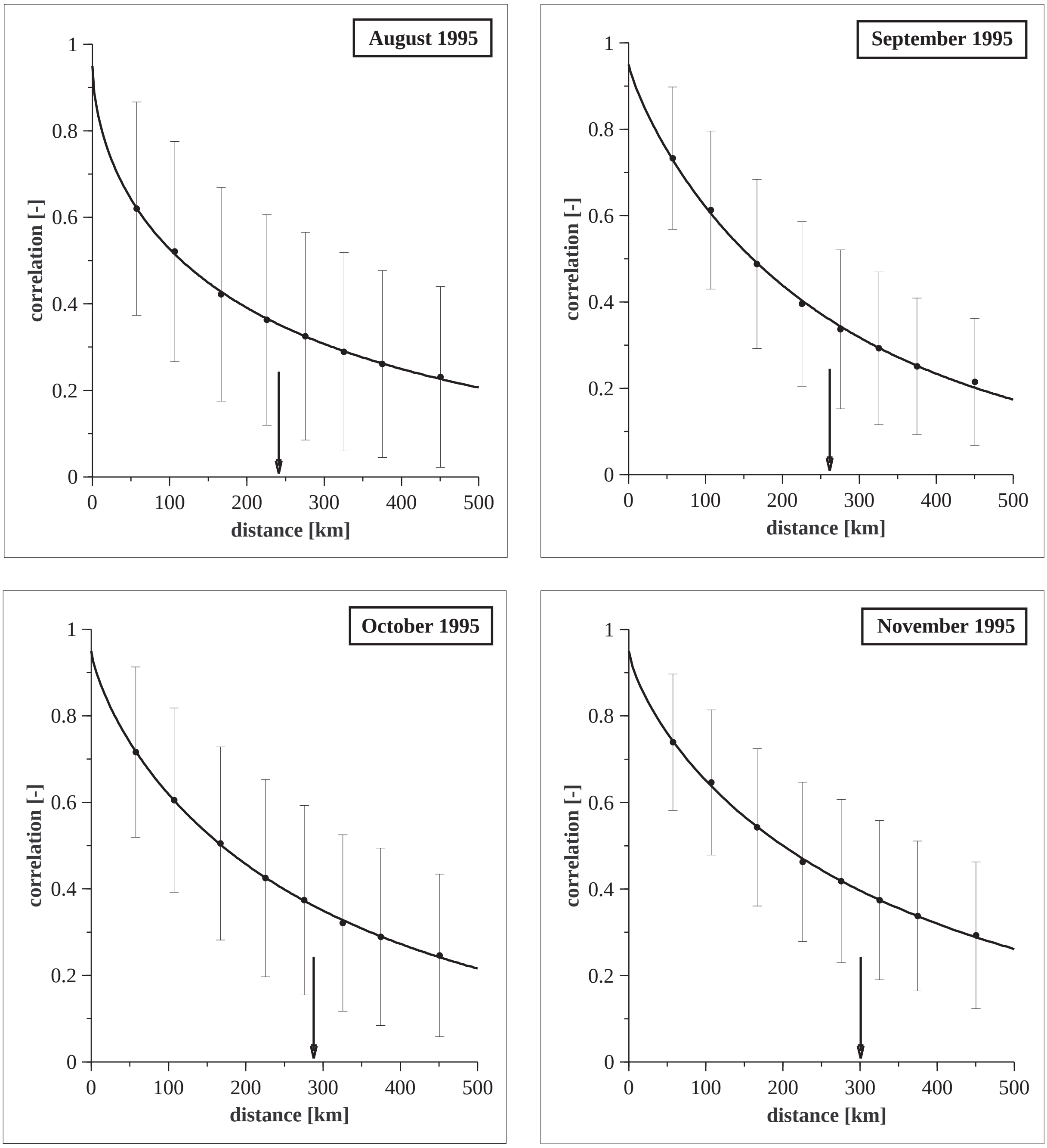

Figure 2 Mean correlations and standard deviations for the 8 groups of interstation distances together with the fitted autocorrelation function of type $\widehat{R}(\rho) = c_1 exp(-c_2\rho^{c_3})$ for the 4 months of the PIDCAP period. The assumed decorrelation distances are marked by arrows.

The model parameters c_1, c_2, and c_3, and therefore the curve of the autocorrelation function, varies with the climatic region and with the season of the year. For a simple characterization of the autocorrelation function, a typical distance, the decorrelation distance, is used. It is defined as the distance for which the correlation decreases to 1/e. From the curve of the autocorrelation function, one can infer the type of precipitation. A strong decrease in the autocorrelation function, corresponding to a short decorrelation distance, is characteristic of convective type precipitation. A weak decrease, corresponding to a wide decorrelation distance, is indicative of stratiform precipitation. The spatial autocorrelation functions, estimated from the 12-hourly accumulated precipitation data during the PIDCAP period over the whole BALTEX model area, are characterized by decorrelation distances of about 240 km for August, 260 km for September, 280 km for October, and 300 km for November. This suggests that the convective component in the precipitation fields over Europe decreases from August to November, which is in accord with the observations.

Note that the relatively large decorrelation distances are caused by the present time aggregation of 12 hours. For 1-hourly accumulated precipitation observations the decorrelation distances are of the order of 50 km (Rubel 1996).

4 STATISTICAL INTERPOLATION

The analysis of the precipitation fields, that is the estimation of the values of precipitation on the location of the grid points from irregularly spaced observations, was performed with the well known method called *optimal averaging with normalized weights* (Gandin 1993), or *ordinary block kriging* (Krige 1981). This method has also been proposed for the areal assessment of precipitation by the WMO (Sevruk 1992), and is discussed in detail in the geostatistical literature (Carr 1995, Wackernagel 1995). Fig. 3 shows the principle of the analysis technique.

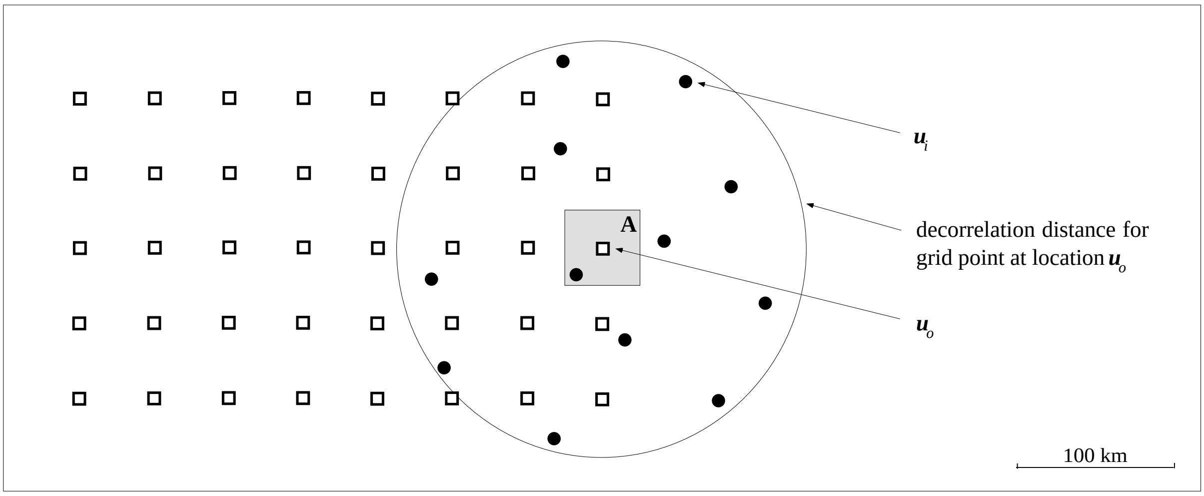

Figure 3 For each area A, represented by a grid point $\mathbf{u}_o$ in its centre, the n=12 closest observations $Z(\mathbf{u}_i) + \delta(\mathbf{u}_i)$, $i = 1, 2, ...n$, within the decorrelation distance are used to estimate the value of the area averaged precipitation $\hat{Z}_A(\mathbf{u}_o)$.

According to the relationship indicated in fig. 3, the true value of the precipitation $Z_A(\mathbf{u}_o)$ is the integral of all precipitation processes $Z(\mathbf{u})$ located at $\mathbf{u} \equiv (x, y)$ within the area A:

$$Z_A(\mathbf{u}_o) = \frac{1}{A} \int\limits_A Z(\mathbf{u})\ dxdy \tag{7}$$

An estimate of Z_A is defined by the following linear combination:

$$\hat{Z}_A(\mathbf{u}_o) = \sum_{i=1}^{n} \lambda_i \left[Z(\mathbf{u}_i) + \delta(\mathbf{u}_i) \right] \tag{8}$$

Here $Z(\mathbf{u}_i)$, $i = 1, 2, ..., n$, are the true precipitation values at the n=12 closest locations $\mathbf{u}_i$, and $\delta(\mathbf{u}_i)$ are the (unknown) observational errors at these locations. It is assumed that the rain gauge errors are random with mean zero, uncorrelated in space, and that their root-mean-square value is constant within the model domain.

The linear combination is a best linear unbiased estimate (BLUE) of the coefficients λ_i, $i = 1, 2, ..., n$ if the following conditions are satisfied.

- **Unbiasedness:** the expectation of the estimate should be equal to the expectation of the true value:

$$E\left[\hat{Z}_A(\mathbf{u}_o)\right] = E\left[Z_A(\mathbf{u}_o)\right] = m(\mathbf{u}_o) \tag{9}$$

- **Minimum variance:** The variance of the estimates from all possible realizations should be minimal with respect to the λ_i:

$$\sigma_E^2(\mathbf{u}_o) = Var\left[\hat{Z}_A(\mathbf{u}_o)\right] = E\left[\left(Z_A(\mathbf{u}_o) - \hat{Z}_A(\mathbf{u}_o)\right)^2\right] = Min. \tag{10}$$

From (10), combined with (7) and (8), follows:

$$\sigma_E^2(\mathbf{u}_o) = E\left[\left(\frac{1}{A}\int_A Z(\mathbf{u})\, dxdy - \sum_{i=1}^{n} \lambda_i \left[Z(\mathbf{u}_i) + \delta(\mathbf{u}_i)\right]\right)^2\right] \tag{11}$$

Assuming that the precipitation field is second order stationary (homogeneous) and isotropic, the weights λ_i can be obtained by minimizing the estimation variance (mean square interpolation error).

$$\begin{aligned} \sigma_E^2(\mathbf{u}_o) &= \frac{1}{A^2}\int_A\int_A E\left[Z(\mathbf{u})\, Z(\mathbf{u}')\right]\; dxdydx'dy' - \\ &- 2\sum_{i=1}^{n}\lambda_i\,\frac{1}{A}\int_A E\left[Z(\mathbf{u})\, Z(\mathbf{u}_i)\right]\; dxdy - 2\sum_{i=1}^{n}\;\lambda_i\;\frac{1}{A}\int_A E\left[Z(\mathbf{u})\,\delta(\mathbf{u}_i)\right]\; dxdy + \\ &+ \sum_{i=1}^{n}\sum_{j=1}^{n}\;\lambda_i\lambda_j E\left[Z(\mathbf{u}_i)\, Z(\mathbf{u}_j)\right] + \sum_{i=1}^{n}\;\lambda_i{}^2 E\left[\delta(\mathbf{u}_i)^2\right] \end{aligned} \tag{12}$$

If it is further assumed that the covariance function

$$Cov\left(\mathbf{u}_i, \mathbf{u}_j\right) = E\left[Z\left(\mathbf{u}_i\right) Z\left(\mathbf{u}_j\right)\right] - m^2 \ , \tag{13}$$

is known, then from eq. (12) follows:

$$\begin{aligned} \sigma_E^2\left(\mathbf{u}_o\right) &= \frac{1}{A^2} \int\limits_A \int\limits_A Cov\left(\mathbf{u}, \mathbf{u}'\right) \ dxdydx'dy' - \\ &- 2\sum_{i=1}^{n} \lambda_i \frac{1}{A} \int\limits_A Cov\left(\mathbf{u}, \mathbf{u}_i\right) \ dxdy + \\ &+ \sum_{i=1}^{n}\sum_{j=1}^{n} \lambda_i\lambda_j \ Cov\left(\mathbf{u}_i, \mathbf{u}_j\right) + \sum_{i=1}^{n} \lambda_i{}^2 E\left[\delta\left(\mathbf{u}_i\right)^2\right] \quad . \end{aligned} \tag{14}$$

Normalized with the variance

$$\sigma^2 = Cov\left(\mathbf{u}_i, \mathbf{u}_i\right) \ , \tag{15}$$

the estimation variance (kriging variance) $\sigma_\epsilon^2 = \sigma_E^2/\sigma^2$ can be written as

$$\begin{aligned} \sigma_\epsilon^2\left(\mathbf{u}_o\right) &= \frac{1}{A^2} \int\limits_A \int\limits_A R\left(\mathbf{u}, \mathbf{u}'\right) \ dxdydx'dy' - \\ &- 2\sum_{i=1}^{n} \lambda_i \frac{1}{A} \int\limits_A R\left(\mathbf{u}, \mathbf{u}_i\right) \ dxdy + \\ &+ \sum_{i=1}^{n}\sum_{j=1}^{n} \lambda_i\lambda_j \ R\left(\mathbf{u}_i, \mathbf{u}_j\right) + \Delta^2 \sum_{i=1}^{n} \lambda_i{}^2 \quad . \end{aligned} \tag{16}$$

In eq. (16) the term

$$R\left(\mathbf{u}_i, \mathbf{u}_j\right) = \frac{Cov\left(\mathbf{u}_i, \mathbf{u}_j\right)}{\sigma^2} \tag{17}$$

is the correlation, and the normalized mean-square observational error is defined as

$$\Delta^2 = \frac{E\left[\delta\left(\mathbf{u}_i\right)^2\right]}{\sigma^2} \quad . \tag{18}$$

The required condition that the measure of the interpolation error is a minimum, had to be performed under the condition that the sum of the weighting factors is equal to unity.

$$\sum_{i=1}^{n} \lambda_i = 1 \tag{19}$$

This additional relationship follows from the unbiasedness condition and is needed, because not the deviations from the expectation values (norms), but the observational values themselves are interpolated.

Extreme values with an additional condition can be calculated by means of *Lagrange's method*. Let us define the function:

$$\sigma^2_{\epsilon_o}(\mathbf{u}_o; \lambda_1, .., \lambda_n; \mu) \equiv \sigma^2_{\epsilon}(\mathbf{u}_o; \lambda_1, .., \lambda_n) + 2\mu \left(\sum_{i=1}^{n} \lambda_i - 1 \right) \tag{20}$$

In order to meet condition (10) above, the derivatives of this quantity with respect to the weights λ_i have to be set equal to zero:

$$\begin{aligned} \frac{\partial \sigma^2_{\epsilon_o}(\mathbf{u}_o; \lambda_1, .., \lambda_n; \mu)}{\partial \lambda_i} &= -2\, \frac{1}{A} \int_A R(\mathbf{u}, \mathbf{u}_i)\ dxdy + \\ &+ \ 2 \sum_{j=1}^{n} \lambda_j\ R(\mathbf{u}_i, \mathbf{u}_j) + 2\, \Delta^2\ \lambda_i + 2\mu = 0 \end{aligned} \tag{21}$$

The still undetermined factor μ is the Lagrangian multiplier. The derivative of (20) with respect to μ reproduces (19). This leads to a set of n+1 linear equations for the weighting factors λ_i and for μ.

$$\begin{aligned} &\sum_{j=1}^{n} \lambda_j \quad R(\mathbf{u}_i, \mathbf{u}_j) + \Delta^2\ \lambda_i + \mu = \frac{1}{A} \int_A R(\mathbf{u}, \mathbf{u}_i)\ dxdy \qquad (i = 1, 2, ..., n) \\ &\sum_{i=1}^{n} \lambda_i \quad = 1 \end{aligned} \tag{22}$$

If we multiply (22) by λ_i and take the sum over i, then we obtain

$$\sum_{i=1}^{n} \sum_{j=1}^{n} \lambda_i \lambda_j \quad R(\mathbf{u}_i, \mathbf{u}_j) + \Delta^2 \sum_{i=1}^{n} \lambda_i^2 + \mu = \sum_{i=1}^{n} \lambda_i \frac{1}{A} \int_A R(\mathbf{u}, \mathbf{u}_i)\ dxdy \tag{23}$$

and the estimation variance (16) can be written as

$$\sigma_\epsilon^2(\mathbf{u}_o) = \frac{1}{A^2}\int\limits_A\int\limits_A R\left(\mathbf{u},\mathbf{u}'\right)\ dxdydx'dy' - \sum_{i=1}^{n}\lambda_i\ \frac{1}{A}\int\limits_A R\left(\mathbf{u},\mathbf{u}_i\right)\ dxdy - \mu \tag{24}$$

Thus, if the correlations are known, the set of equations can be solved immediately. Note, that an increasing observational error leads to a decrease in the difference between the weighting factors λ_i, and therefore to a smoothed precipitation field.

In practice the true correlation function $R(\rho)$ is not known. Instead, an empirically estimated function $\hat{R}(\rho)$ according to eqs. (4), (5) is used. With the correlation model:

$$\begin{aligned} \hat{R}(\rho) &= R(\rho) - \Delta^2 \quad &\text{for } \rho > 0 \\ \hat{R}(\rho) &= 1 &\text{for } \rho = 0 \end{aligned} \tag{25}$$

which has a discontinuity at the origin, and with picking the corresponding values at the discrete interstation distances, the system of equations (22) reads:

$$\begin{aligned} &\sum_{j=1}^{n}\lambda_j\quad \hat{R}(\mathbf{u}_i,\mathbf{u}_j) + \mu = \frac{1}{A}\int\limits_A \hat{R}(\mathbf{u},\mathbf{u}_i)\ dxdy \qquad (i = 1,2,...,n) \\ &\sum_{i=1}^{n}\lambda_i\quad = 1\ . \end{aligned} \tag{26}$$

Δ^2 is now part of the correlation model $\hat{R}(\rho)$ and the normalized estimation variance follows as

$$\sigma_\epsilon^2(\mathbf{u}_o) = \frac{1}{A^2}\int\limits_A\int\limits_A \hat{R}\left(\mathbf{u},\mathbf{u}'\right)\ dxdydx'dy' - \sum_{i=1}^{n}\lambda_i\ \frac{1}{A}\int\limits_A \hat{R}\left(\mathbf{u},\mathbf{u}_i\right)\ dxdy - \mu \tag{27}$$

It can be obtained immediately, because the double integral has to be calculated only once for the model domain, while the second integral has already been calculated in order to solve eq. (26).

The estimation variance (27) is given separately for each grid point, and is a measure of the quality of the analysis. First, it depends on the size of the analysed area. If the area is large, then the double integral term is small. If the area decreases to a point, this term increases to unity. Second, the estimation variance depends on the station density, and third, on the statistical structure of the precipitation field. Therefore, the estimation variance defined for the grid area A - that is the normalized mean square interpolation error - decreases with increasing station density, and increasing decorrelation distance.

5 NUMERICAL IMPLEMENTATION

In the following, the practical calculations for the estimation of grid area averaged precipitation values (fig. 3) is described. In a first step the input data, the routinely distributed synoptic observations, are checked against a plausibility criterion. This means that observed values exceeding a climatological threshold, defined as 300 mm/12h (Rubel 1994), are assumed to be unrealistic. These values are therefore treated as missing values. An additional correction of the observations with respect to wind induced errors or losses due to evaporation and wetting (Sevruk 1986, Førland 1996), has not been performed in the present analysis.

After this crude data check, in a second step the actual precipitation analysis is performed grid area by grid area. Since it is assumed that only observations within the decorrelation distance of the central point of the grid area will affect the analysis, these observations had to be selected. To do this, the observations are sorted with respect to their distance from the central point of the area. The *Quick Sort* algorithm, which is standard in numerical computation (Press et al. 1987), is used. Finally, only the 12 closest observations $[Z(\mathbf{u}_i)+\delta(\mathbf{u}_i)]$, $i=1,...,12$, are chosen for the analysis. The areally averaged precipitation is calculated from eq. (8), after determination of the unknown weighting factors from eq. (26).

To simplify the writing of the numerical solution of the *kriging system* (26), the following terminology is defined:

$$\hat{R}_{ij} = \hat{R}\left(\mathbf{u}_i, \mathbf{u}_j\right) \tag{28}$$

$$\hat{R}_{oi} = \frac{1}{A}\int\limits_A \hat{R}\left(\mathbf{u}, \mathbf{u}_i\right)\ dxdy \tag{29}$$

$$\hat{R}_{oo} = \frac{1}{A^2}\int\limits_A\int\limits_A \hat{R}\left(\mathbf{u}, \mathbf{u}'\right)\ dxdydx'dy' \tag{30}$$

With the above definitions, (26) can also be written in matrix form

$$\left|\begin{array}{cccccc} 1 & \hat{R}_{12} & \hat{R}_{13} & ... & \hat{R}_{1n} & 1 \\ \hat{R}_{21} & 1 & \hat{R}_{23} & ... & \hat{R}_{2n} & 1 \\ \hat{R}_{31} & \hat{R}_{32} & 1 & ... & \hat{R}_{3n} & 1 \\ ... & ... & ... & ... & ... & 1 \\ \hat{R}_{n1} & \hat{R}_{n2} & \hat{R}_{n3} & ... & 1 & 1 \\ 1 & 1 & 1 & ... & 1 & 0 \end{array}\right| \cdot \left|\begin{array}{c} \lambda_1 \\ \lambda_2 \\ \lambda_3 \\ ... \\ \lambda_n \\ \mu \end{array}\right| = \left|\begin{array}{c} \hat{R}_{o1} \\ \hat{R}_{o2} \\ \hat{R}_{o3} \\ ... \\ \hat{R}_{on} \\ 1 \end{array}\right| \tag{31}$$

and the estimation variance (also called kriging variance) can be written as:

$$\sigma_\epsilon^2 = \hat{R}_{oo} - \sum_{i=1}^{n} \lambda_i \, \hat{R}_{oi} - \mu \tag{32}$$

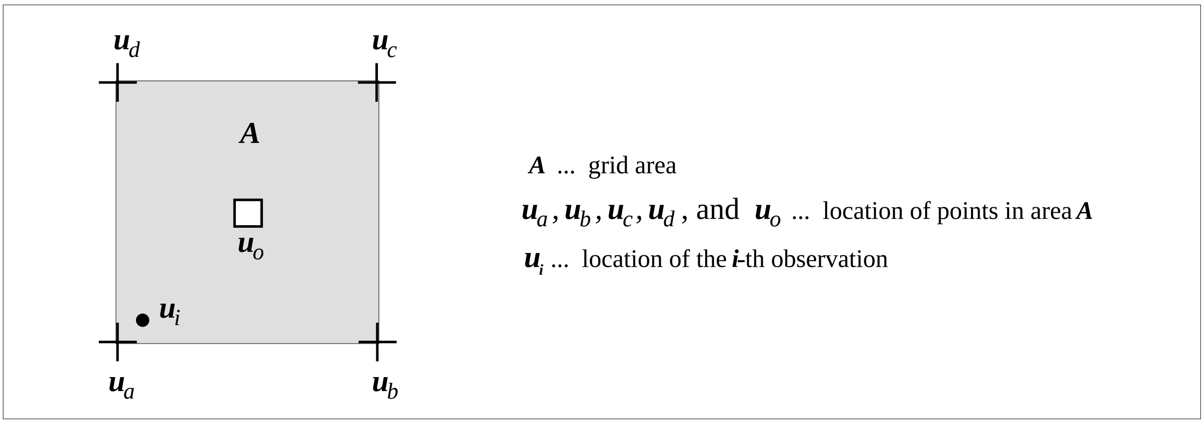

Figure 4 Location of the points $\mathbf{u}_a$, $\mathbf{u}_b$, $\mathbf{u}_c$, $\mathbf{u}_d$, and $\mathbf{u}_o$ in the area $\mathbf{A}$ as used for the numerical integration of the autocorrelation function.

The location of the points used for the numerical integration of (29) and (30) is shown in fig. 4. With this, the numerical approximation of $\hat{R}_{oi}$ was performed with:

$$\hat{R}_{oi} = \frac{1}{8}\left[\hat{R}(\mathbf{u}_a, \mathbf{u}_i) + \hat{R}(\mathbf{u}_b, \mathbf{u}_i) + \hat{R}(\mathbf{u}_c, \mathbf{u}_i) + \hat{R}(\mathbf{u}_d, \mathbf{u}_i) + 4\hat{R}(\mathbf{u}_o, \mathbf{u}_i)\right] \tag{33}$$

Parallel to that, the approximation for $\hat{R}_{oo}$ is calculated from:

$$\begin{aligned}
\hat{R}_{oo} &= \frac{1}{8}\cdot\frac{1}{8}\left[\hat{R}(\mathbf{u}_a, \mathbf{u}_a) + \hat{R}(\mathbf{u}_b, \mathbf{u}_a) + \hat{R}(\mathbf{u}_c, \mathbf{u}_a) + \hat{R}(\mathbf{u}_d, \mathbf{u}_a) + 4\hat{R}(\mathbf{u}_o, \mathbf{u}_a)\right] + \\
&+ \frac{1}{8}\cdot\frac{1}{8}\left[\hat{R}(\mathbf{u}_a, \mathbf{u}_b) + \hat{R}(\mathbf{u}_b, \mathbf{u}_b) + \hat{R}(\mathbf{u}_c, \mathbf{u}_b) + \hat{R}(\mathbf{u}_d, \mathbf{u}_b) + 4\hat{R}(\mathbf{u}_o, \mathbf{u}_b)\right] + \\
&+ \frac{1}{8}\cdot\frac{1}{8}\left[\hat{R}(\mathbf{u}_a, \mathbf{u}_c) + \hat{R}(\mathbf{u}_b, \mathbf{u}_c) + \hat{R}(\mathbf{u}_c, \mathbf{u}_c) + \hat{R}(\mathbf{u}_d, \mathbf{u}_c) + 4\hat{R}(\mathbf{u}_o, \mathbf{u}_c)\right] + \\
&+ \frac{1}{8}\cdot\frac{1}{8}\left[\hat{R}(\mathbf{u}_a, \mathbf{u}_d) + \hat{R}(\mathbf{u}_b, \mathbf{u}_d) + \hat{R}(\mathbf{u}_c, \mathbf{u}_d) + \hat{R}(\mathbf{u}_d, \mathbf{u}_d) + 4\hat{R}(\mathbf{u}_o, \mathbf{u}_d)\right] + \\
&+ \frac{4}{8}\cdot\frac{1}{8}\left[\hat{R}(\mathbf{u}_a, \mathbf{u}_o) + \hat{R}(\mathbf{u}_b, \mathbf{u}_o) + \hat{R}(\mathbf{u}_c, \mathbf{u}_o) + \hat{R}(\mathbf{u}_d, \mathbf{u}_o) + 4\hat{R}(\mathbf{u}_o, \mathbf{u}_o)\right]
\end{aligned} \tag{34}$$

Because of the exclusive dependence of the correlations on the interstation distance, e.g. $\hat{R}(\mathbf{u}_a, \mathbf{u}_b) = \hat{R}(\mathbf{u}_a, \mathbf{u}_d) = \hat{R}(\mathbf{u}_b, \mathbf{u}_c) = \hat{R}(\mathbf{u}_c, \mathbf{u}_d)$ is valid. Then, from (34) follows

$$\begin{aligned} \hat{R}_{oo} &= \frac{1}{64}\left[4\hat{R}\left(\mathbf{u}_a, \mathbf{u}_a\right) + 8\hat{R}\left(\mathbf{u}_a, \mathbf{u}_b\right) + 4\hat{R}\left(\mathbf{u}_a, \mathbf{u}_c\right) + 16\hat{R}\left(\mathbf{u}_a, \mathbf{u}_o\right)\right] + \\ &+ \frac{1}{16}\left[4\hat{R}\left(\mathbf{u}_a, \mathbf{u}_o\right) + 4\hat{R}\left(\mathbf{u}_a, \mathbf{u}_a\right)\right] \end{aligned} \tag{35}$$

and the final solution for the numerical approximation of $\hat{R}_{oo}$ can be written as

$$\hat{R}_{oo} = \frac{1}{16}\left[8\hat{R}\left(\mathbf{u}_a, \mathbf{u}_o\right) + 5\hat{R}\left(\mathbf{u}_a, \mathbf{u}_a\right) + 2\hat{R}\left(\mathbf{u}_a, \mathbf{u}_b\right) + 1\hat{R}\left(\mathbf{u}_a, \mathbf{u}_c\right)\right] \tag{36}$$

Note, that $\hat{R}\left(\mathbf{u}_a, \mathbf{u}_a\right) = 1$, and if all grid boxes within the model domain are of same area A, then eq. (36) has to be calculated only once. Conversely, eq. (33) has to be calculated for each area A for which an observation located at $\mathbf{u}_i$ is used to estimate the value of its areally averaged precipitation. By knowing $\hat{R}_{ij}$ and $\hat{R}_{oi}$, the weights λ_i for the observations $[Z(\mathbf{u}_i) + \delta(\mathbf{u}_i)]$ can be calculated from eq. (31). The analyzed areally averaged precipitation then follows from (8).

In fig. 5, an example of the described precipitation analysis is presented. The precipitation field for 26 August 1995, 18:00 UTC (accumulated from 06:00 to 18:00 UTC), reaches from the north of Scandinavia south to Greece and covers nearly the entire drainage basin of the Baltic Sea (green boundaries). A scale, ranging from precipitation values from 1 mm/12h to values equal to or greater than 256 mm/12h, is used. Areas of heavy rain shows precipitation values of 16 - 32 mm/12h.

For the interpretation of an analyzed precipitation value, it is useful to have some prior knowledge of the interpolation error. Fig. 6 shows this interpolation error, called kriging variance, for the 26 August 1995, 18:00 UTC. This kind of interpolation error is a relative measure of the reliability of the analyzed values, and depends on the station density, the autocorrelation function, as well as the extension of the analyzed grid areas. The kriging variance is the mean square difference between the true and the estimated precipitation value, normalized with the variance of the precipitation field. A zero value means no interpolation error, a value of unity indicates that the mean square difference between the true and the estimated precipitation value is of the same order as the variance. The lowest values of the kriging variance (lower than 0.1) are over Switzerland and Austria, both outside the Baltic drainage basin, and the highest values (greater than 0.8) are over the Atlantic Ocean and the Black Sea. Over the latter regions, no data are available. Over the Baltic Sea, values of the kriging variance are between 0.3 and 0.4. In other words, the absolute interpolation error is 30 - 40 % of the variance of the precipitation field. Note, that it is not possible to interprete the interpolation error as a percentage of the precipitation value itself, because the value of the variance is unknown. The latter is an implicit part of the autocorrelation function.

Nevertheless, the kriging variance allows us to detect areas with low accuracy. If one uses the analyzed precipitation fields as model input (Dorninger et al. 1995) or for model verification, then a kriging variance threshold of e.g. 0.3 can be defined for usable precipitation values. Model results or model verifications of grid areas with kriging variances above this threshold have to be interpreted with respect to the low analysis quality.

Figure 5 Page 22: Objectively analyzed precipitation field for 26 August 1995, 18:00 UTC. Units are in mm/12h.

Figure 6 Page 23: Normalized interpolation error (kriging variance) of the objectively analyzed precipitation field for 26 August 1995, 18:00 UTC.

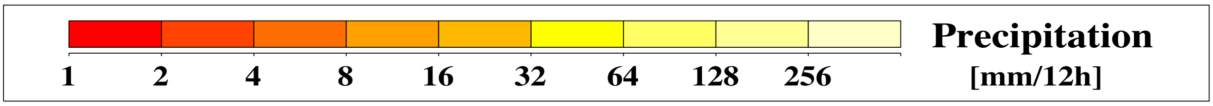
1
2
4
8
16
32
64
128
256
Precipitation
[mm/12h]

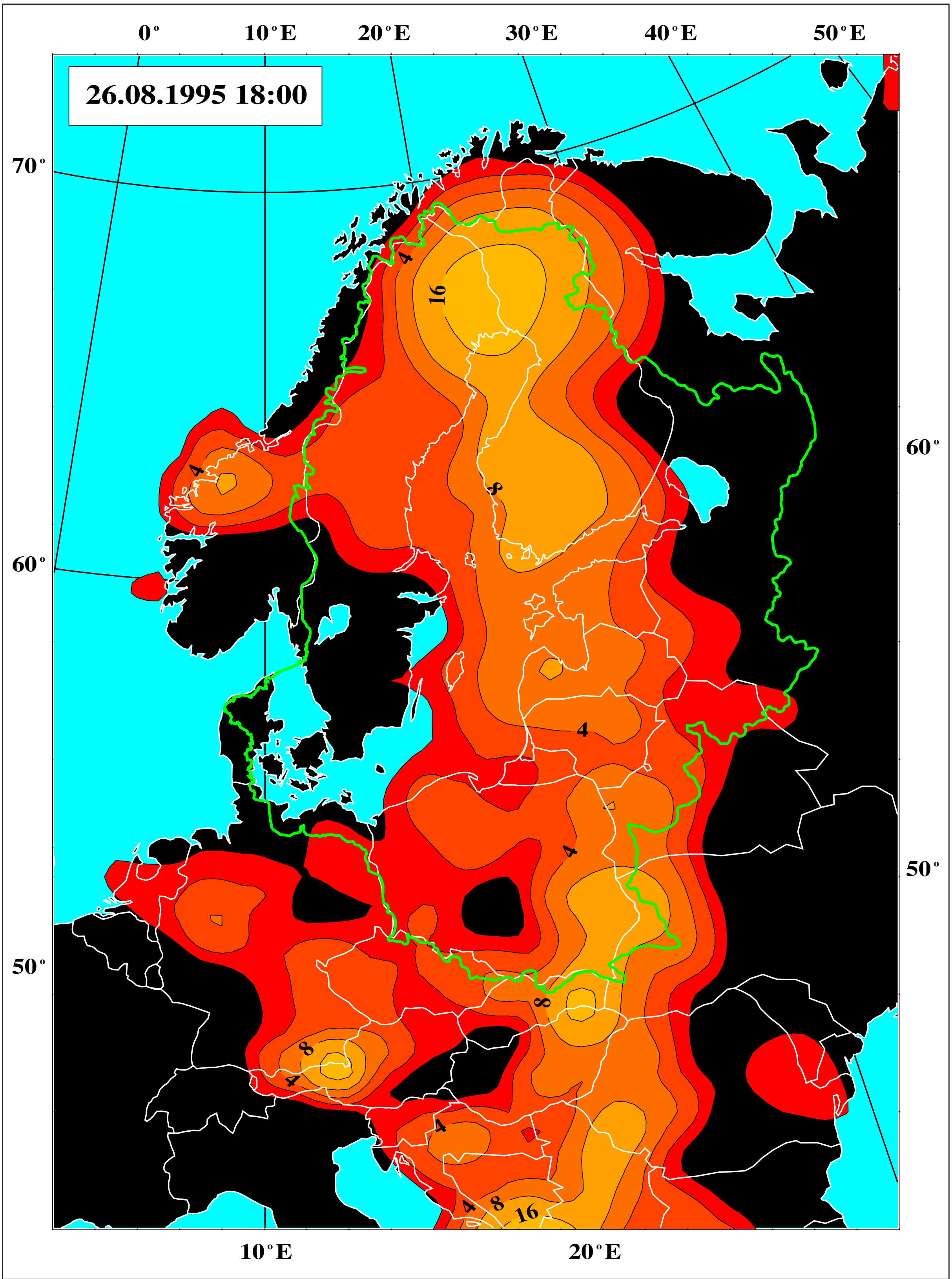
26.08.1995 18:00
0°
10°E
20°E
30°E
40°E
50°E
70°
60°
50°
4
16
8
4
4
8
4
8
4
4
8
16

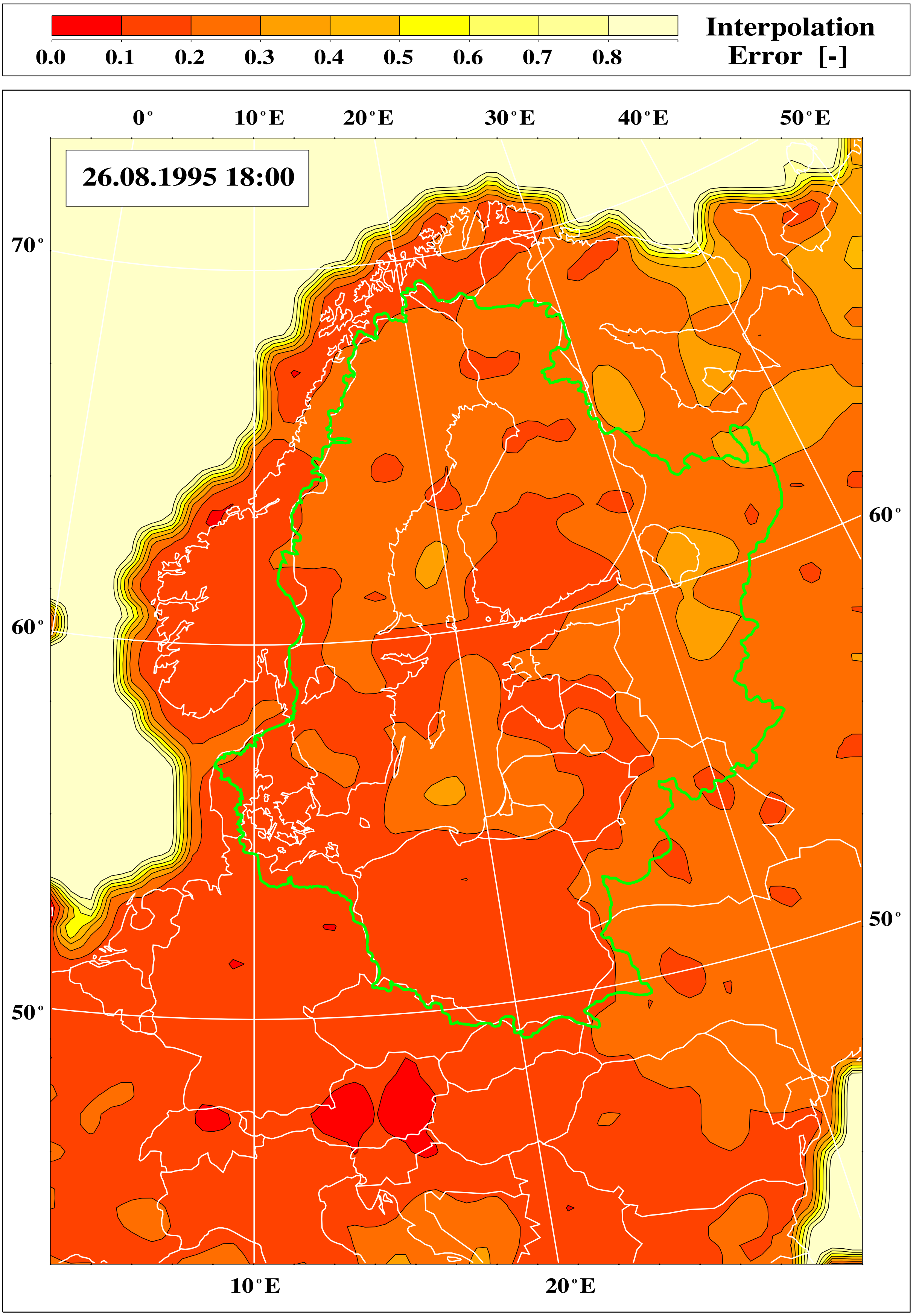
0.0
0.1
0.2
0.3
0.4
0.5
0.6
0.7
0.8
Interpolation Error [-]
0°
10°E
20°E
30°E
40°E
50°E
26.08.1995 18:00
70°
60°
50°
60°
50°
10°E
20°E

6 COMPARISON WITH ECMWF FORECASTS

To be sure that the structure of the analyzed precipitation fields is realistic, forecasts from the ECMWF T213 model are used for comparison. The modelled fields are 12-hourly accumulated, from 18 to 30 hour forecast.

As a first visual comparison with 4 days of the PIDCAP period, 27 - 30 September 1995, the forecast vs. the observed precipitation fields are plotted against each other (fig. 7). There is a good agreement in both the pattern and the values, between the forecast and analyzed fields, which points to the high quality of the ECMWF precipitation forecasts. Furthermore, this good agreement shows that the structure of the analyzed fields is consistent with model fields. This is important, because the analysis procedure is based on an averaging process which can therefore lead to precipitation fields which are to smooth.

In the discussion of the comparison, one has to consider the absence of observations over the North Sea. A comparison of the fields over this region is therefore not possible. Beyond this, the observations are uncorrected. The slight overestimation of the predicted precipitation in regions of heavy rain might be caused by the underestimation of the gauge values due to e.g. wind-induced losses (Førland 1996).

It is planned to analyze selected precipitation events of the PIDCAP period with additional observations from national climate and hydrological networks. This high resolution analysis will be performed on the full resolution REMO grid (18 km grid distance), and will take into account the proposed gauge-corrections (Sevruk 1986, Førland 1996). The resulting objectively analyzed precipitation fields can then be used for quantitative verifications of mesoscale models (HIRLAM, DM, and REMO).

Figure 7 Pages 25 - 26: Precipitation from ECMWF, 12-hourly accumulated from 18 to 30 hour forecast (left) vs. precipitation analyzed from synoptic observations (right). Dates are 27 - 30 September 1995, 18:00 UTC. Units are in mm/12h.

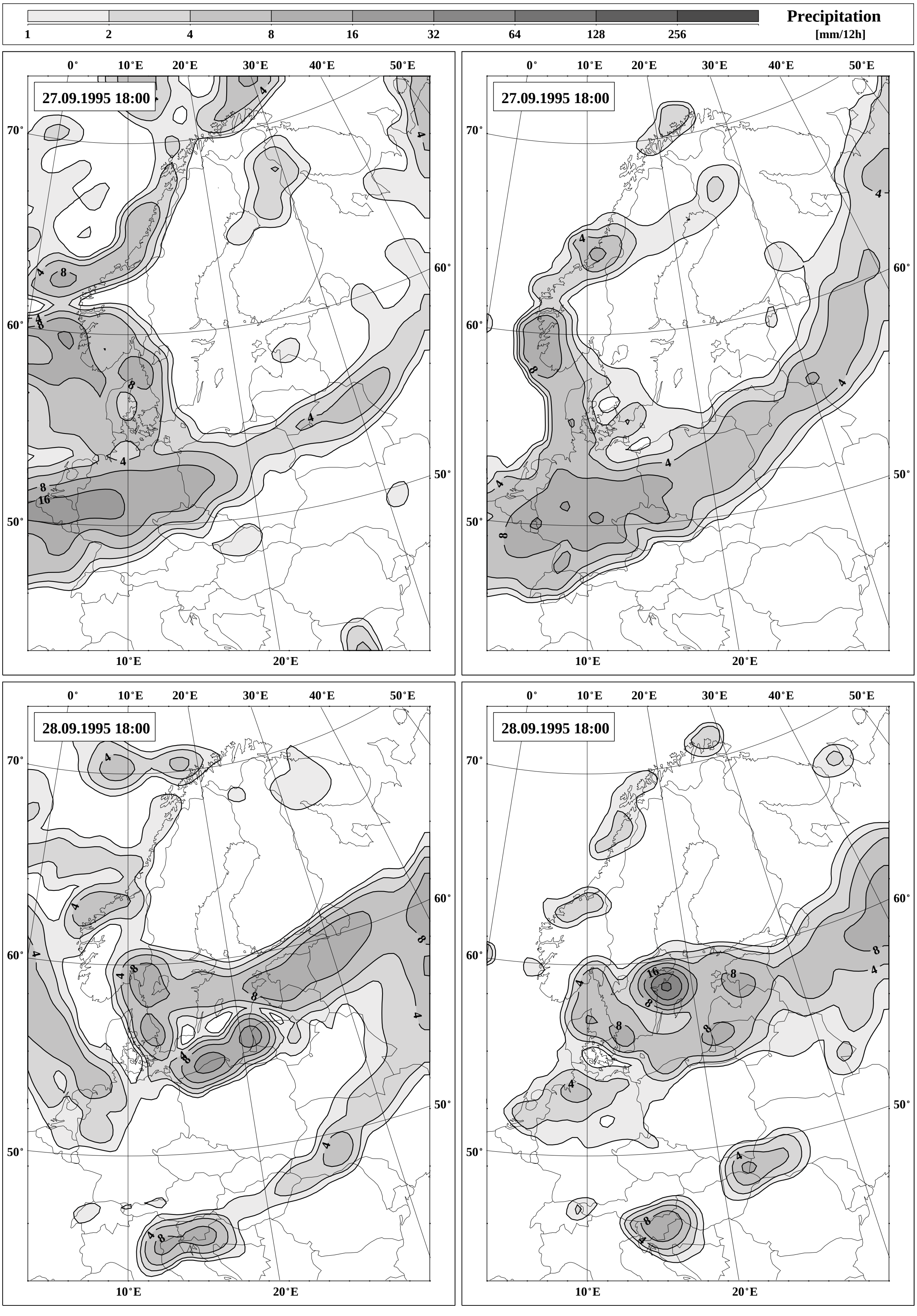
Precipitation
[mm/12h]
1 2 4 8 16 32 64 128 256
27.09.1995 18:00
27.09.1995 18:00
28.09.1995 18:00
28.09.1995 18:00
0° 10°E 20°E 30°E 40°E 50°E
70° 60° 50°
10°E 20°E

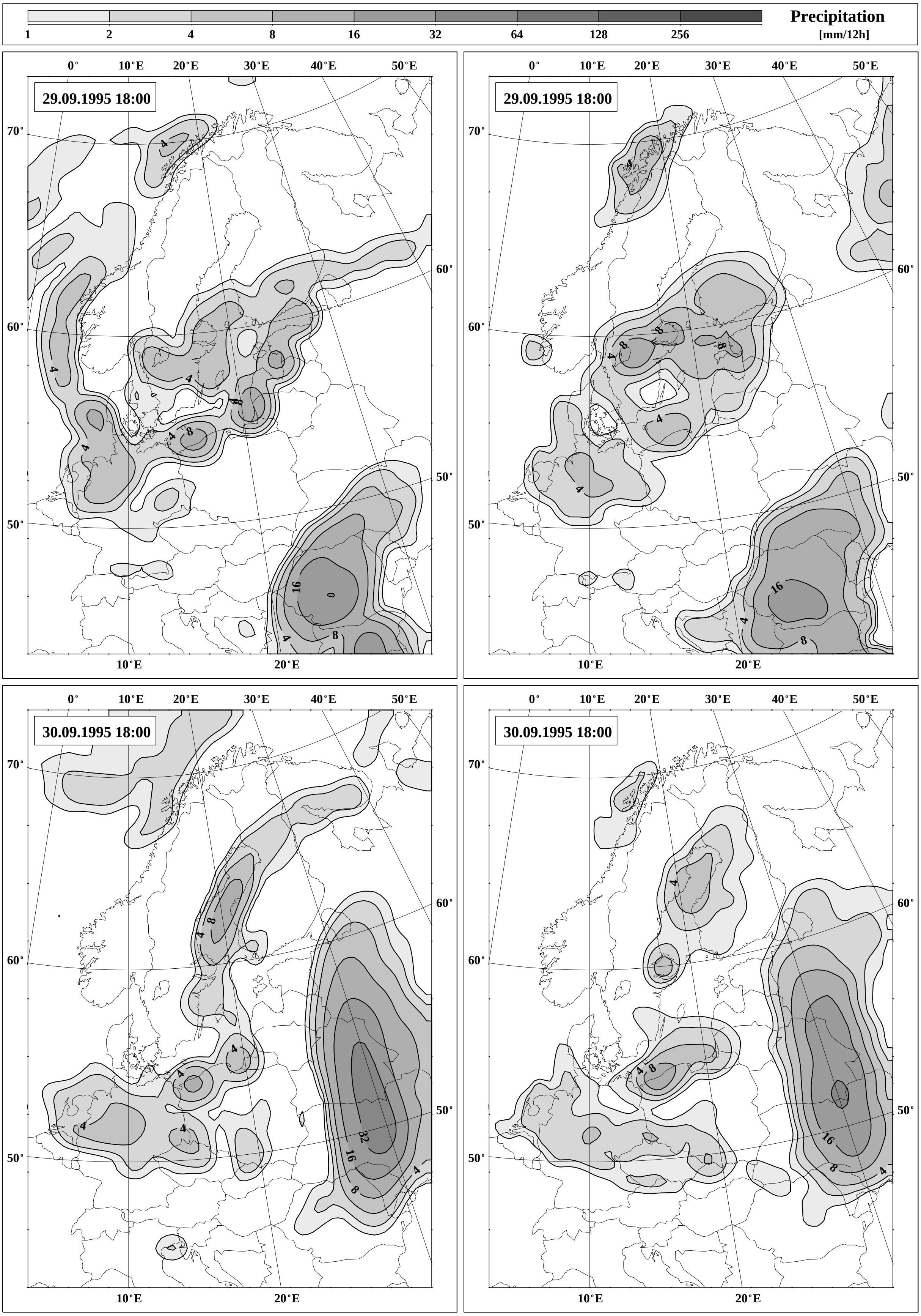
Precipitation
[mm/12h]
1
2
4
8
16
32
64
128
256
29.09.1995 18:00
29.09.1995 18:00
30.09.1995 18:00
30.09.1995 18:00
0°
10°E
20°E
30°E
40°E
50°E
70°
60°
50°

7 TWICE DAILY PRECIPITATION FIELDS

This is the main chapter of the PIDCAP quick look precipitation atlas, containing 4 month (August to November 1995) twice daily gridded precipitation fields. Fig. 8 shows the precipitation fields, objectively analyzed with block kriging, for 06:00 UTC (left) and 18:00 UTC (right) in units mm/12h. The precipitation fields are estimated from synoptic gauge observations accumulated over the last 12 hours. The typical density of the synoptic network together with the analysis grid, can be seen in fig. 1. The scaling of the contour lines is defined by powers of base 2, starting with 2^0 for values ≥ 1 mm/12h, and ending with 2^8 for values ≥ 256 mm/12h.

The twice daily precipitation fields (fig. 8) are used to select interesting periods for further investigations. Three periods with heavy precipitation over the catchment of the Baltic Sea are found. These are:

- **23 August to 5 September, 1995:** Heavy precipitation over the whole Baltic region was caused by a cyclone moving from the North Sea over Sweden to the North Cap, followed from 3 cyclones moving northwards from their developing region near the Black Sea.
- **24 September to 2 October, 1995:** Two frontal systems moved across the BALTEX region from west to east. The structure of these systems is well defined by the corresponding precipitation field.
- **31 October to 4 November, 1995:** This period contains a regionally confined, but very strong north storm. In almost the entire Baltic region, the precipitation occurred in the form of snow, which is unusual for this time of the year.

Beside these periods, several other periods, possibly interesting for case studies, can be selected from the pictures in fig. 8:

- 9 September to 12 September, 1995
- 14 September to 17 September, 1995
- 4 October to 8 October, 1995
- 18 October to 23 October, 1995
- 27 October to 28 October, 1995
- 15 November to 19 November, 1995
- 23 November to 28 November, 1995

This atlas does not contain detailed analyses and descriptions of weather situations, since additional information concerning this field, together with selected precipitation records, is available from other authors (Isemer 1996).

Figure 8 Pages 28 - 88: Objectively analyzed precipitation fields for the period 1 August 1995 - 30 November 1995, 06:00 and 18:00 UTC. Units are in mm/12h.

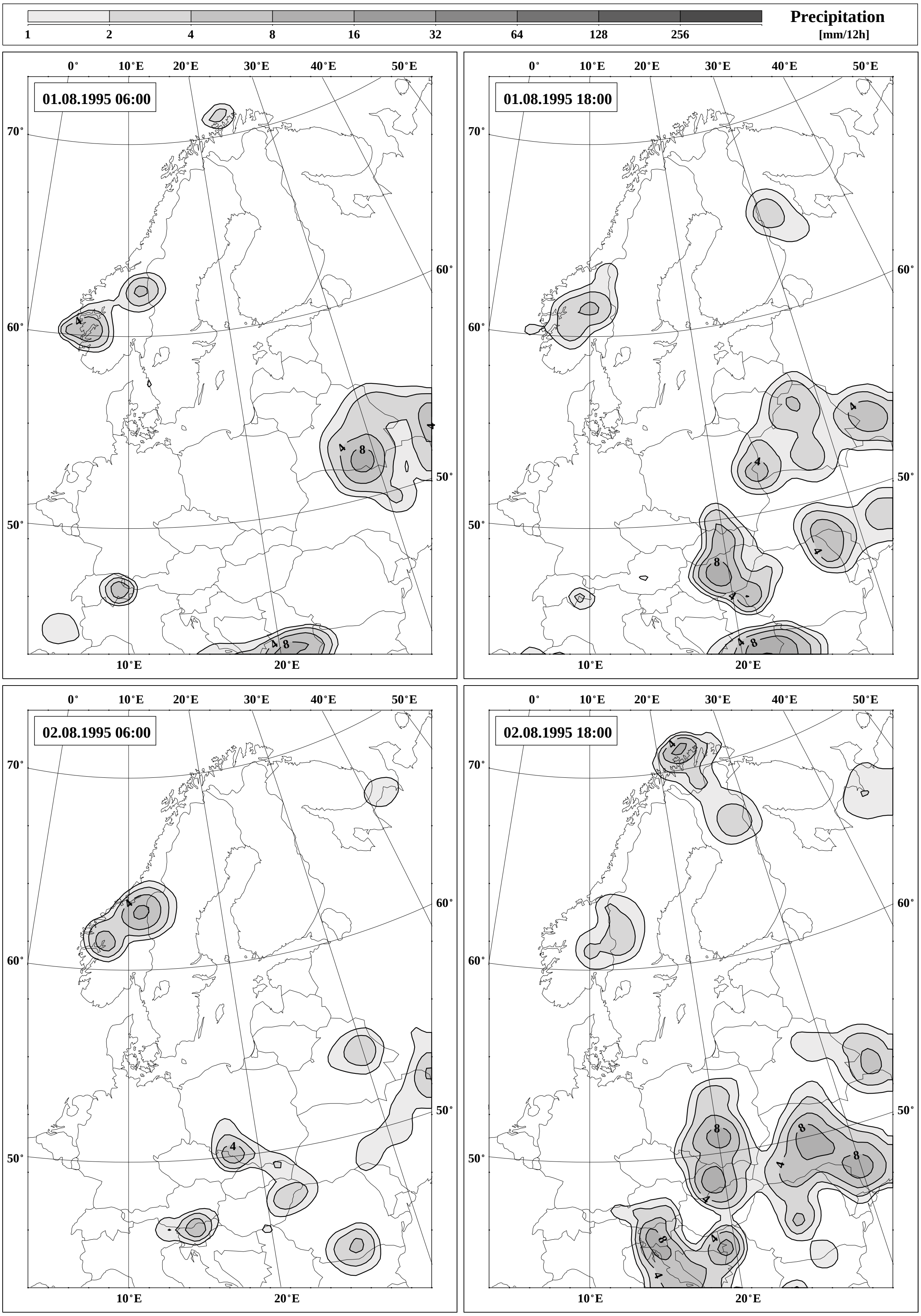

Precipitation
[mm/12h]
1
2
4
8
16
32
64
128
256
01.08.1995 06:00
01.08.1995 18:00
02.08.1995 06:00
02.08.1995 18:00
0°
10°E
20°E
30°E
40°E
50°E
70°
60°
50°

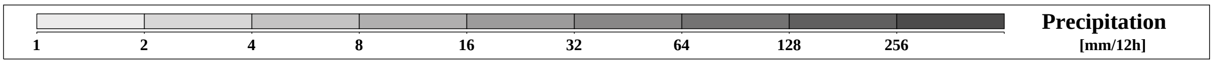
1
2
4
8
16
32
64
128
256
Precipitation
[mm/12h]

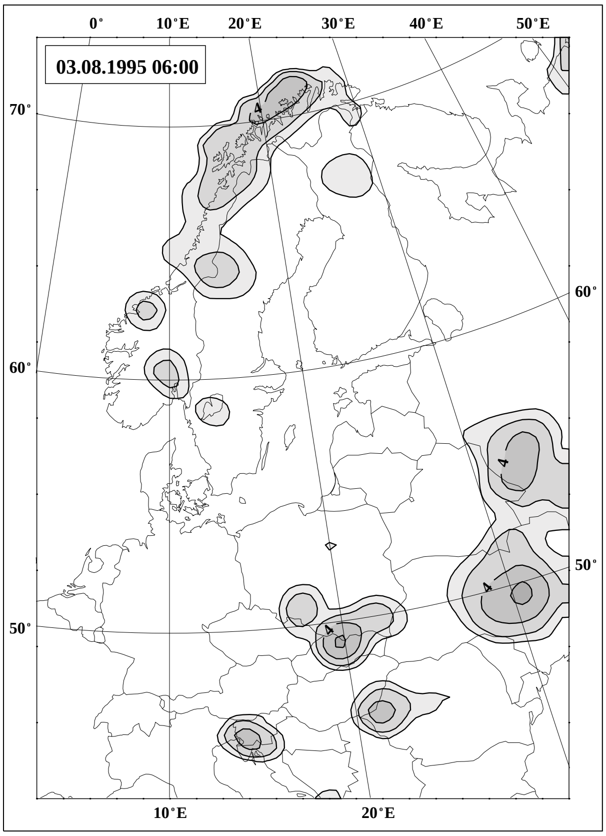
03.08.1995 06:00
0°
10°E
20°E
30°E
40°E
50°E
70°
60°
50°
10°E
20°E

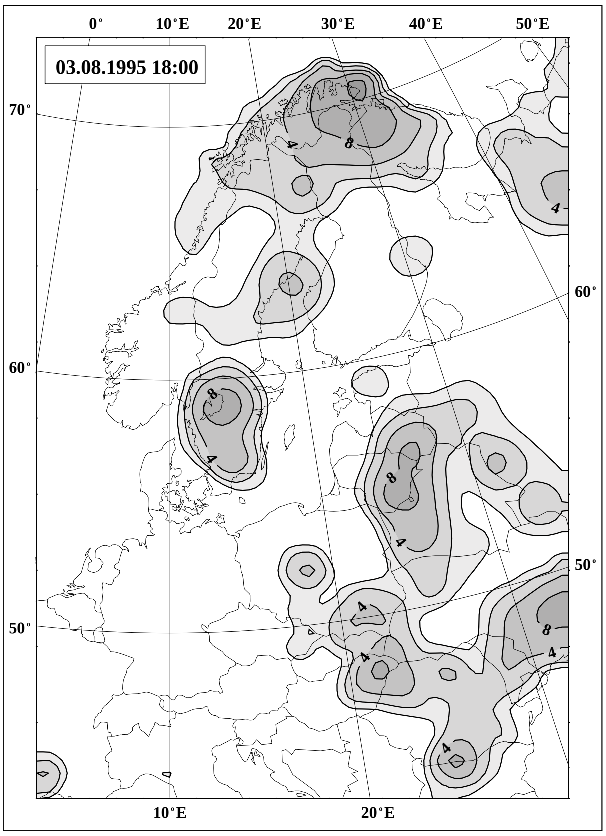
03.08.1995 18:00
0°
10°E
20°E
30°E
40°E
50°E
70°
60°
50°
10°E
20°E

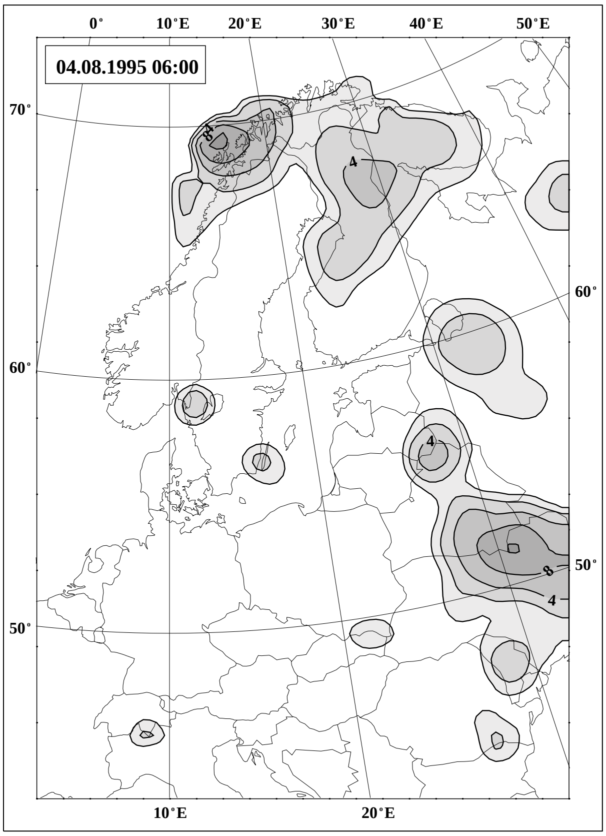
04.08.1995 06:00
0°
10°E
20°E
30°E
40°E
50°E
70°
60°
50°
10°E
20°E

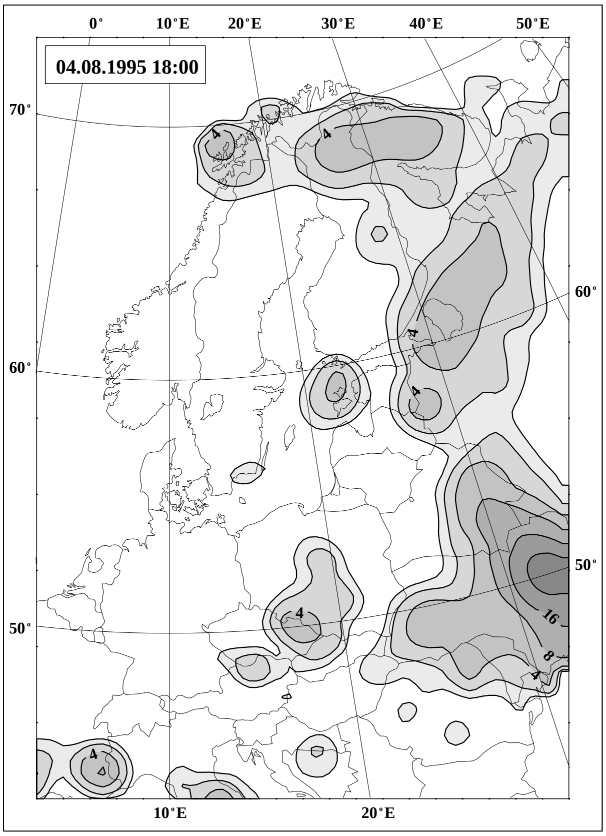
04.08.1995 18:00
0°
10°E
20°E
30°E
40°E
50°E
70°
60°
50°
10°E
20°E

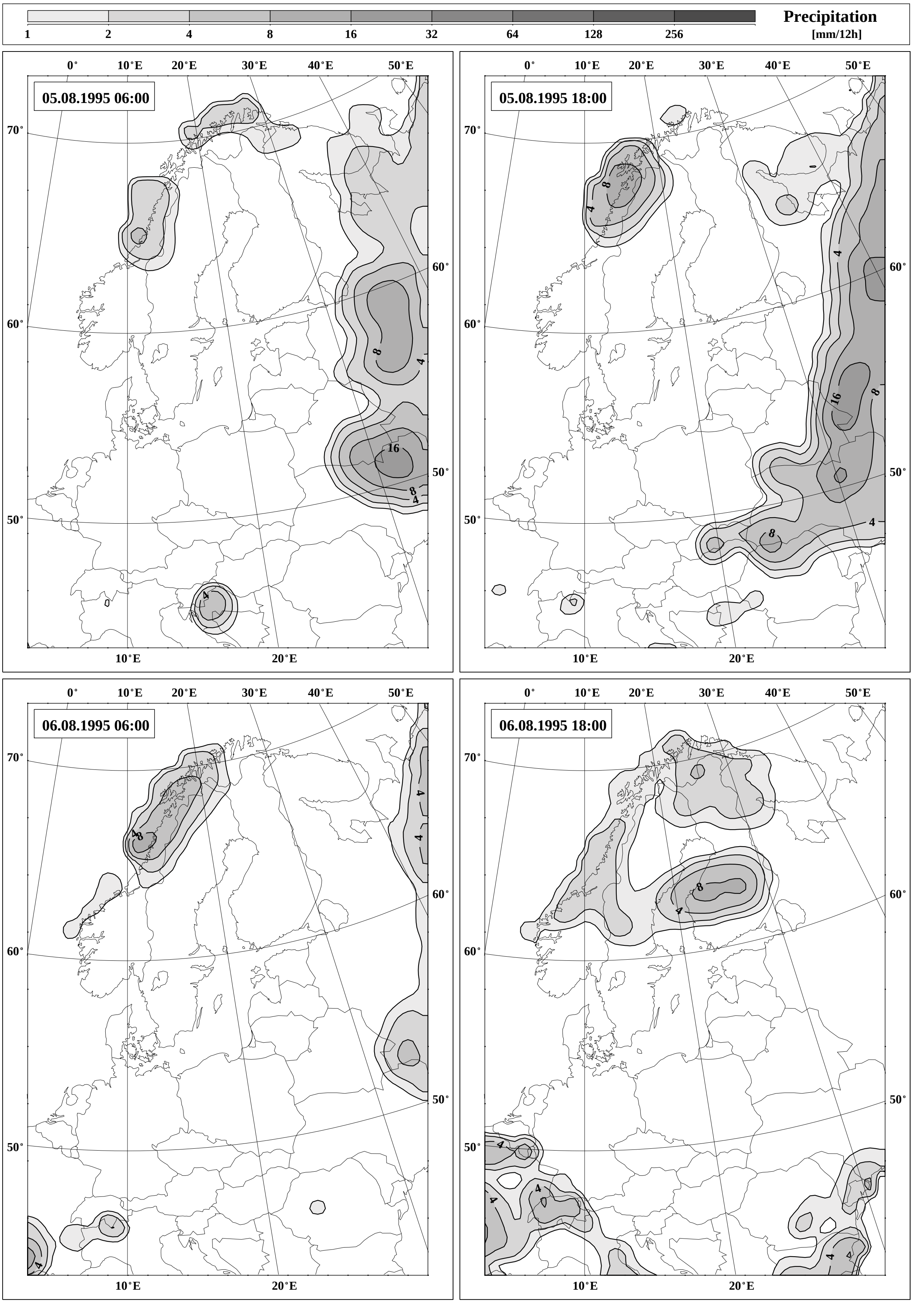
Precipitation
[mm/12h]
1
2
4
8
16
32
64
128
256
05.08.1995 06:00
05.08.1995 18:00
06.08.1995 06:00
06.08.1995 18:00
0°
10°E
20°E
30°E
40°E
50°E
70°
60°
50°

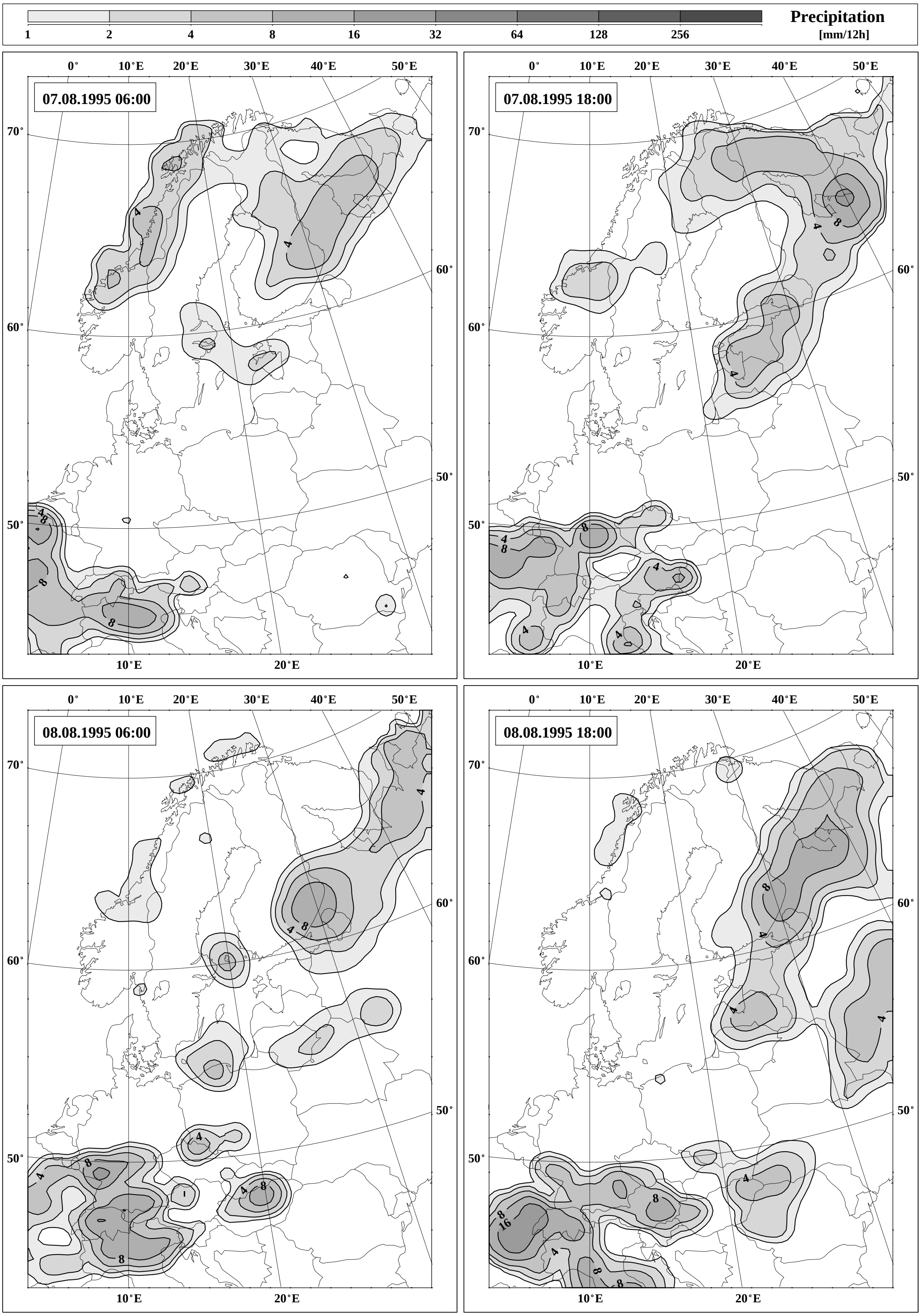
Precipitation
[mm/12h]
1
2
4
8
16
32
64
128
256
07.08.1995 06:00
07.08.1995 18:00
08.08.1995 06:00
08.08.1995 18:00
0°
10°E
20°E
30°E
40°E
50°E
70°
60°
50°

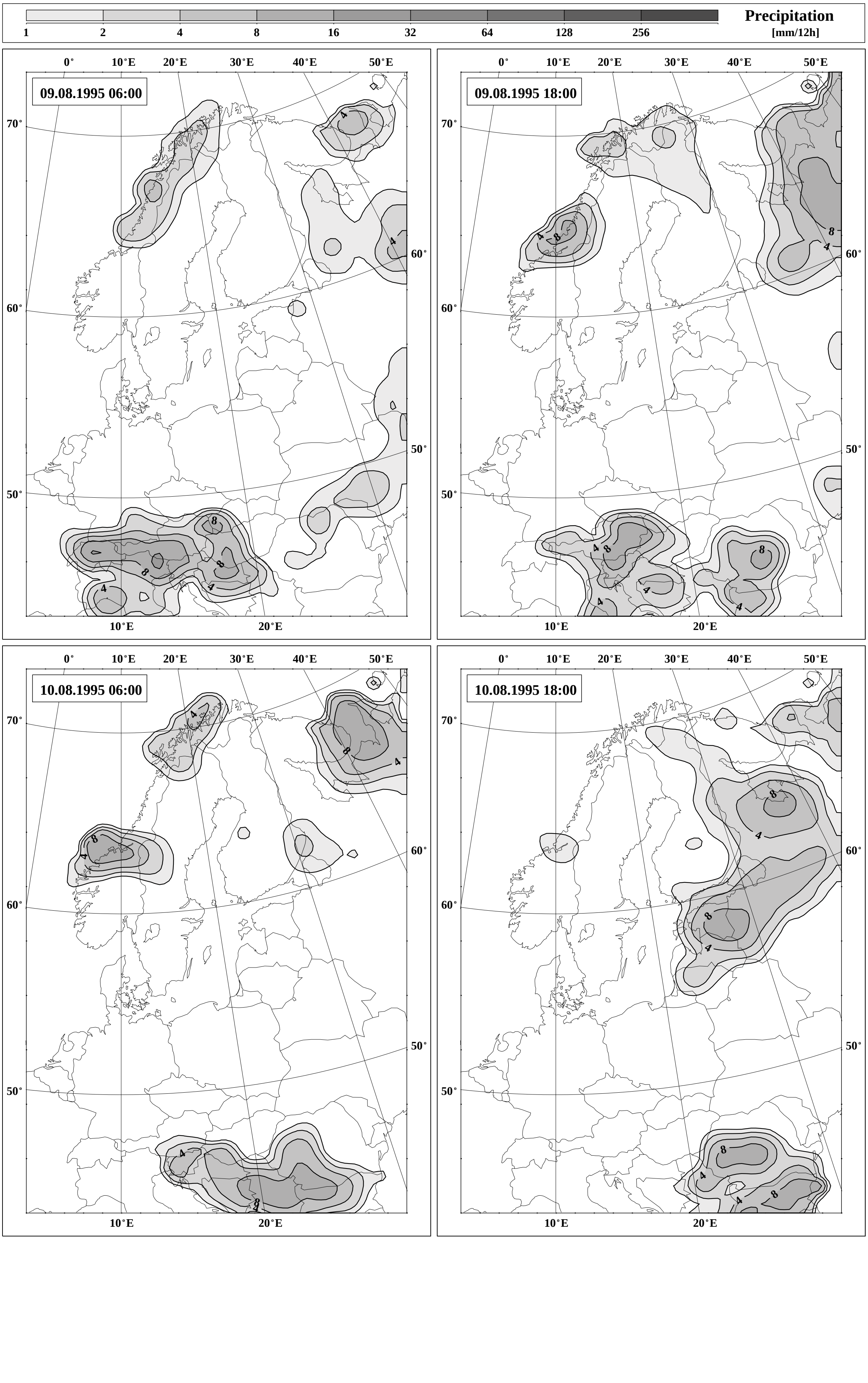
1
2
4
8
16
32
64
128
256
Precipitation
[mm/12h]
09.08.1995 06:00
09.08.1995 18:00
10.08.1995 06:00
10.08.1995 18:00
0°
10°E
20°E
30°E
40°E
50°E
70°
60°
50°

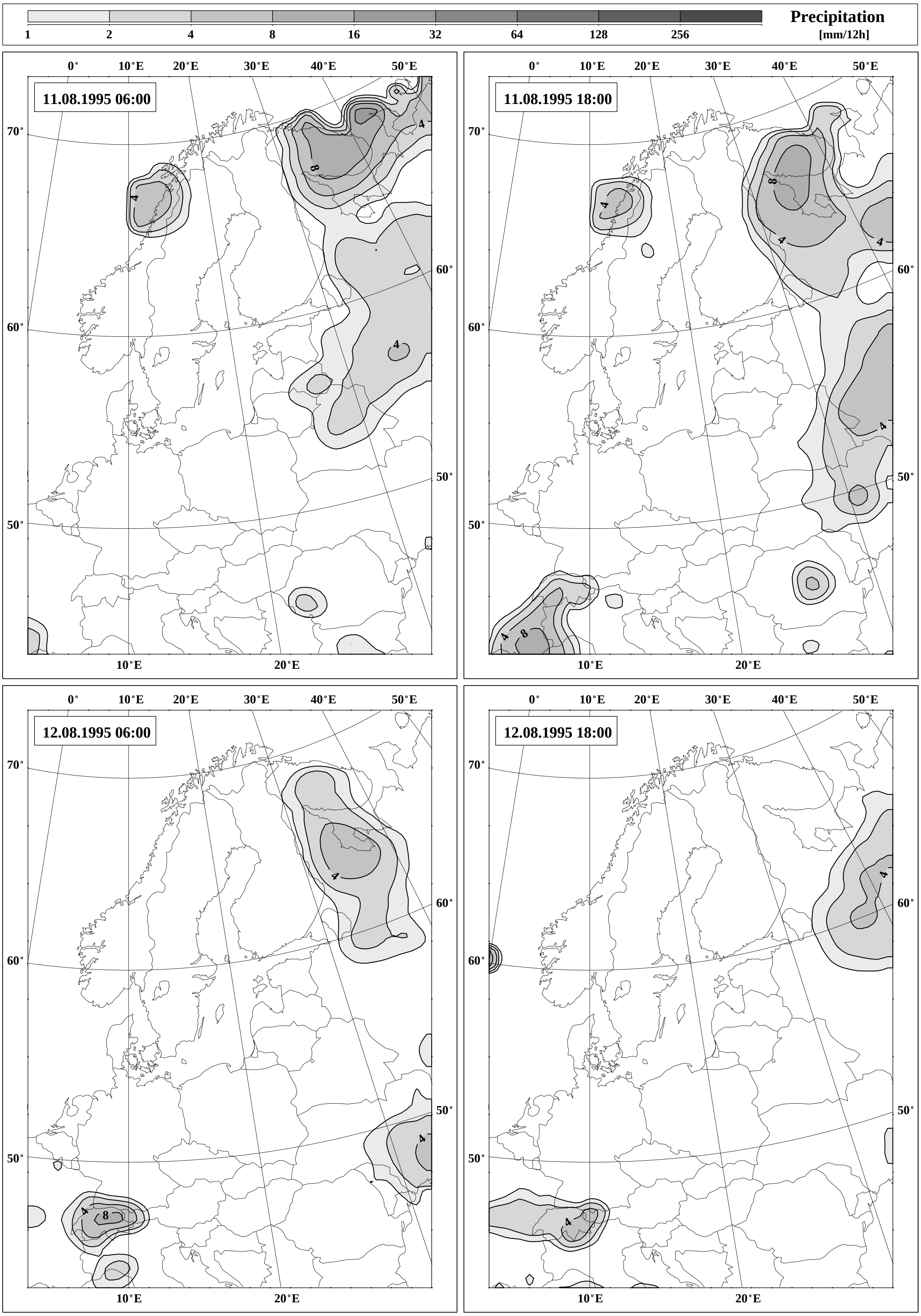
Precipitation
[mm/12h]
1 2 4 8 16 32 64 128 256
11.08.1995 06:00
11.08.1995 18:00
12.08.1995 06:00
12.08.1995 18:00
0° 10°E 20°E 30°E 40°E 50°E
70° 60° 50°
10°E 20°E

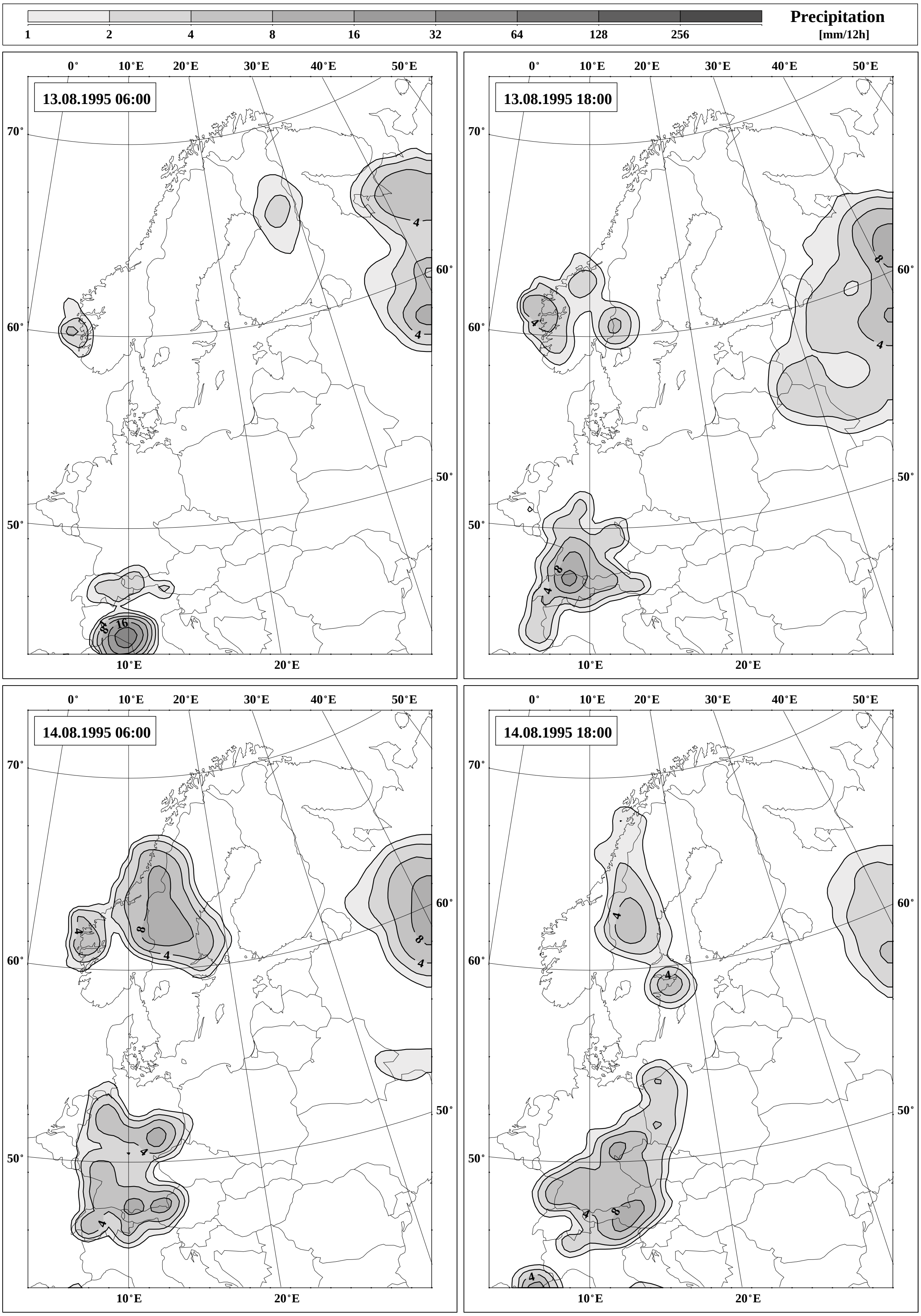
Precipitation
[mm/12h]
1 2 4 8 16 32 64 128 256
13.08.1995 06:00
13.08.1995 18:00
14.08.1995 06:00
14.08.1995 18:00
0° 10°E 20°E 30°E 40°E 50°E
70° 60° 50°
10°E 20°E

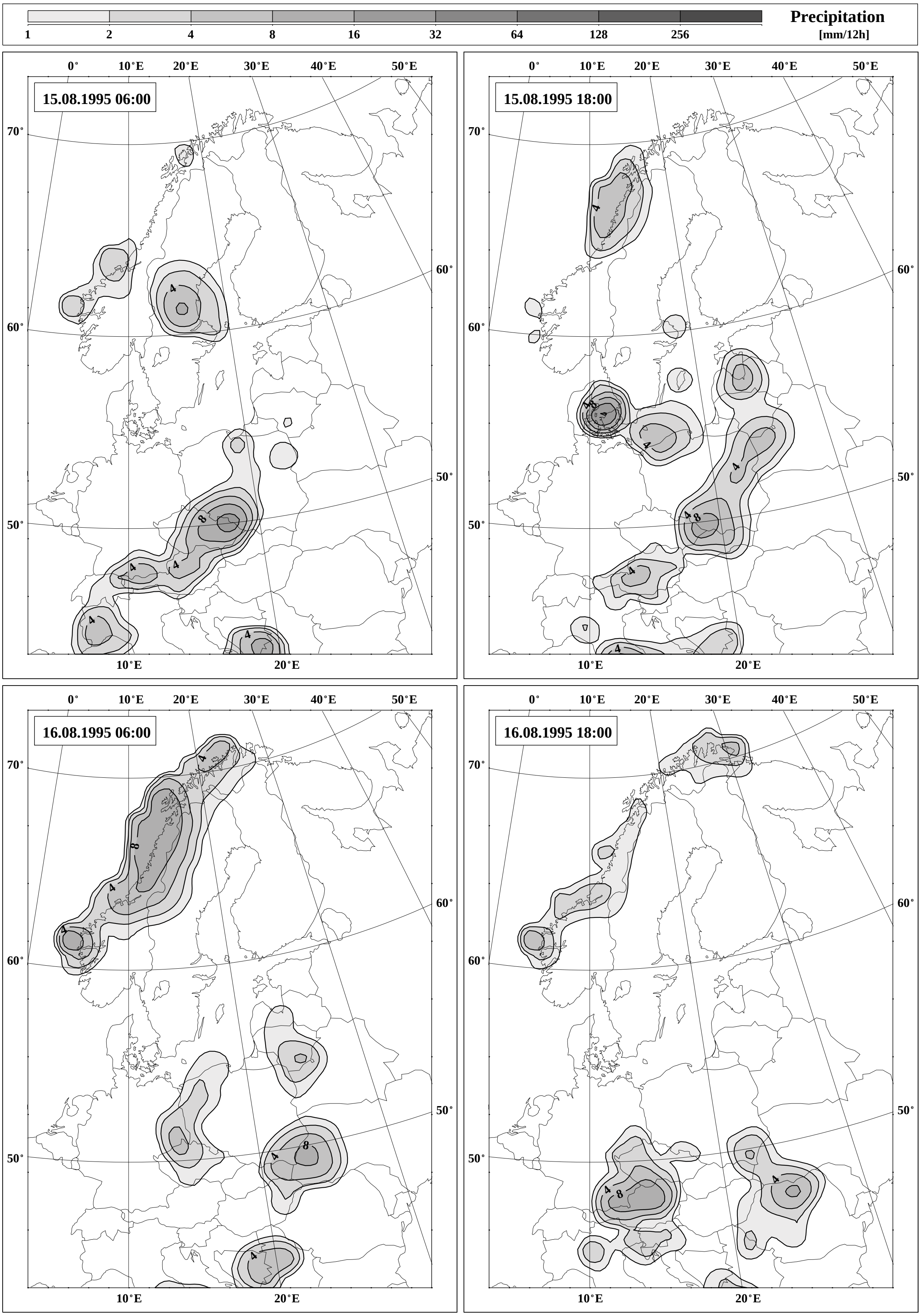
Precipitation
[mm/12h]
1
2
4
8
16
32
64
128
256
15.08.1995 06:00
15.08.1995 18:00
16.08.1995 06:00
16.08.1995 18:00
0°
10°E
20°E
30°E
40°E
50°E
70°
60°
50°

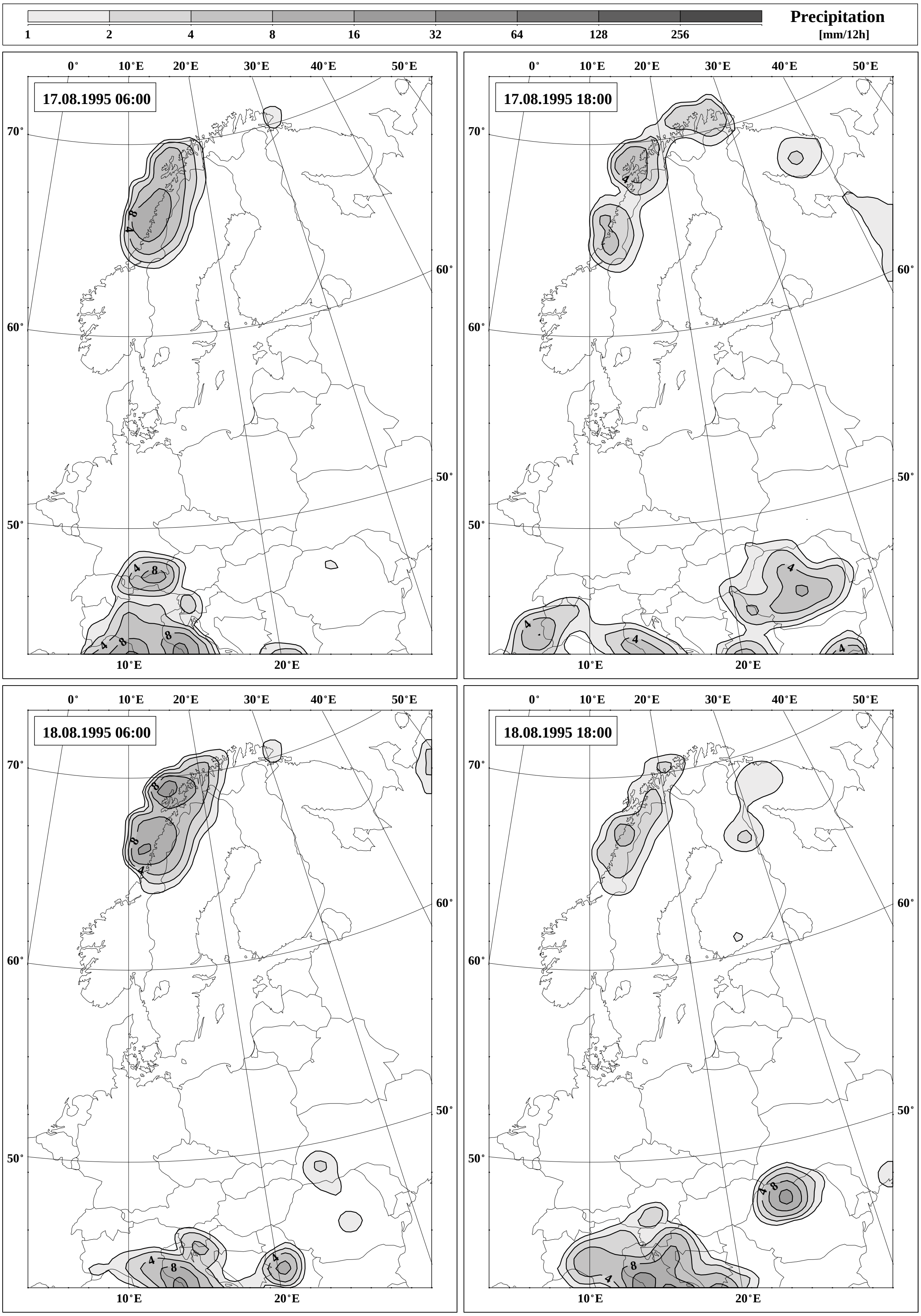

Precipitation
[mm/12h]
1 2 4 8 16 32 64 128 256
17.08.1995 06:00
17.08.1995 18:00
18.08.1995 06:00
18.08.1995 18:00
0° 10°E 20°E 30°E 40°E 50°E
70° 60° 50°

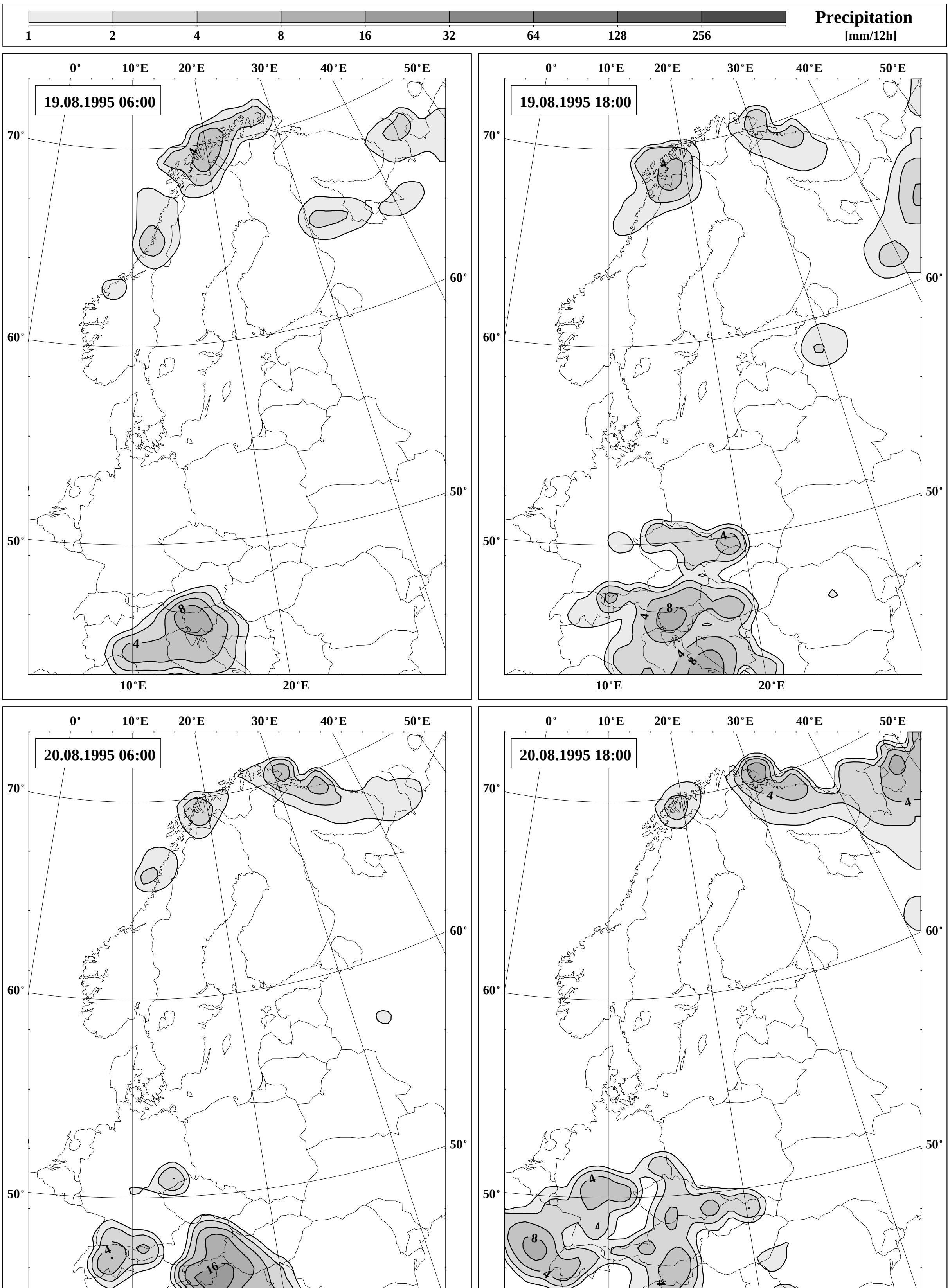

Precipitation
[mm/12h]
1 2 4 8 16 32 64 128 256
19.08.1995 06:00
19.08.1995 18:00
20.08.1995 06:00
20.08.1995 18:00
0° 10°E 20°E 30°E 40°E 50°E
70° 60° 50°

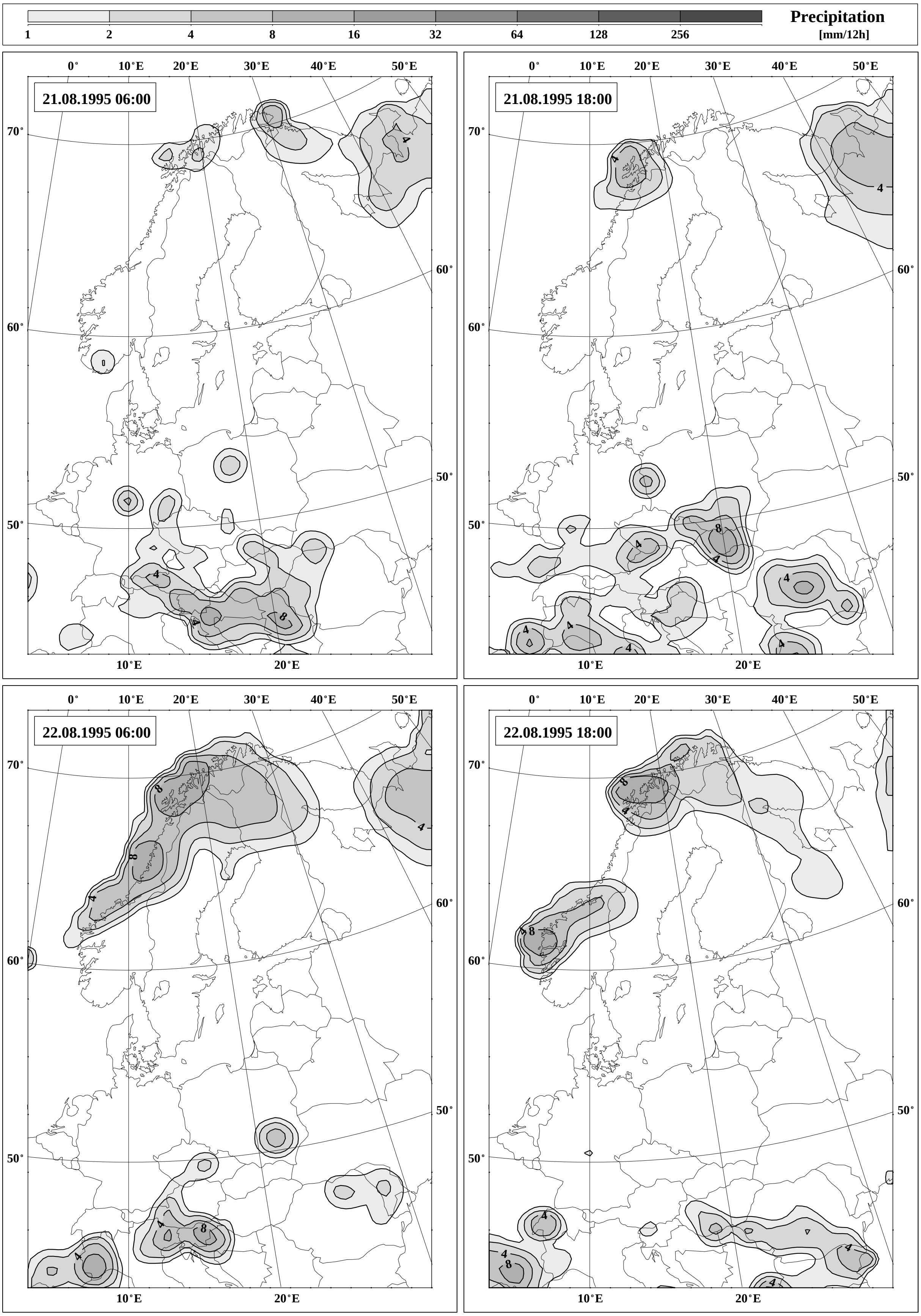
Precipitation
[mm/12h]
1
2
4
8
16
32
64
128
256
21.08.1995 06:00
21.08.1995 18:00
22.08.1995 06:00
22.08.1995 18:00
0°
10°E
20°E
30°E
40°E
50°E
70°
60°
50°

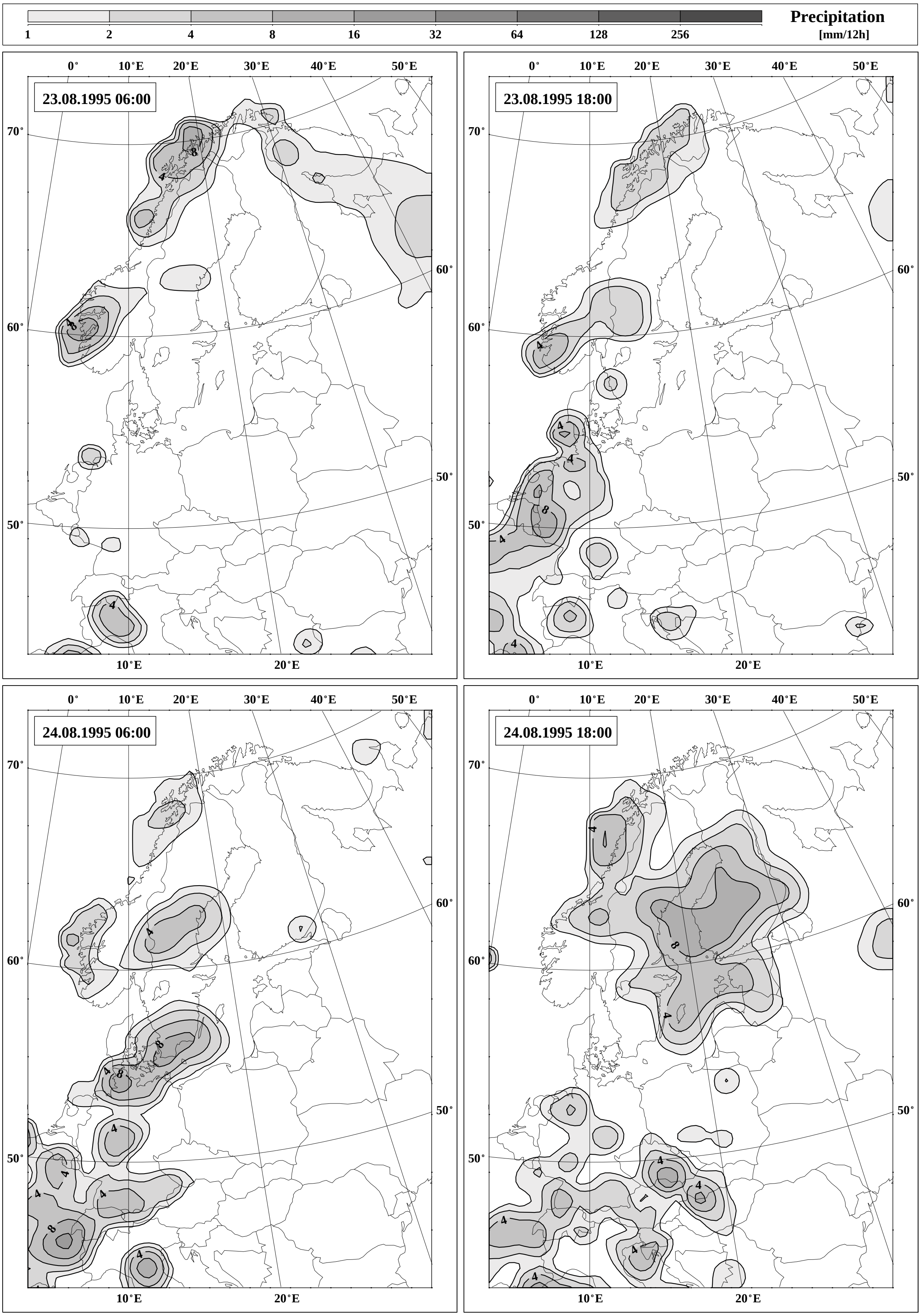
1 2 4 8 16 32 64 128 256
Precipitation
[mm/12h]
23.08.1995 06:00
23.08.1995 18:00
24.08.1995 06:00
24.08.1995 18:00
0°
10°E
20°E
30°E
40°E
50°E
70°
60°
50°

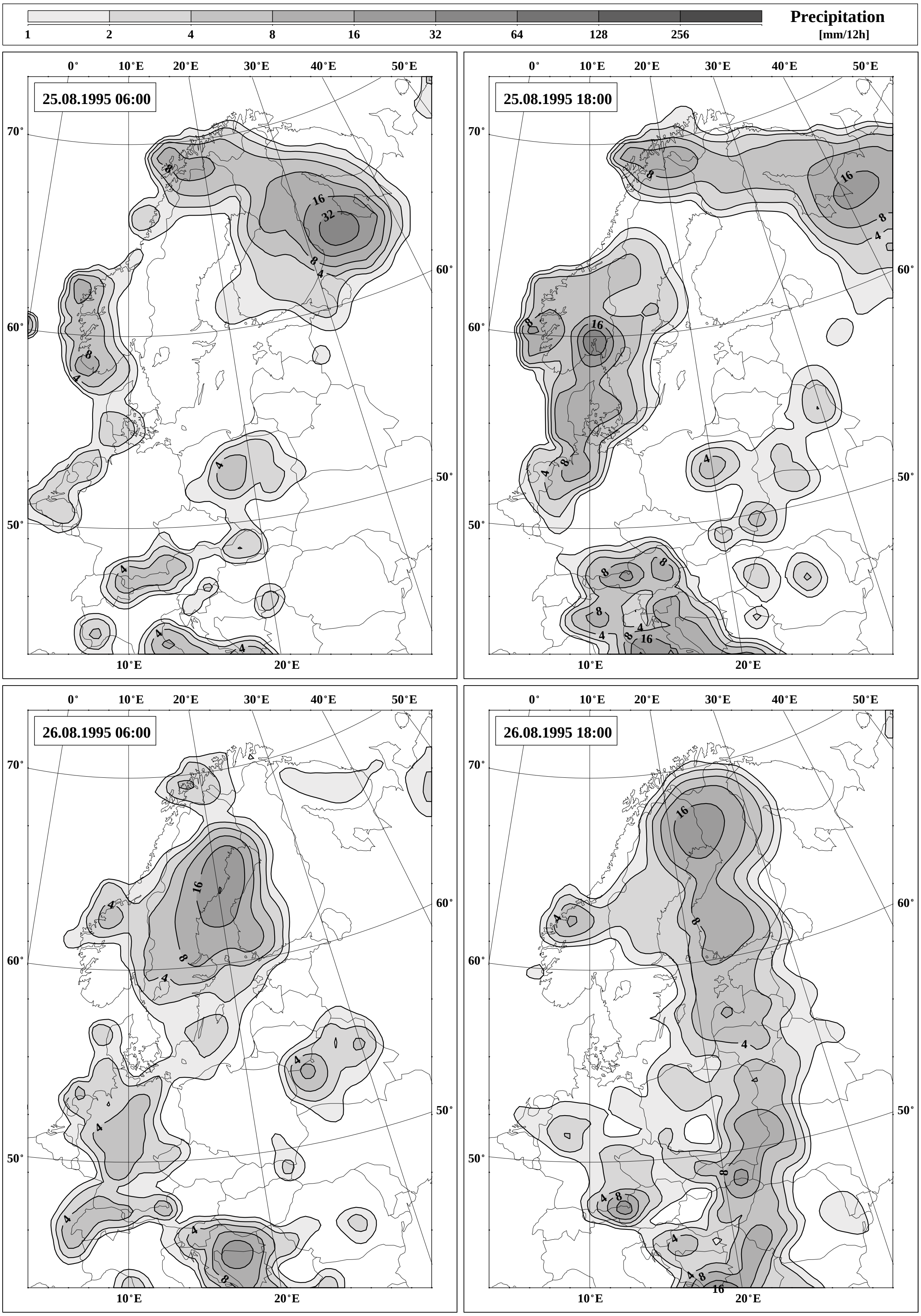
Precipitation
[mm/12h]
1
2
4
8
16
32
64
128
256
25.08.1995 06:00
25.08.1995 18:00
26.08.1995 06:00
26.08.1995 18:00
0°
10°E
20°E
30°E
40°E
50°E
70°
60°
50°

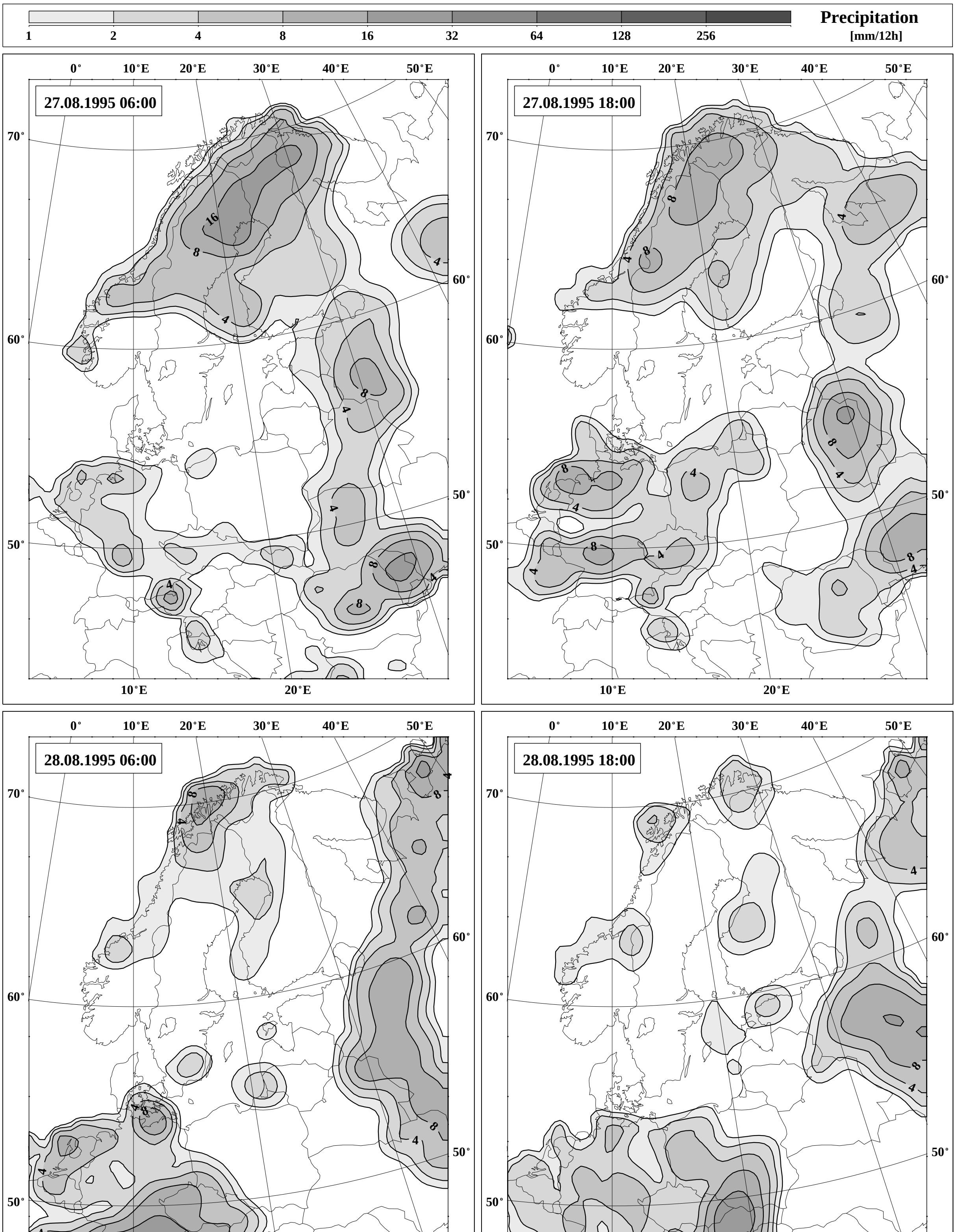
Precipitation
[mm/12h]
1 2 4 8 16 32 64 128 256
27.08.1995 06:00
27.08.1995 18:00
28.08.1995 06:00
28.08.1995 18:00
0° 10°E 20°E 30°E 40°E 50°E
70° 60° 50°
10°E 20°E

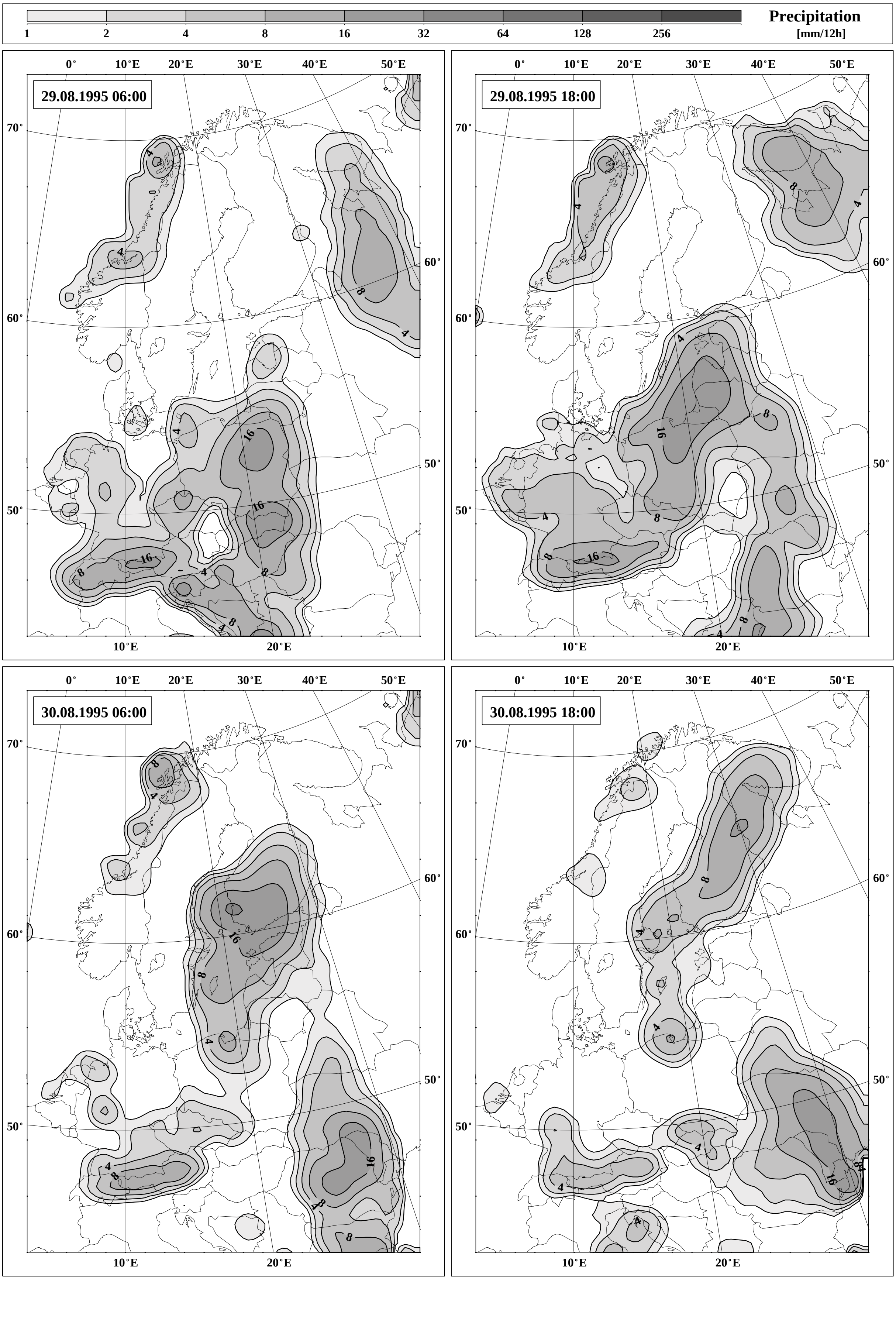
Precipitation
[mm/12h]
1
2
4
8
16
32
64
128
256
29.08.1995 06:00
29.08.1995 18:00
30.08.1995 06:00
30.08.1995 18:00

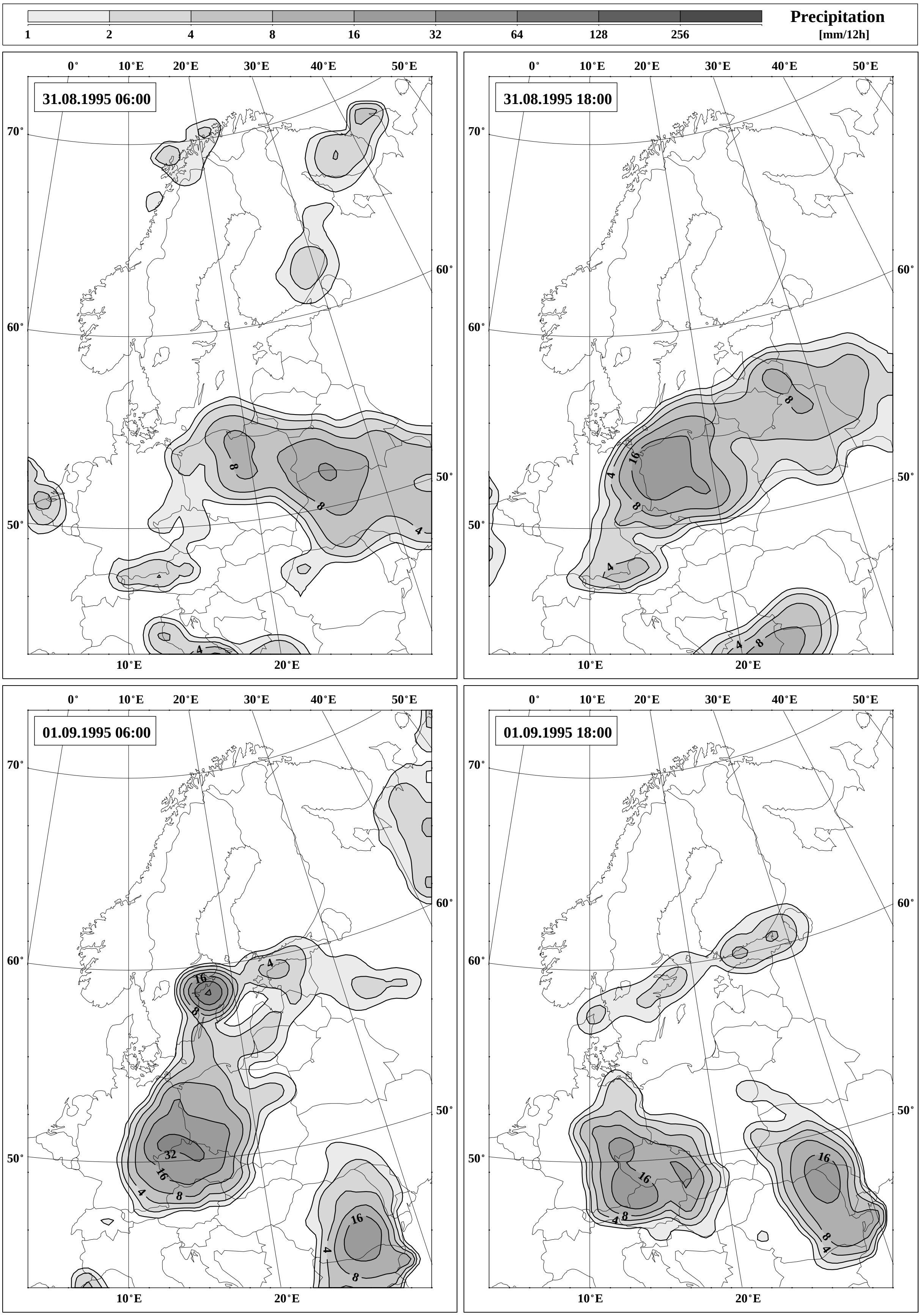
Precipitation
[mm/12h]
1
2
4
8
16
32
64
128
256
31.08.1995 06:00
31.08.1995 18:00
01.09.1995 06:00
01.09.1995 18:00
0°
10°E
20°E
30°E
40°E
50°E
70°
60°
50°

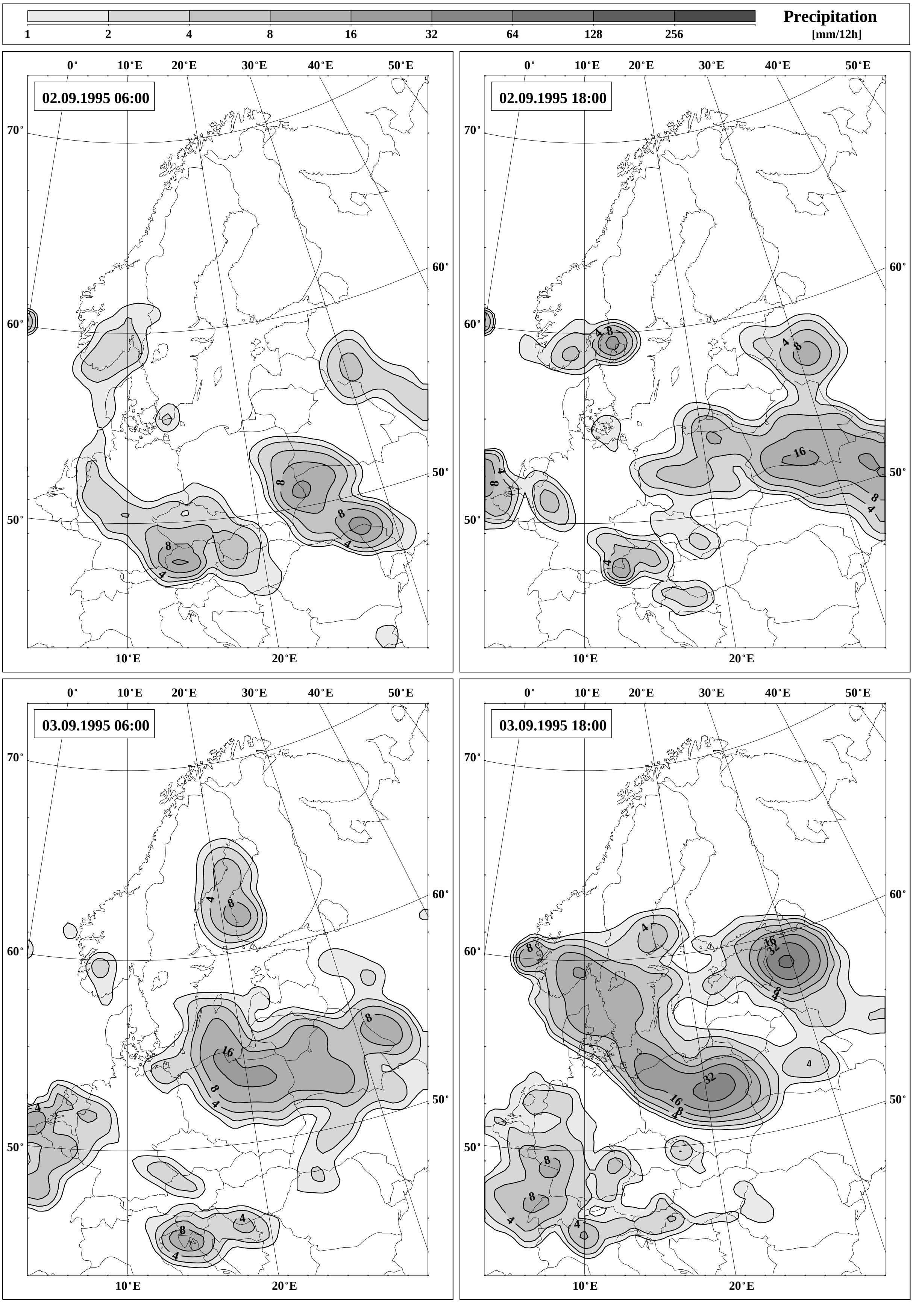
Precipitation
[mm/12h]
1
2
4
8
16
32
64
128
256
02.09.1995 06:00
02.09.1995 18:00
03.09.1995 06:00
03.09.1995 18:00
0°
10°E
20°E
30°E
40°E
50°E
70°
60°
50°

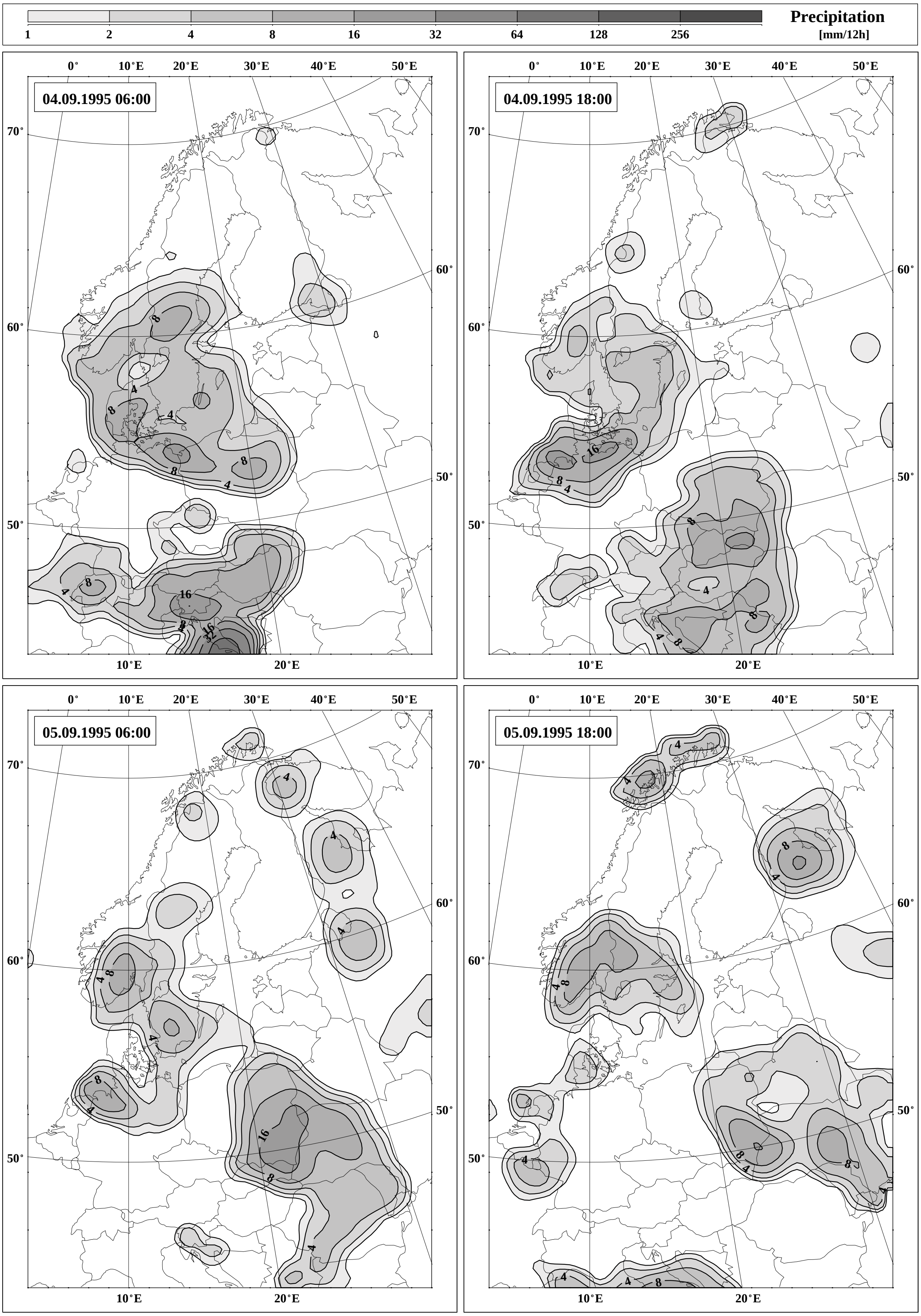
Precipitation
[mm/12h]
1 2 4 8 16 32 64 128 256
04.09.1995 06:00
04.09.1995 18:00
05.09.1995 06:00
05.09.1995 18:00
0° 10°E 20°E 30°E 40°E 50°E
70° 60° 50°
10°E 20°E

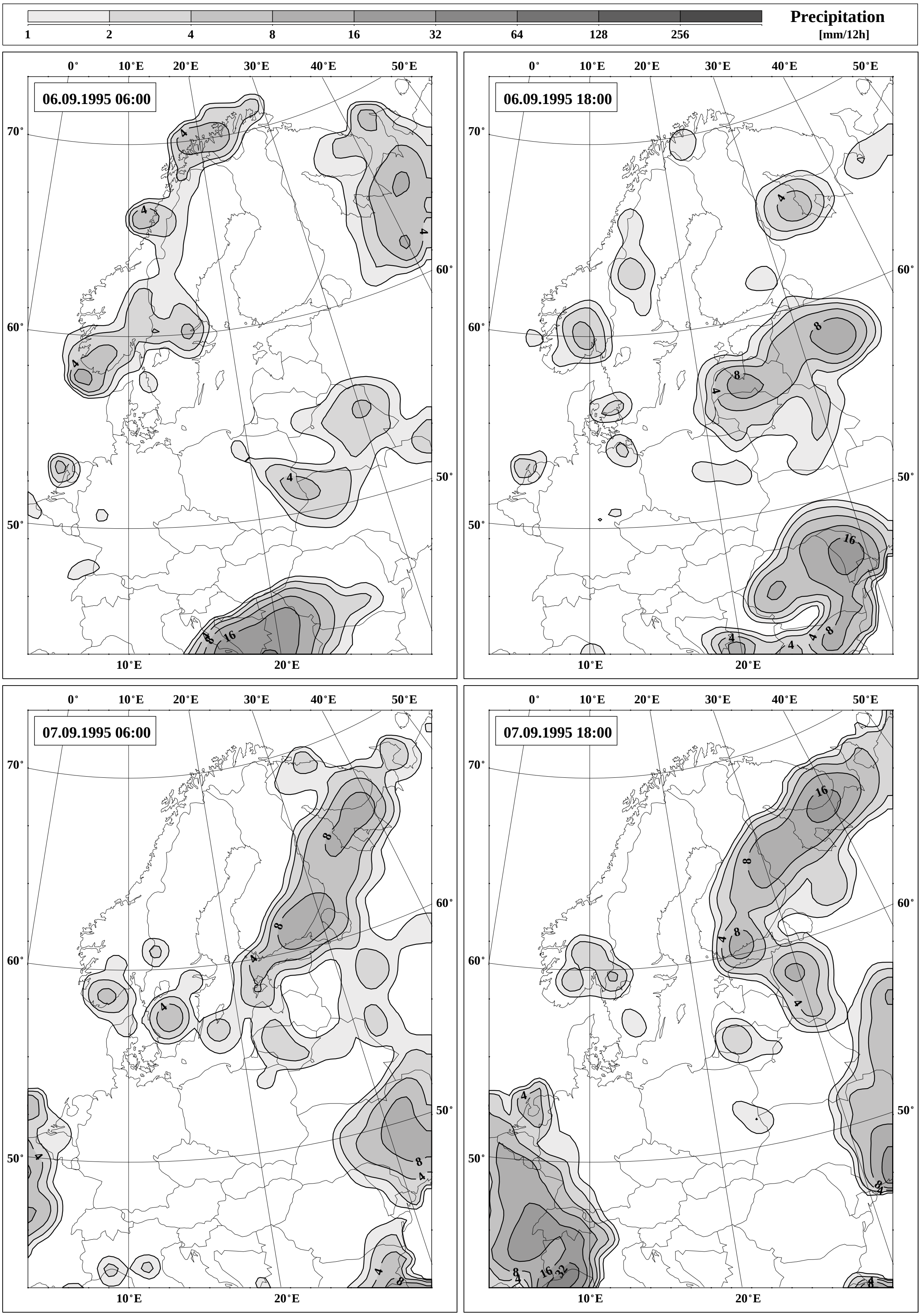
Precipitation
[mm/12h]
1 2 4 8 16 32 64 128 256
06.09.1995 06:00
06.09.1995 18:00
07.09.1995 06:00
07.09.1995 18:00
0° 10°E 20°E 30°E 40°E 50°E
70° 60° 50°
10°E 20°E

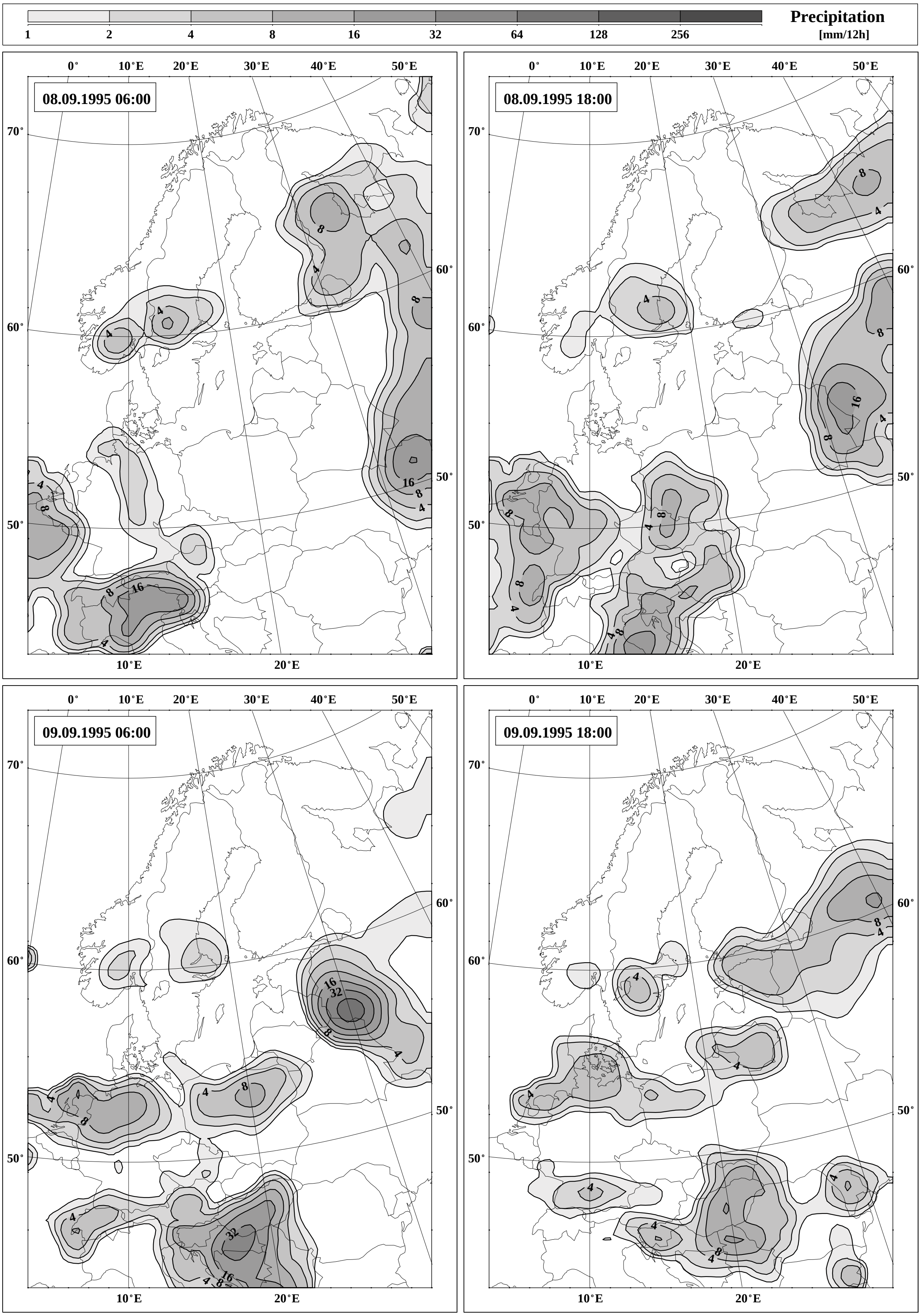
Precipitation
[mm/12h]
1 2 4 8 16 32 64 128 256
08.09.1995 06:00
08.09.1995 18:00
09.09.1995 06:00
09.09.1995 18:00
0° 10°E 20°E 30°E 40°E 50°E
70° 60° 50°
10°E 20°E

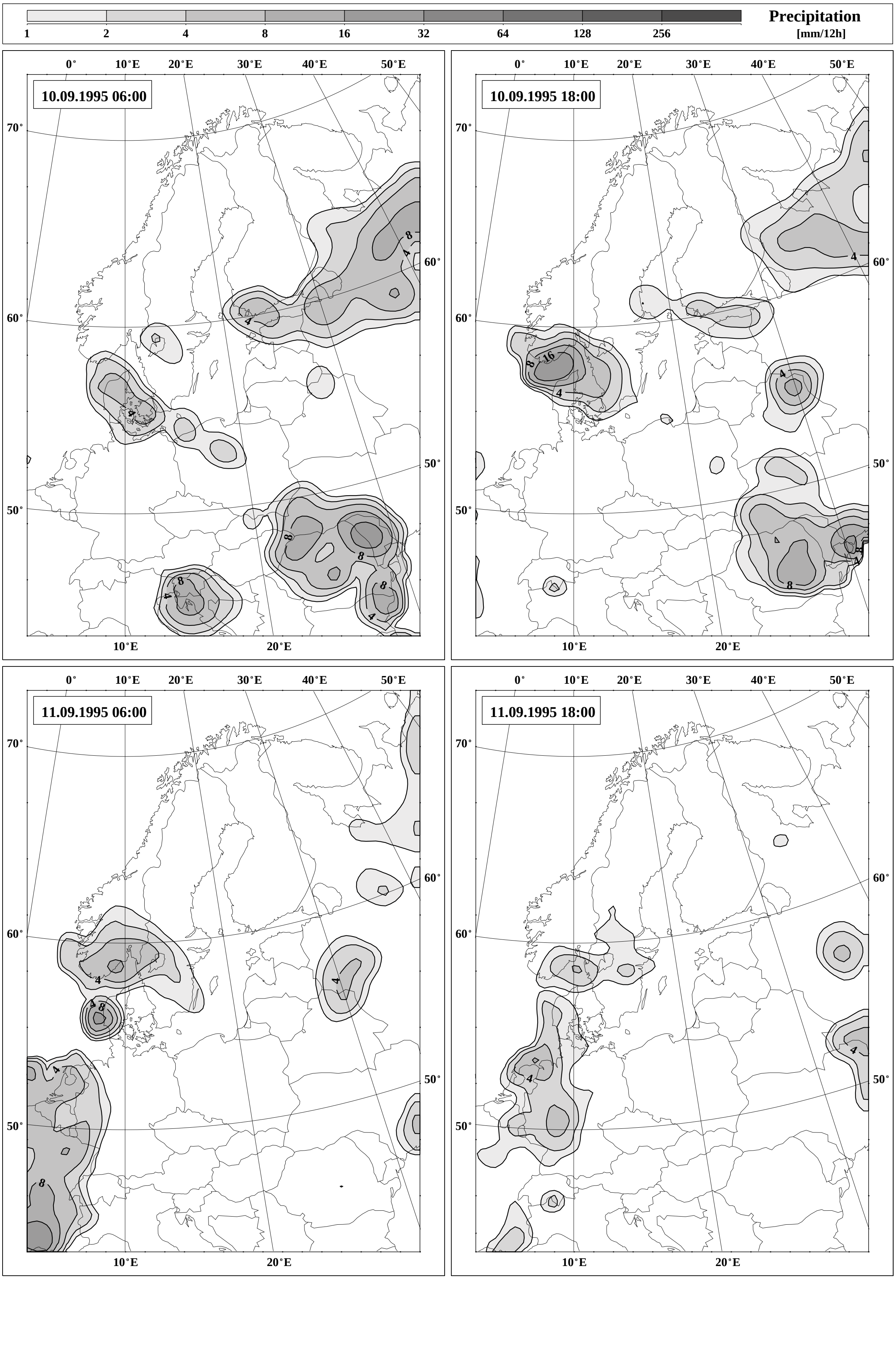
Precipitation
[mm/12h]
1 2 4 8 16 32 64 128 256
10.09.1995 06:00
10.09.1995 18:00
11.09.1995 06:00
11.09.1995 18:00
0° 10°E 20°E 30°E 40°E 50°E
70° 60° 50°
10°E 20°E

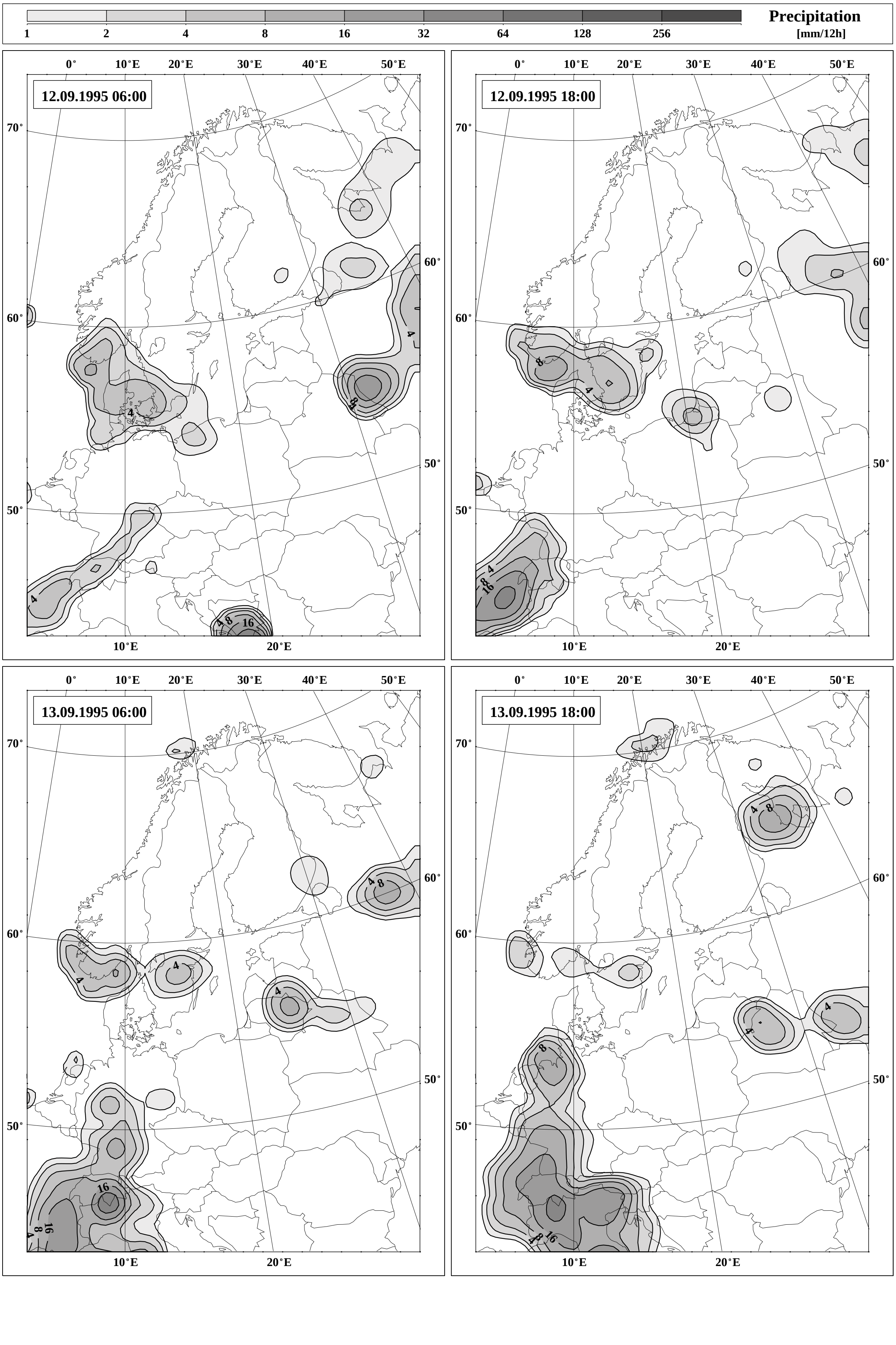

1 2 4 8 16 32 64 128 256
Precipitation
[mm/12h]
12.09.1995 06:00
12.09.1995 18:00
13.09.1995 06:00
13.09.1995 18:00
0° 10°E 20°E 30°E 40°E 50°E
70°
60°
50°
10°E 20°E

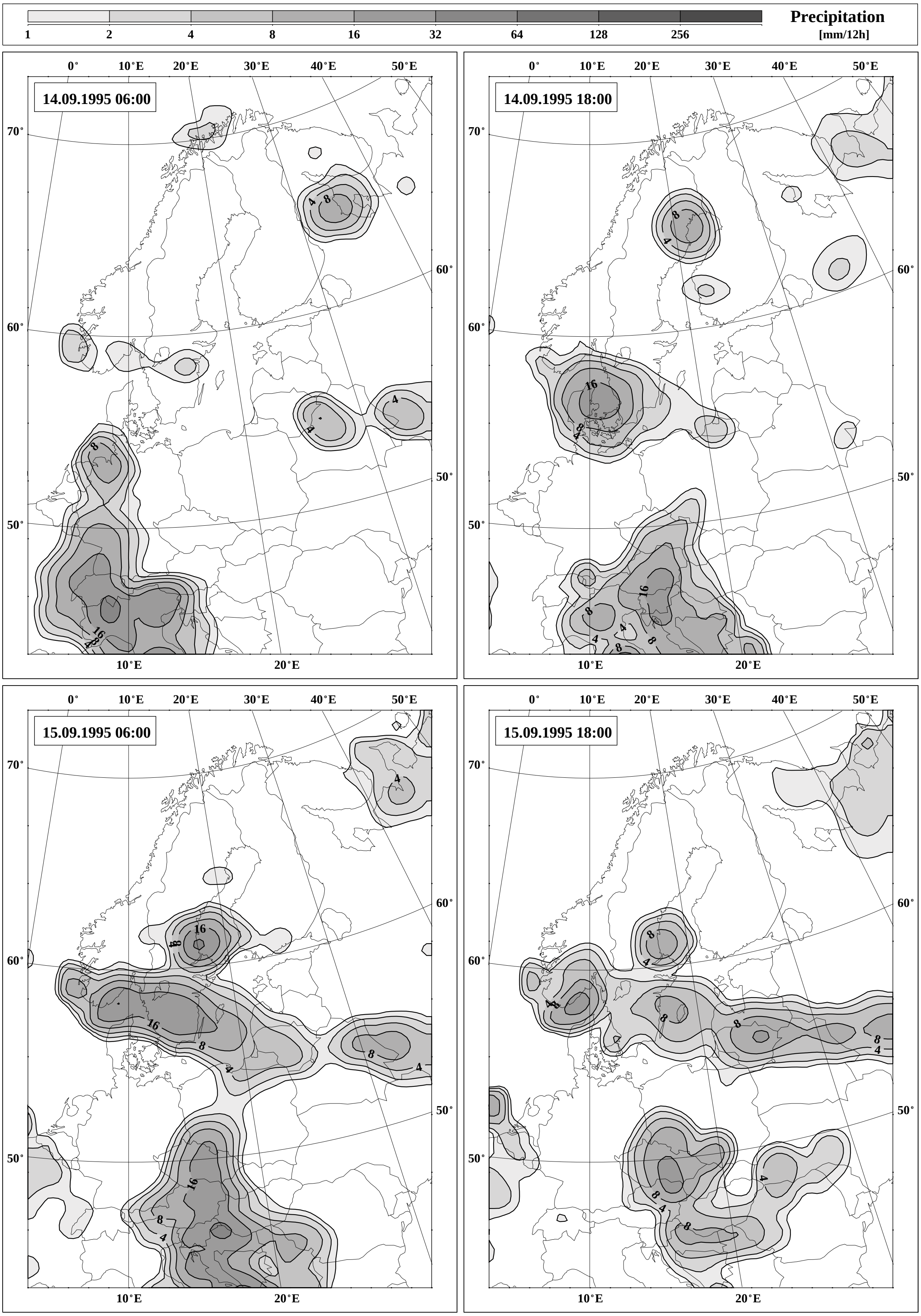

Precipitation
[mm/12h]
1 2 4 8 16 32 64 128 256
14.09.1995 06:00
14.09.1995 18:00
15.09.1995 06:00
15.09.1995 18:00
0° 10°E 20°E 30°E 40°E 50°E
70° 60° 50°
10°E 20°E

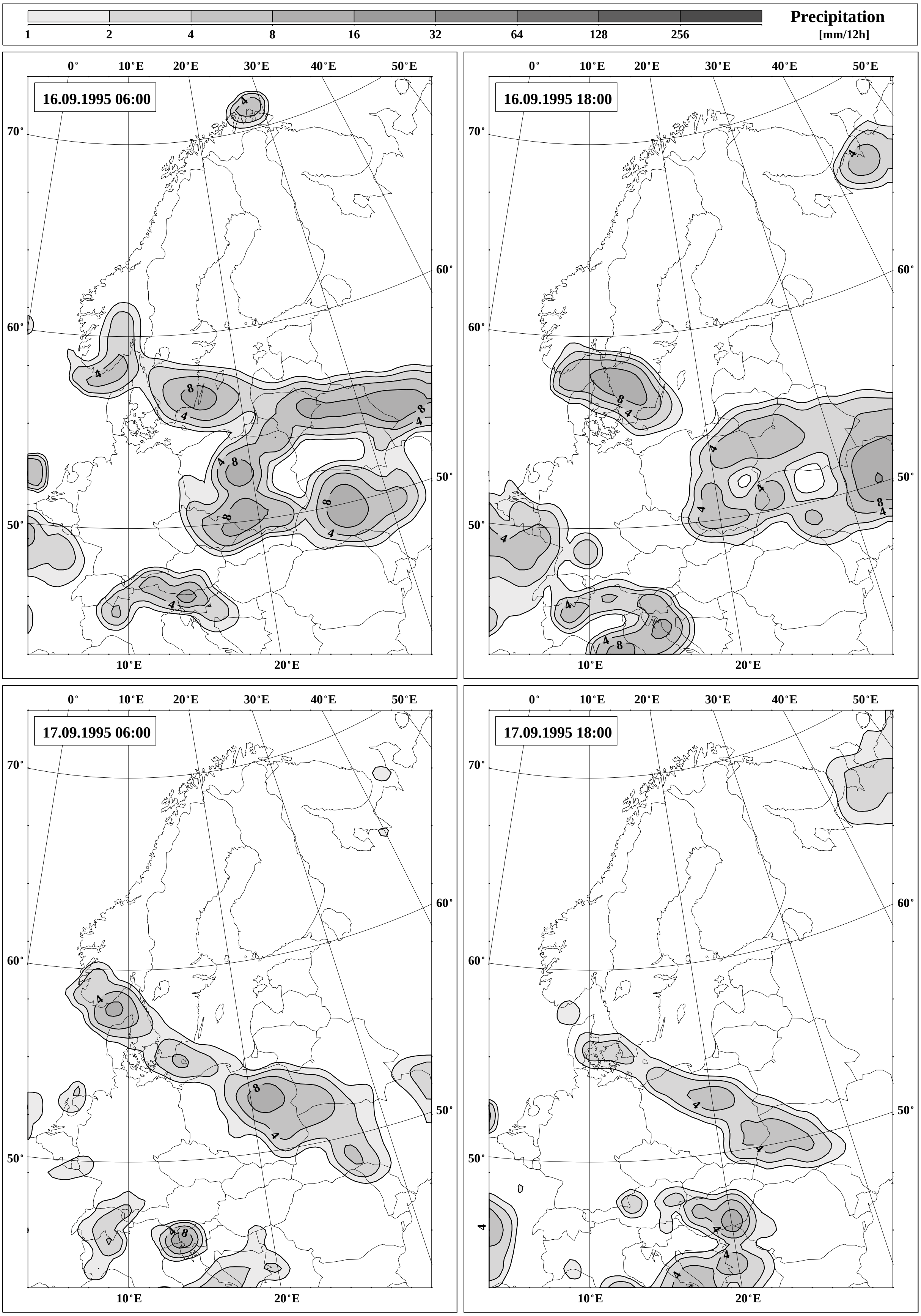
Precipitation
[mm/12h]
1 2 4 8 16 32 64 128 256
16.09.1995 06:00
16.09.1995 18:00
17.09.1995 06:00
17.09.1995 18:00
0° 10°E 20°E 30°E 40°E 50°E
70° 60° 50°
10°E 20°E

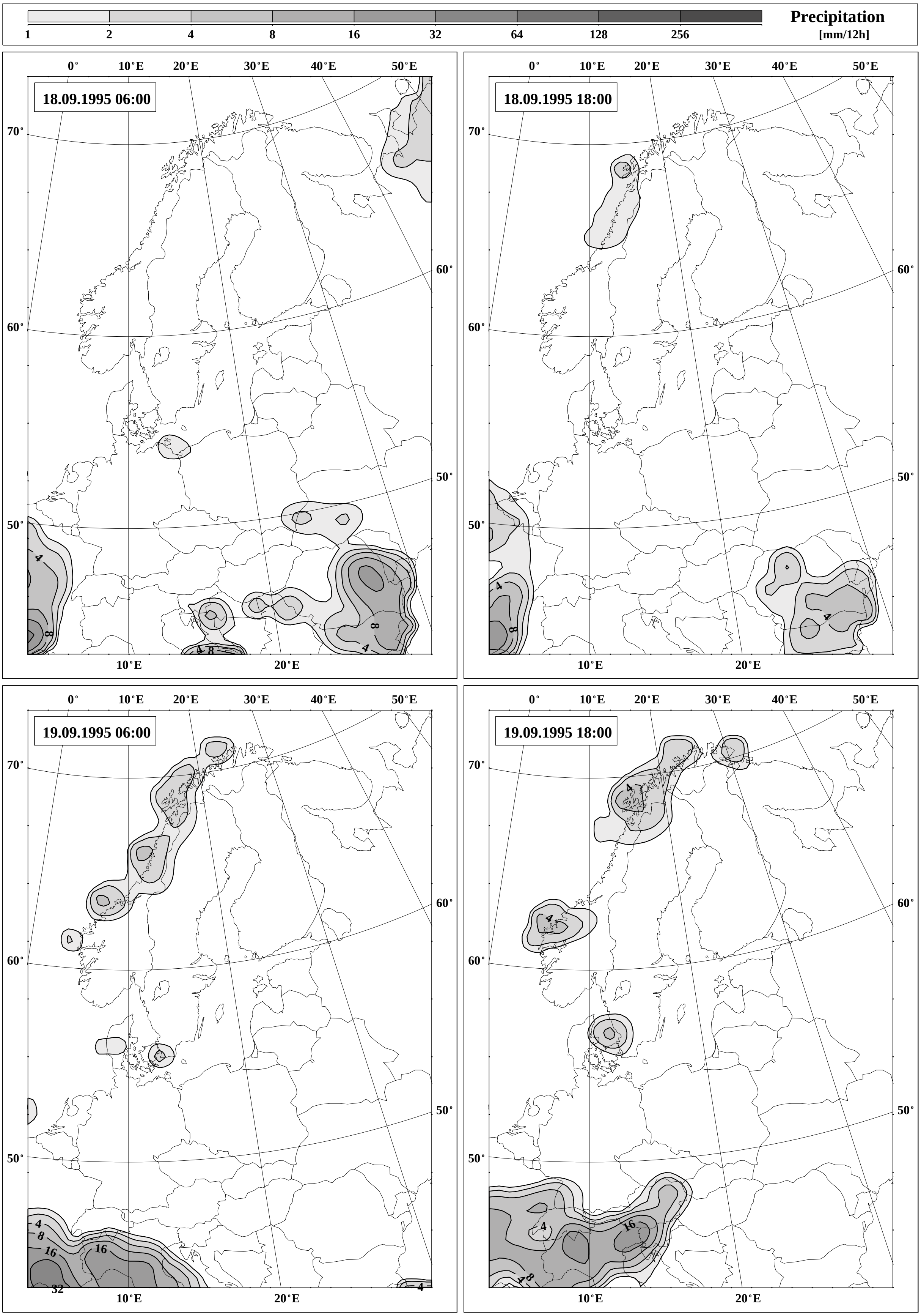
Precipitation
[mm/12h]
1
2
4
8
16
32
64
128
256
18.09.1995 06:00
18.09.1995 18:00
19.09.1995 06:00
19.09.1995 18:00
0°
10°E
20°E
30°E
40°E
50°E
70°
60°
50°

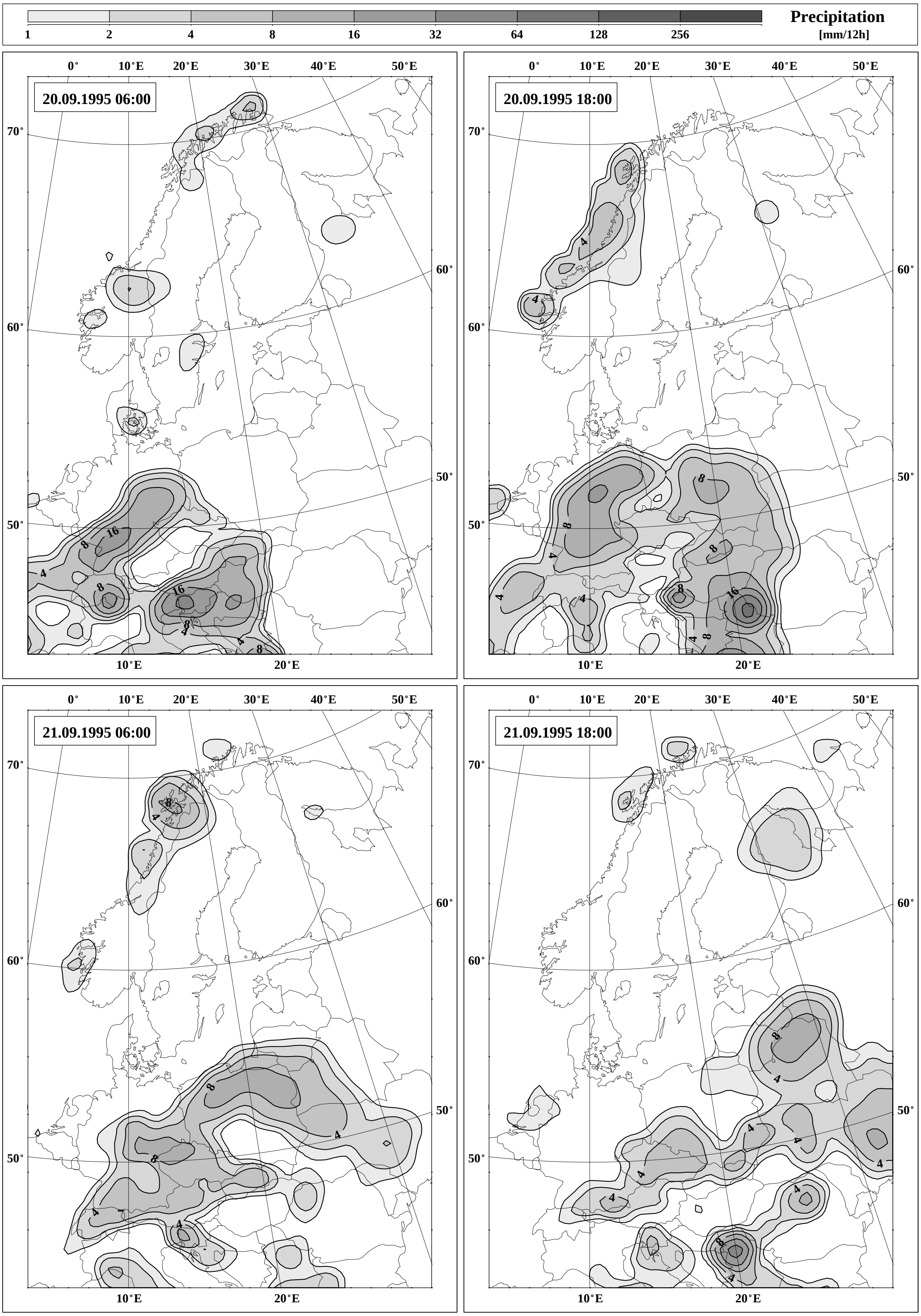
1 2 4 8 16 32 64 128 256
Precipitation
[mm/12h]
20.09.1995 06:00
20.09.1995 18:00
21.09.1995 06:00
21.09.1995 18:00
0° 10°E 20°E 30°E 40°E 50°E
70°
60°
50°
10°E 20°E

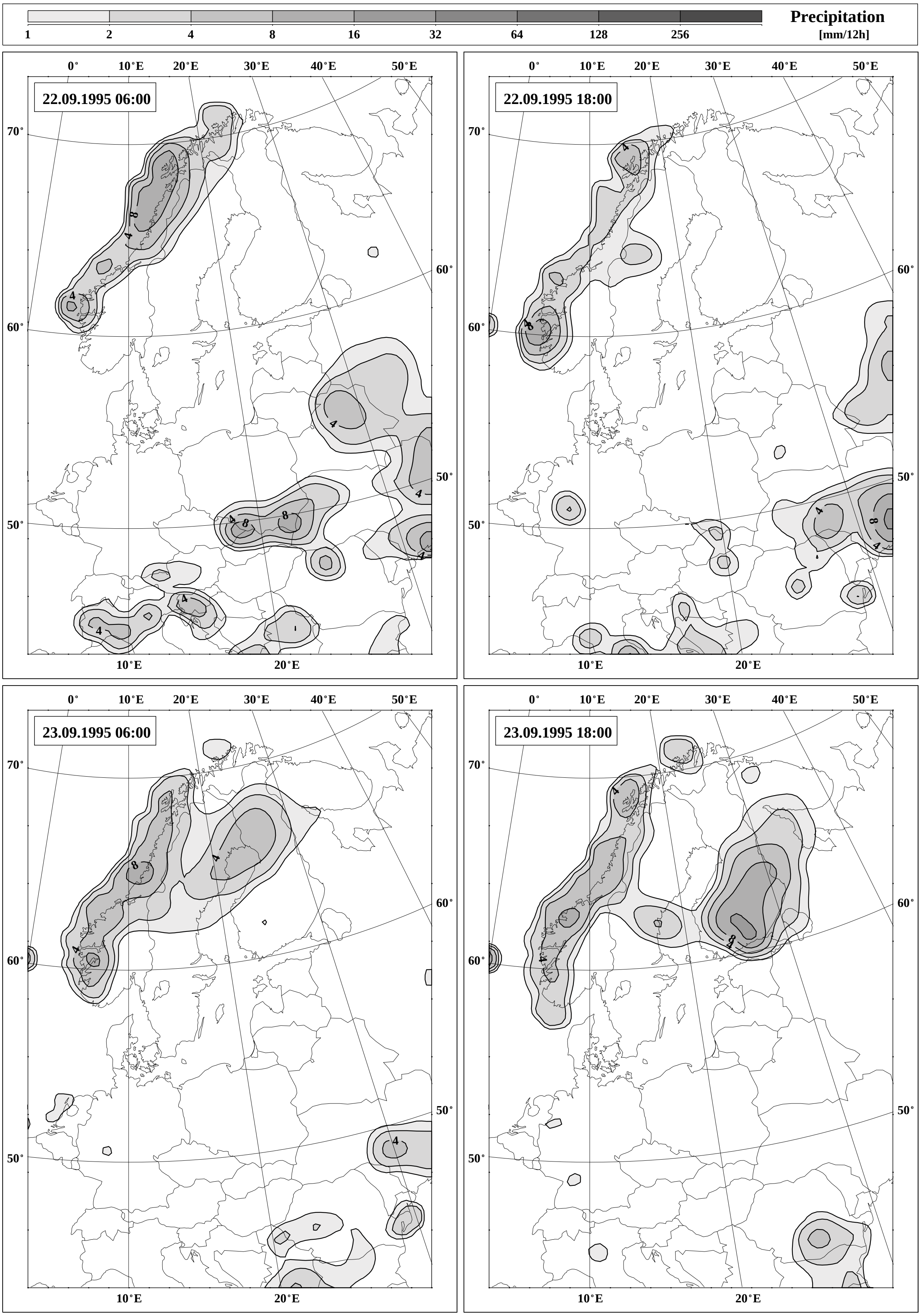
Precipitation
[mm/12h]
1 2 4 8 16 32 64 128 256
22.09.1995 06:00
22.09.1995 18:00
23.09.1995 06:00
23.09.1995 18:00
0° 10°E 20°E 30°E 40°E 50°E
70° 60° 50°
10°E 20°E

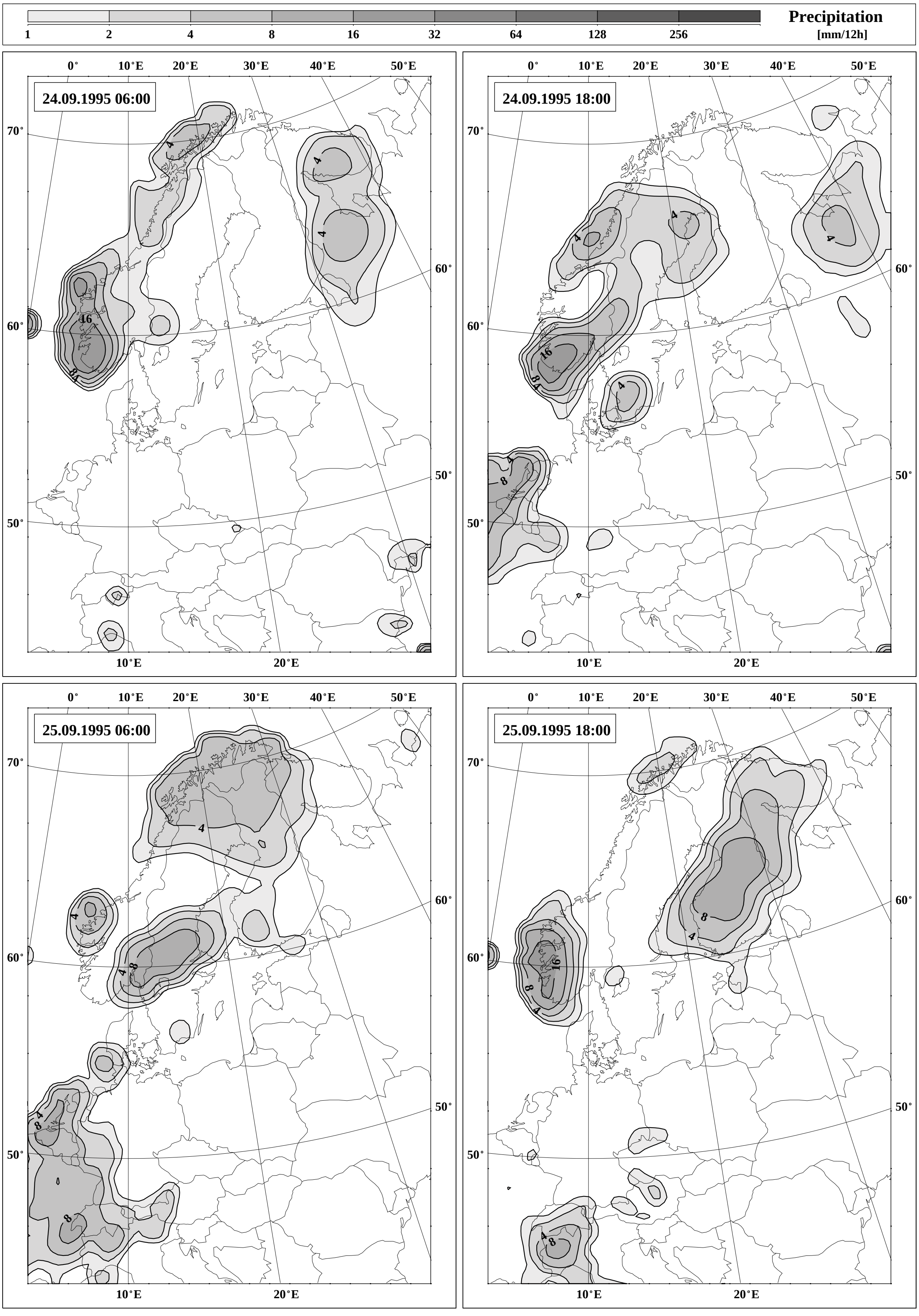
Precipitation
[mm/12h]
1
2
4
8
16
32
64
128
256
24.09.1995 06:00
24.09.1995 18:00
25.09.1995 06:00
25.09.1995 18:00
0°
10°E
20°E
30°E
40°E
50°E
70°
60°
50°

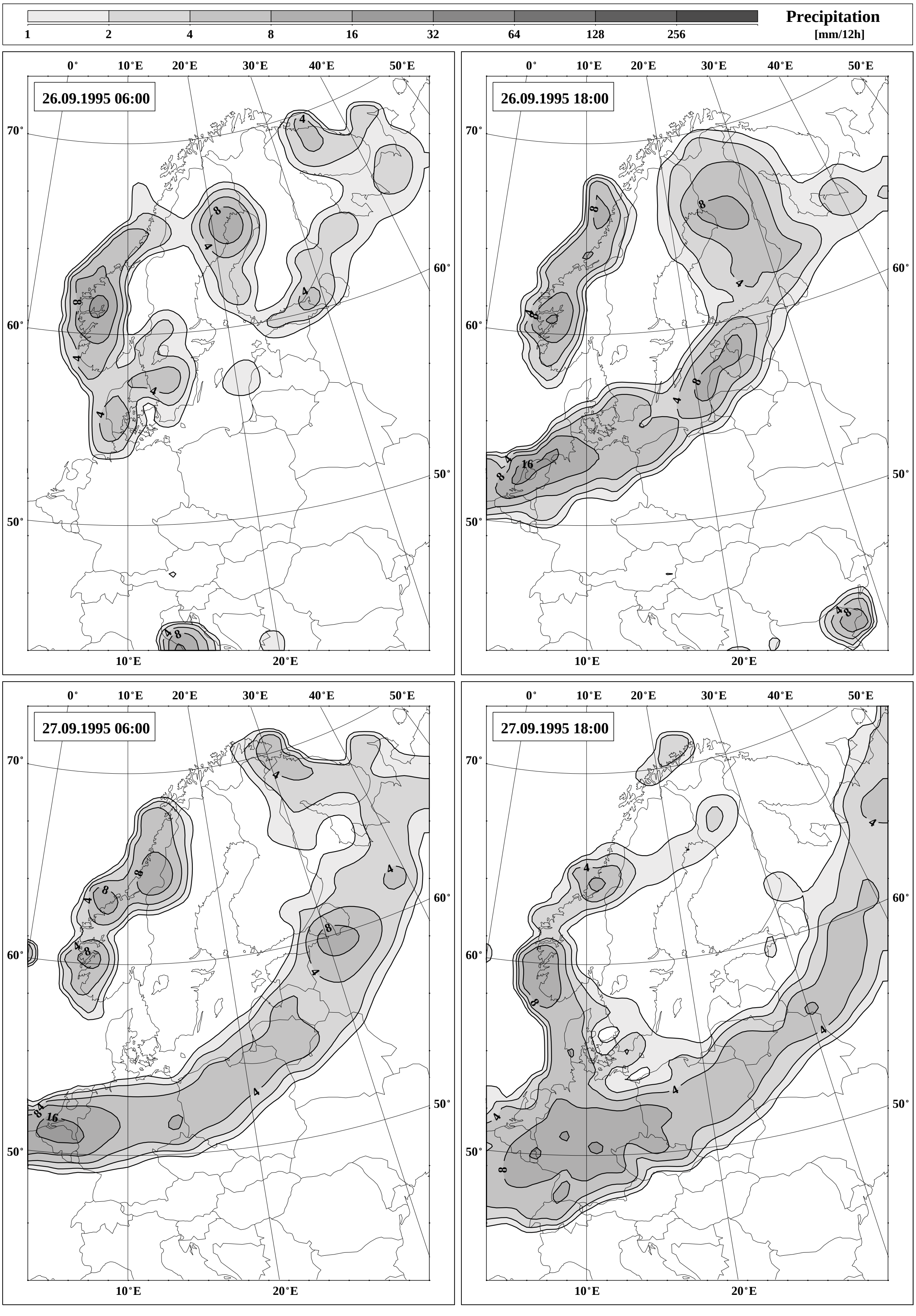
Precipitation
[mm/12h]
1
2
4
8
16
32
64
128
256
26.09.1995 06:00
26.09.1995 18:00
27.09.1995 06:00
27.09.1995 18:00
0°
10°E
20°E
30°E
40°E
50°E
70°
60°
50°
10°E
20°E

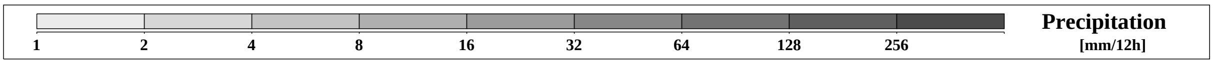
1
2
4
8
16
32
64
128
256
Precipitation
[mm/12h]

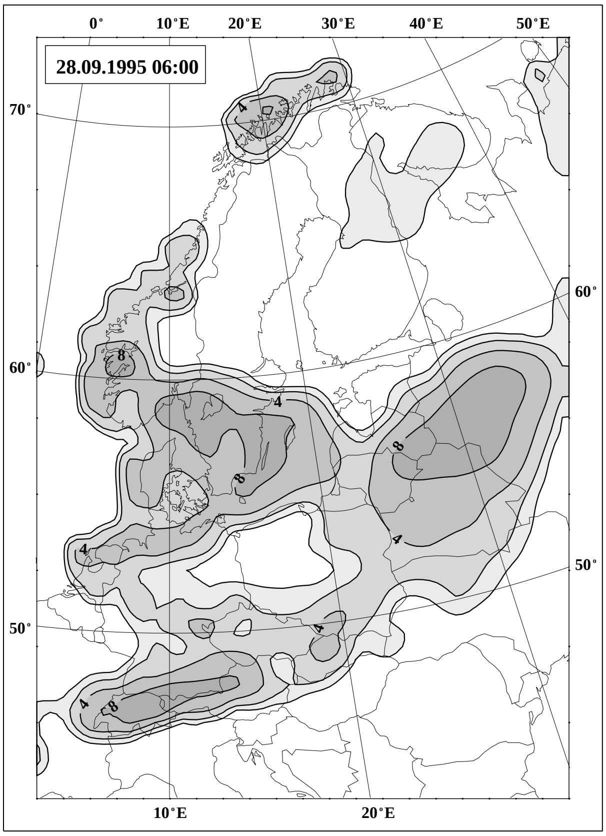
28.09.1995 06:00
0°
10°E
20°E
30°E
40°E
50°E
70°
60°
50°
60°
50°
10°E
20°E

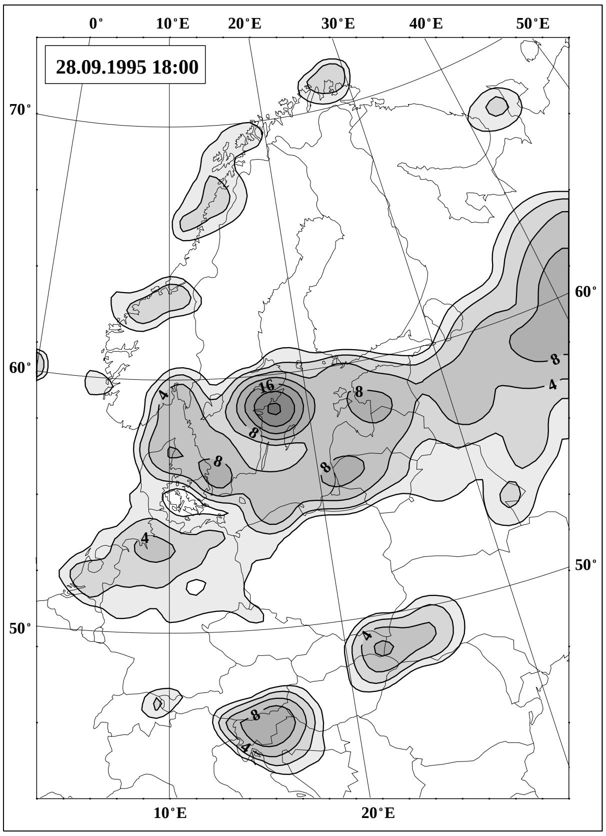
28.09.1995 18:00
0°
10°E
20°E
30°E
40°E
50°E
70°
60°
50°
60°
50°
10°E
20°E

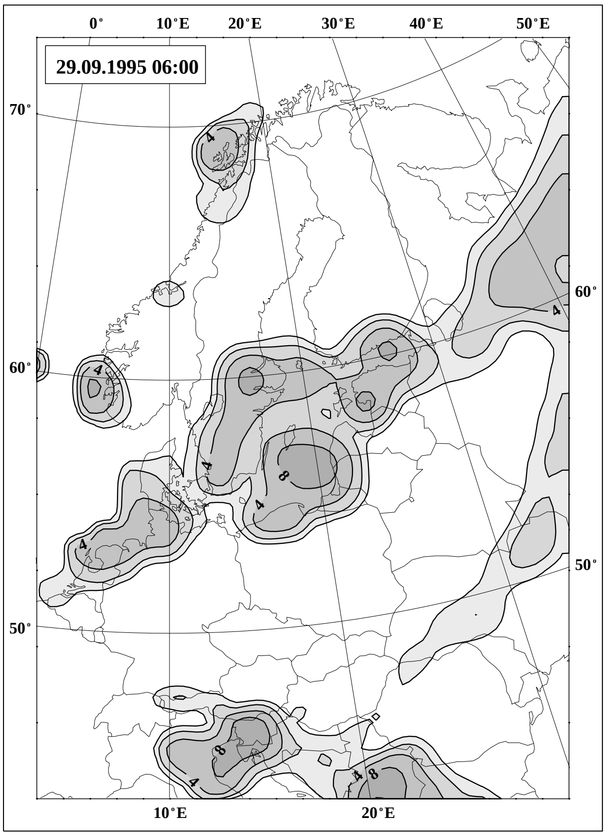
29.09.1995 06:00
0°
10°E
20°E
30°E
40°E
50°E
70°
60°
50°
60°
50°
10°E
20°E

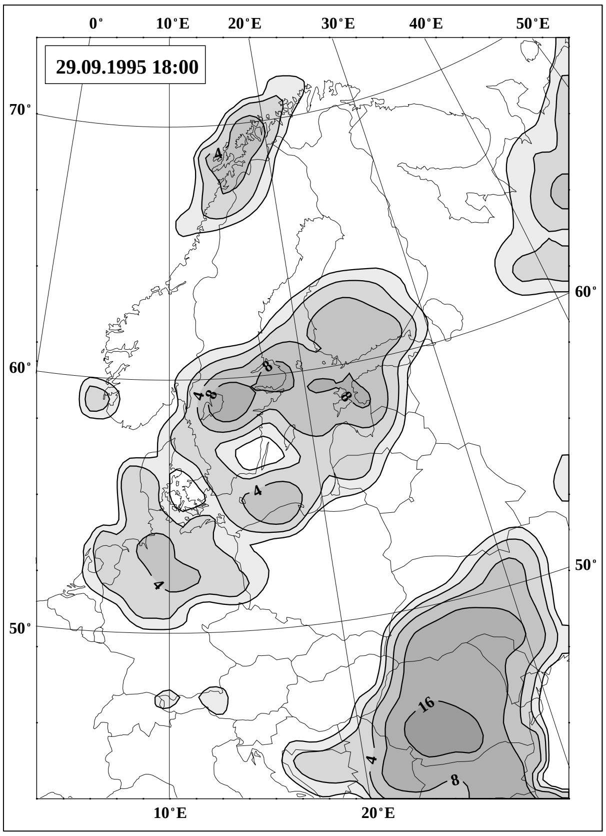
29.09.1995 18:00
0°
10°E
20°E
30°E
40°E
50°E
70°
60°
50°
60°
50°
10°E
20°E

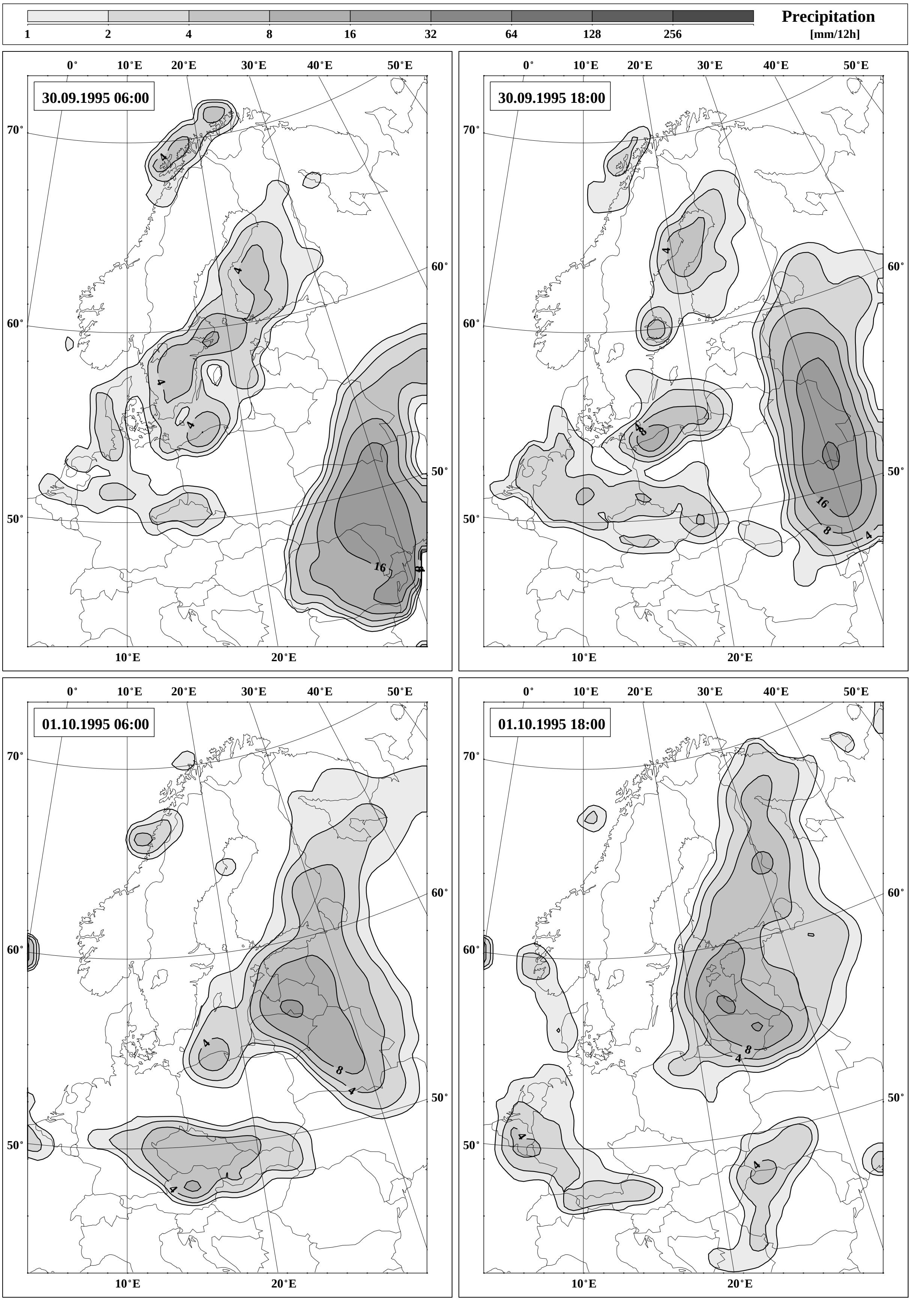
Precipitation
[mm/12h]
1
2
4
8
16
32
64
128
256
30.09.1995 06:00
30.09.1995 18:00
01.10.1995 06:00
01.10.1995 18:00
0°
10°E
20°E
30°E
40°E
50°E
70°
60°
50°

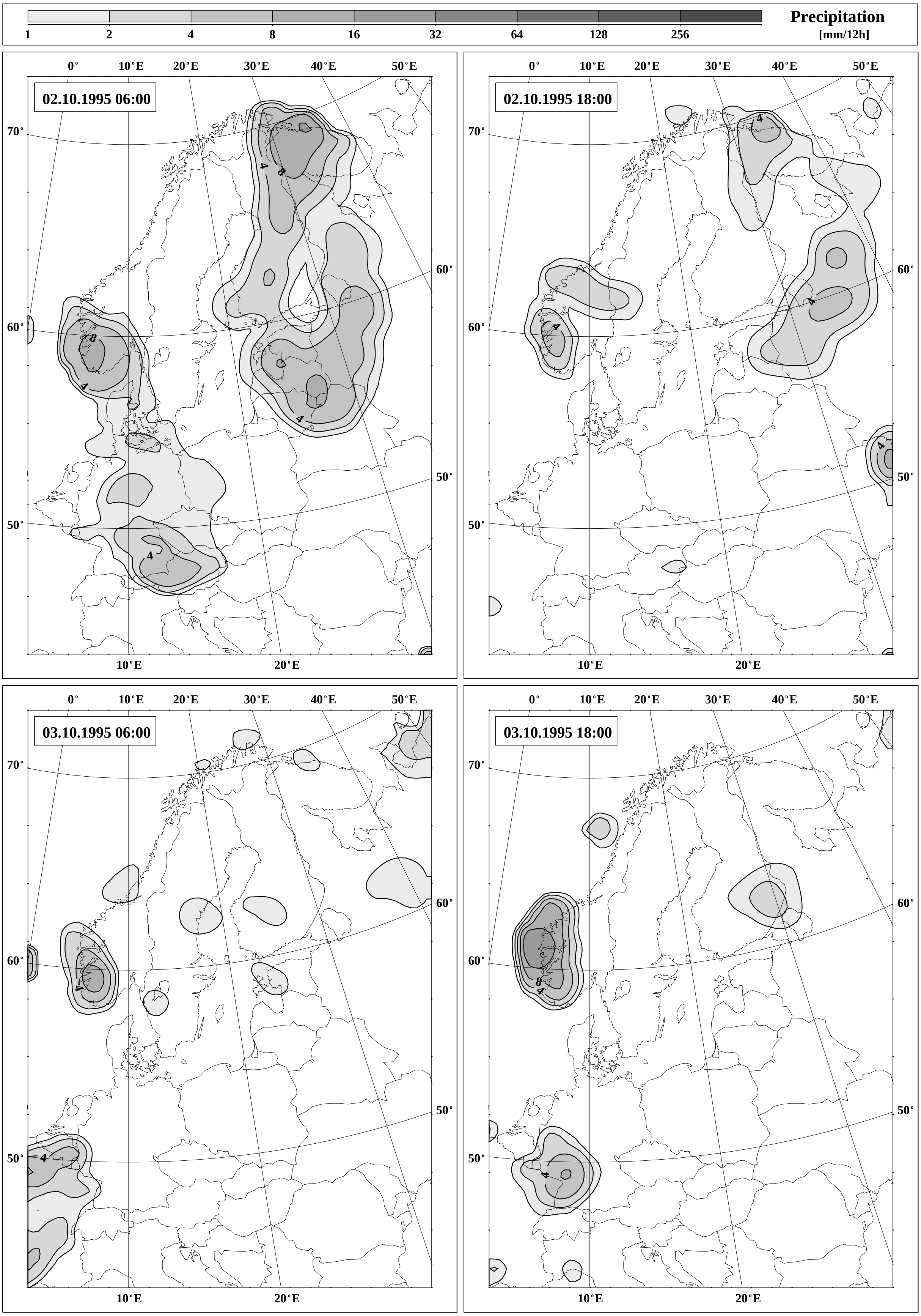
Precipitation
[mm/12h]
1
2
4
8
16
32
64
128
256
02.10.1995 06:00
02.10.1995 18:00
03.10.1995 06:00
03.10.1995 18:00
0°
10°E
20°E
30°E
40°E
50°E
70°
60°
50°

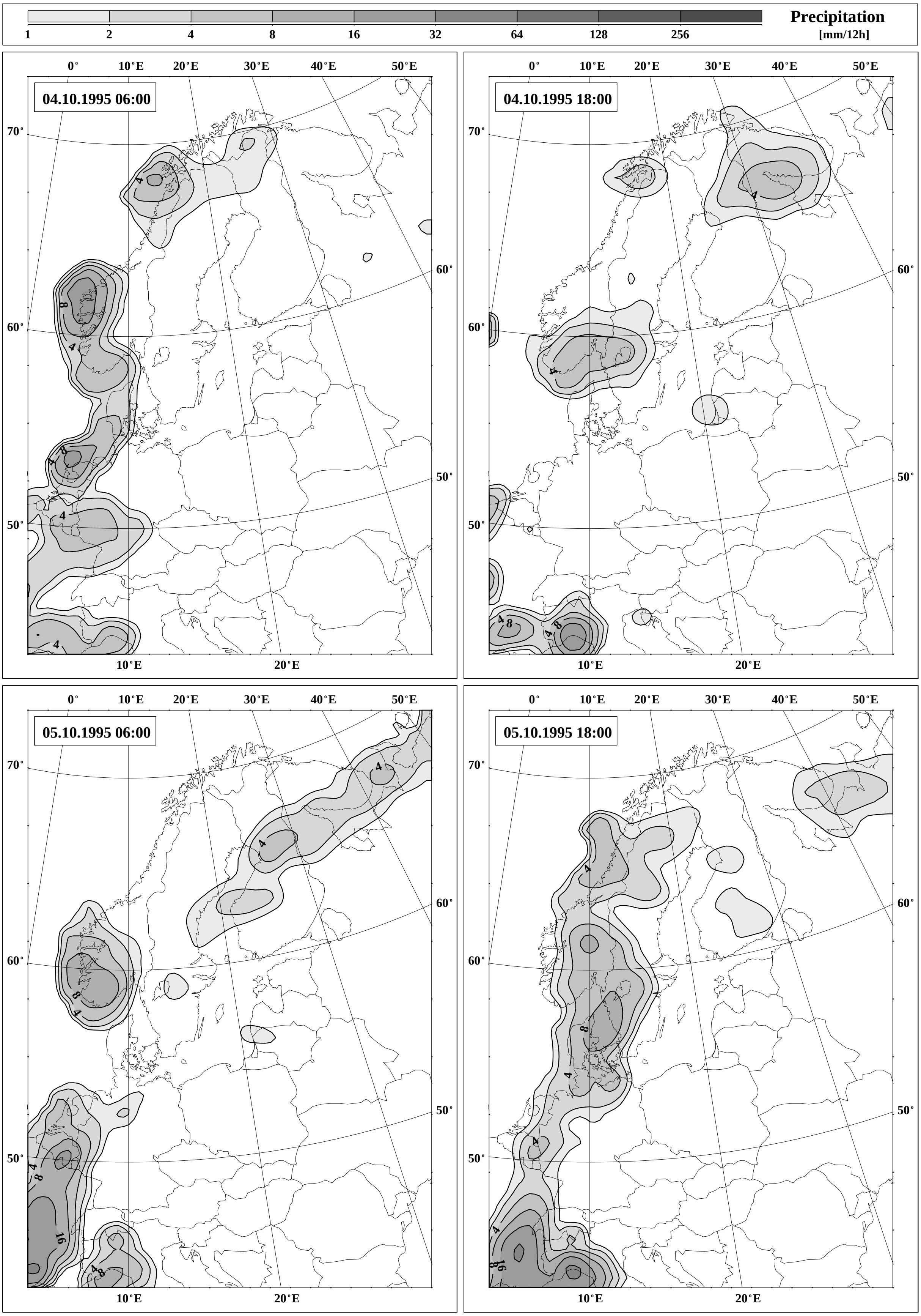
Precipitation
[mm/12h]
1 2 4 8 16 32 64 128 256
04.10.1995 06:00
04.10.1995 18:00
05.10.1995 06:00
05.10.1995 18:00
0° 10°E 20°E 30°E 40°E 50°E
70° 60° 50°
10°E 20°E

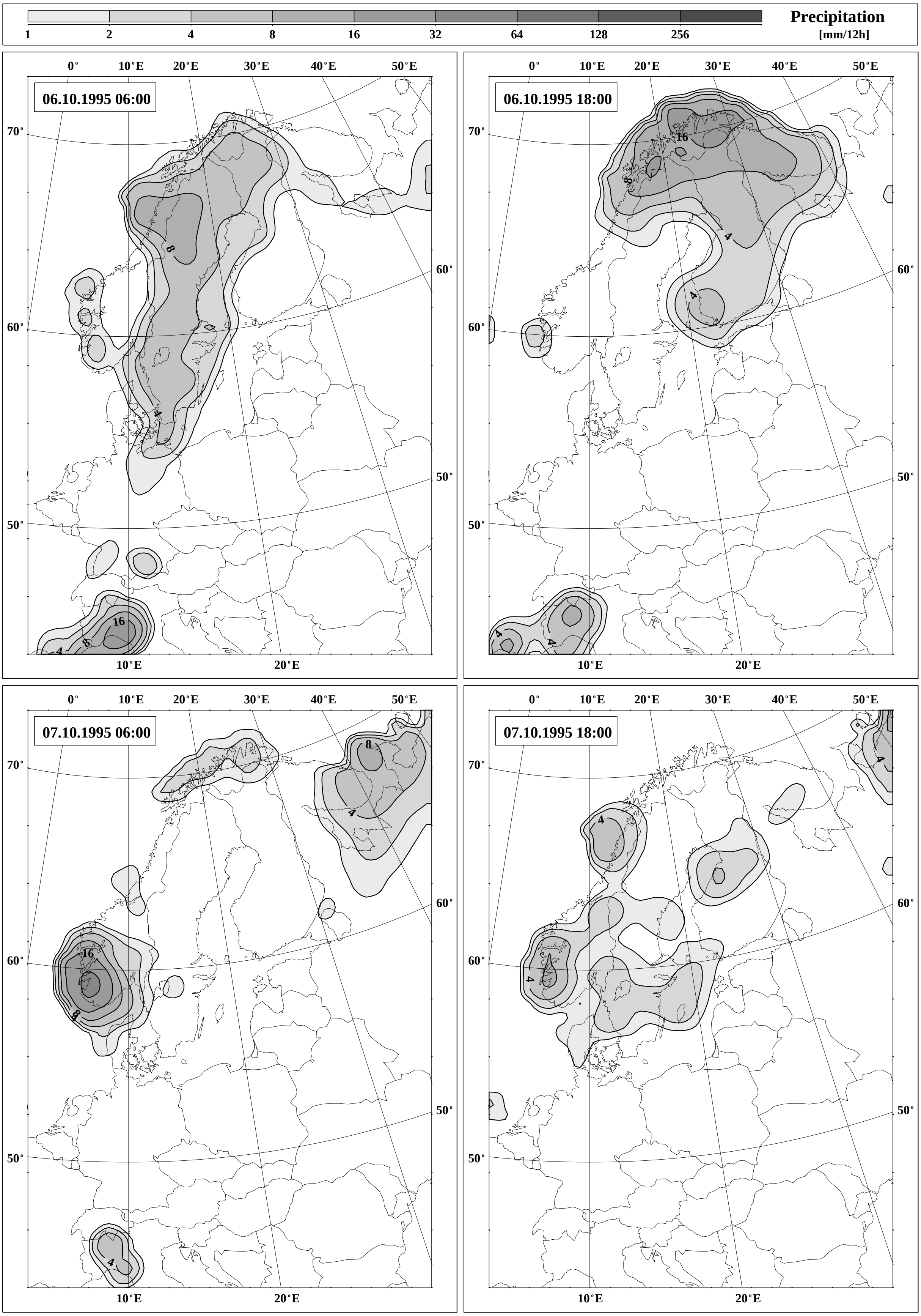
1
2
4
8
16
32
64
128
256
Precipitation
[mm/12h]
06.10.1995 06:00
06.10.1995 18:00
07.10.1995 06:00
07.10.1995 18:00
0°
10°E
20°E
30°E
40°E
50°E
70°
60°
50°

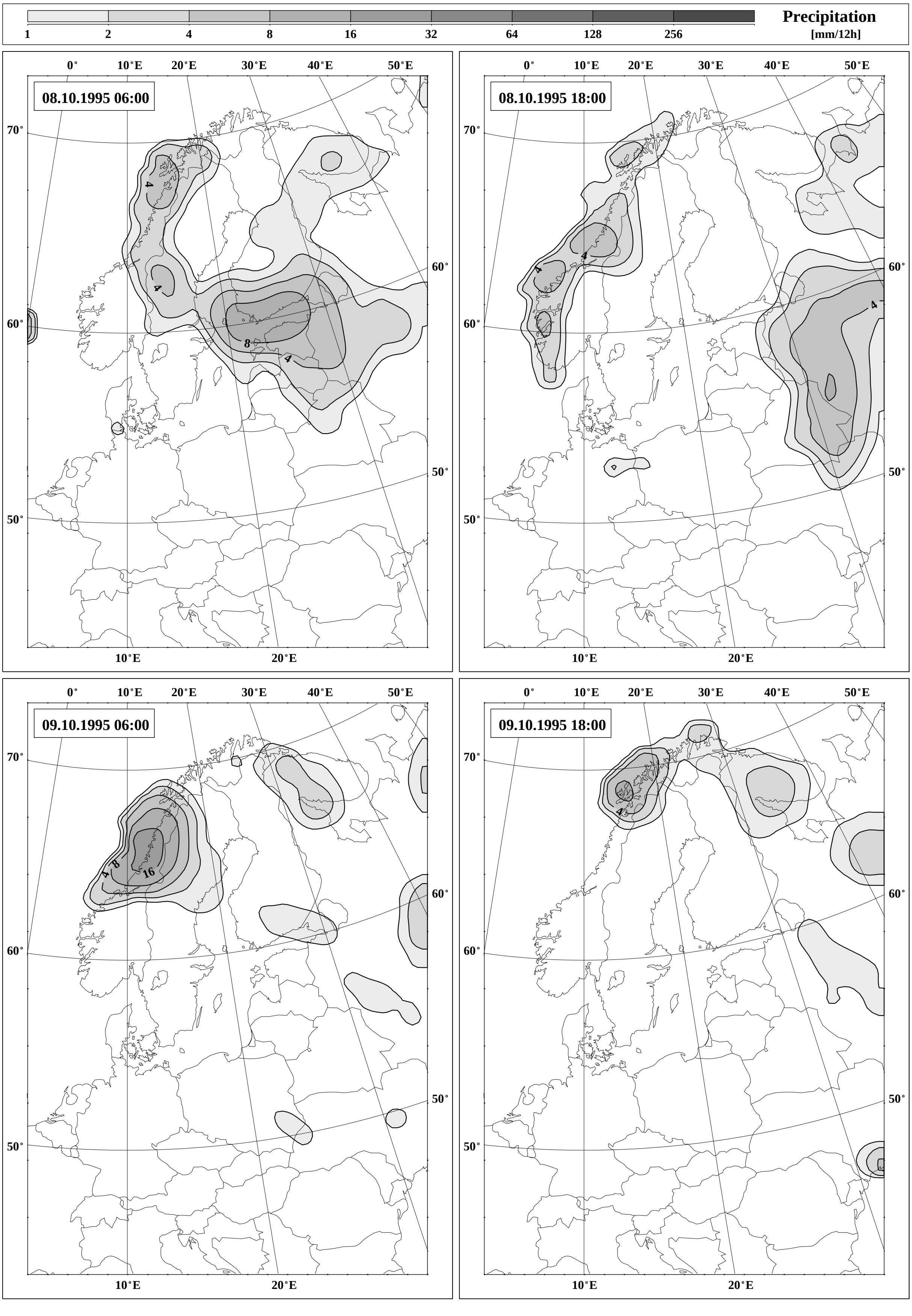
Precipitation
[mm/12h]
1
2
4
8
16
32
64
128
256
08.10.1995 06:00
08.10.1995 18:00
09.10.1995 06:00
09.10.1995 18:00
0°
10°E
20°E
30°E
40°E
50°E
70°
60°
50°

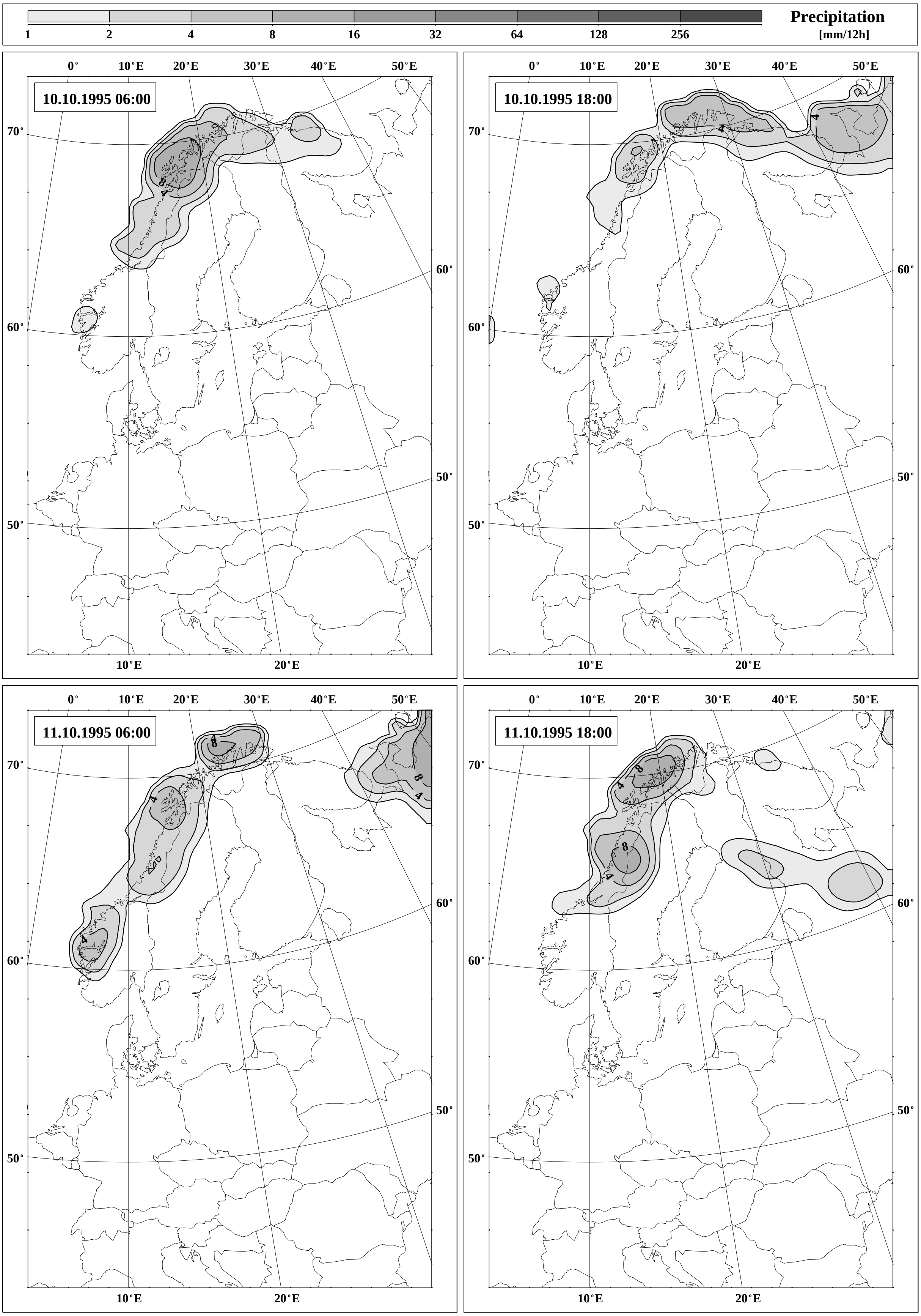
Precipitation
[mm/12h]
1
2
4
8
16
32
64
128
256
10.10.1995 06:00
10.10.1995 18:00
11.10.1995 06:00
11.10.1995 18:00
0°
10°E
20°E
30°E
40°E
50°E
70°
60°
50°

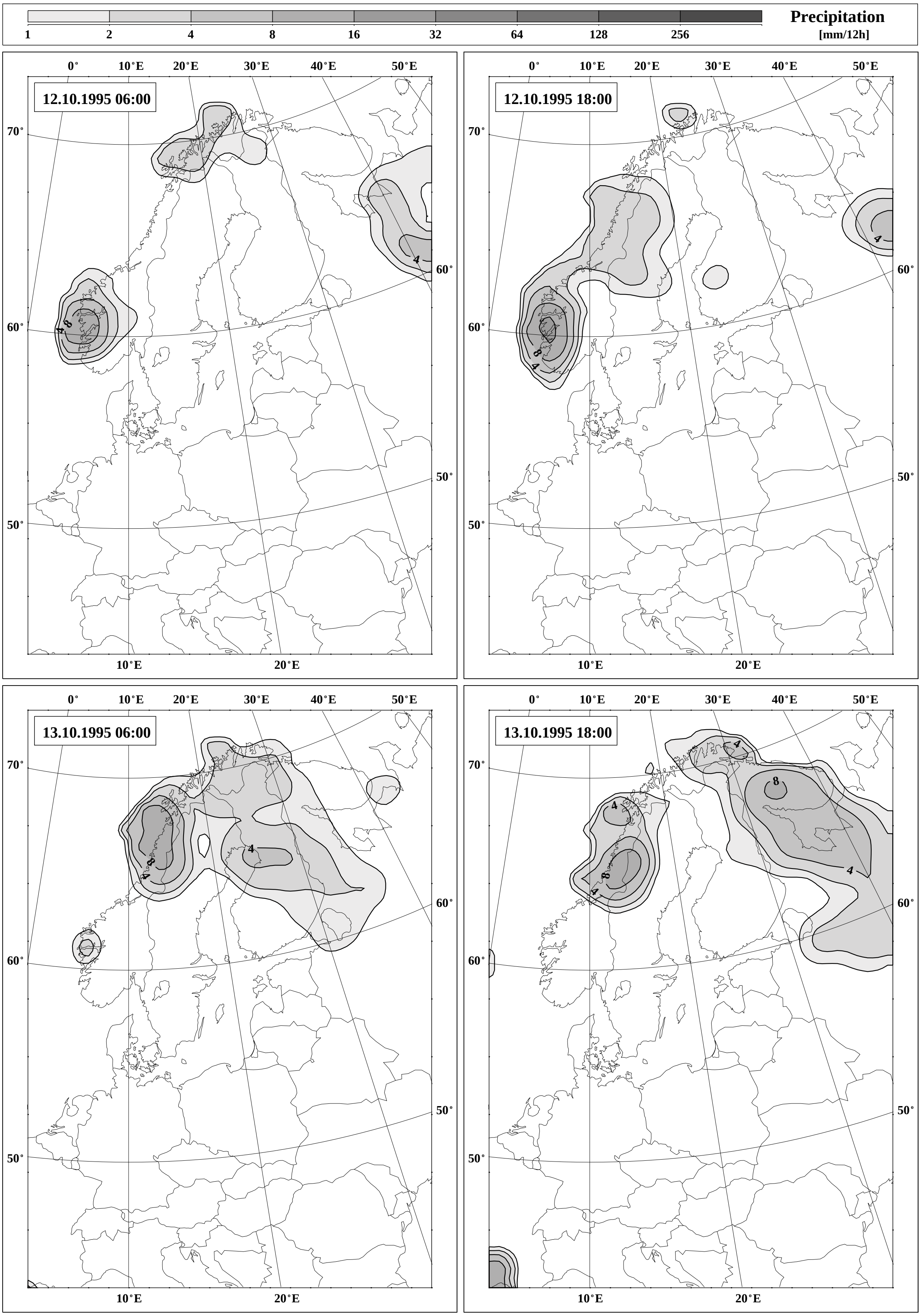
Precipitation
[mm/12h]
1
2
4
8
16
32
64
128
256
12.10.1995 06:00
12.10.1995 18:00
13.10.1995 06:00
13.10.1995 18:00
0°
10°E
20°E
30°E
40°E
50°E
70°
60°
50°

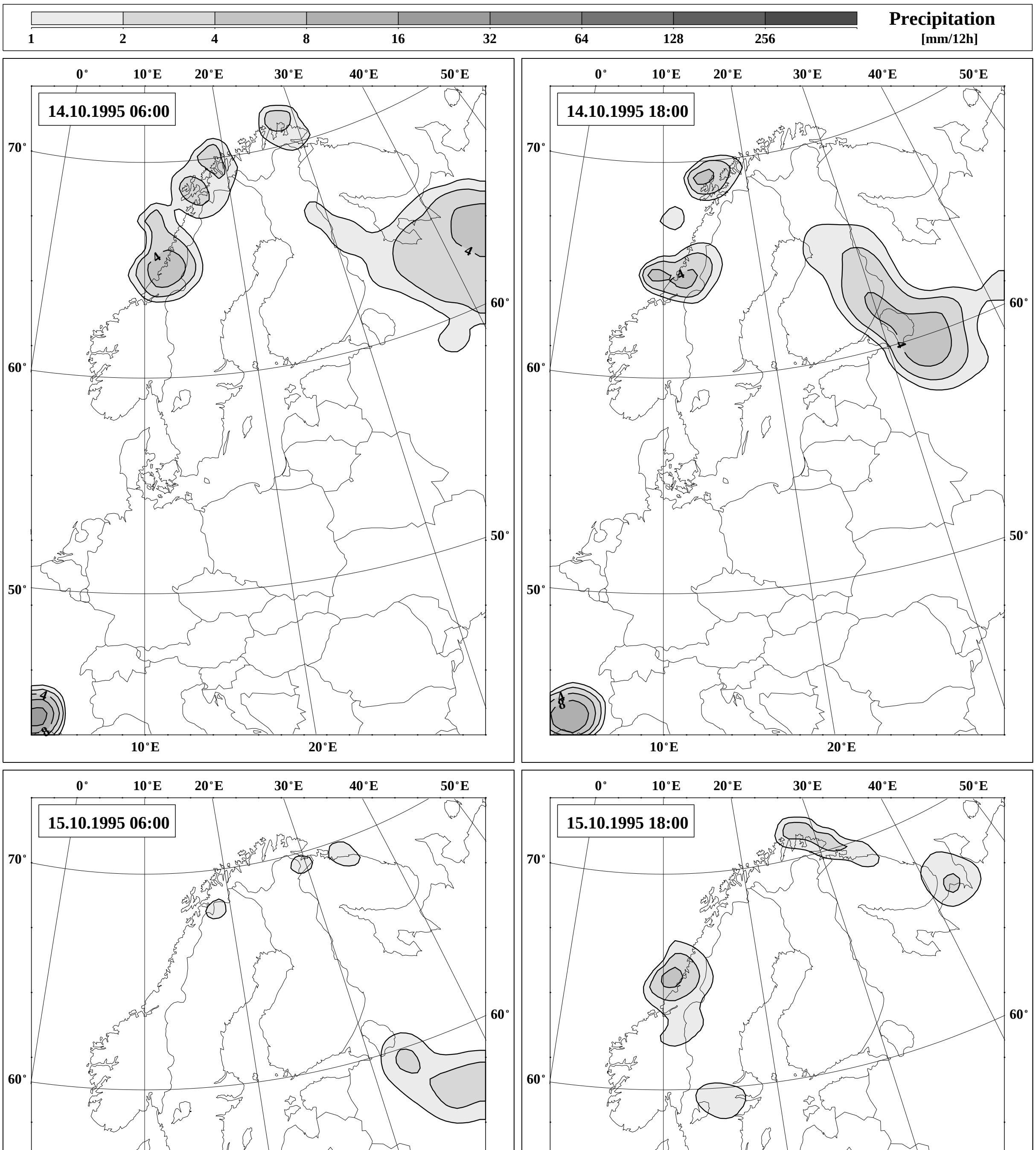
1 2 4 8 16 32 64 128 256
Precipitation
[mm/12h]
14.10.1995 06:00
14.10.1995 18:00
15.10.1995 06:00
15.10.1995 18:00
0° 10°E 20°E 30°E 40°E 50°E
70°
60°
50°
10°E 20°E

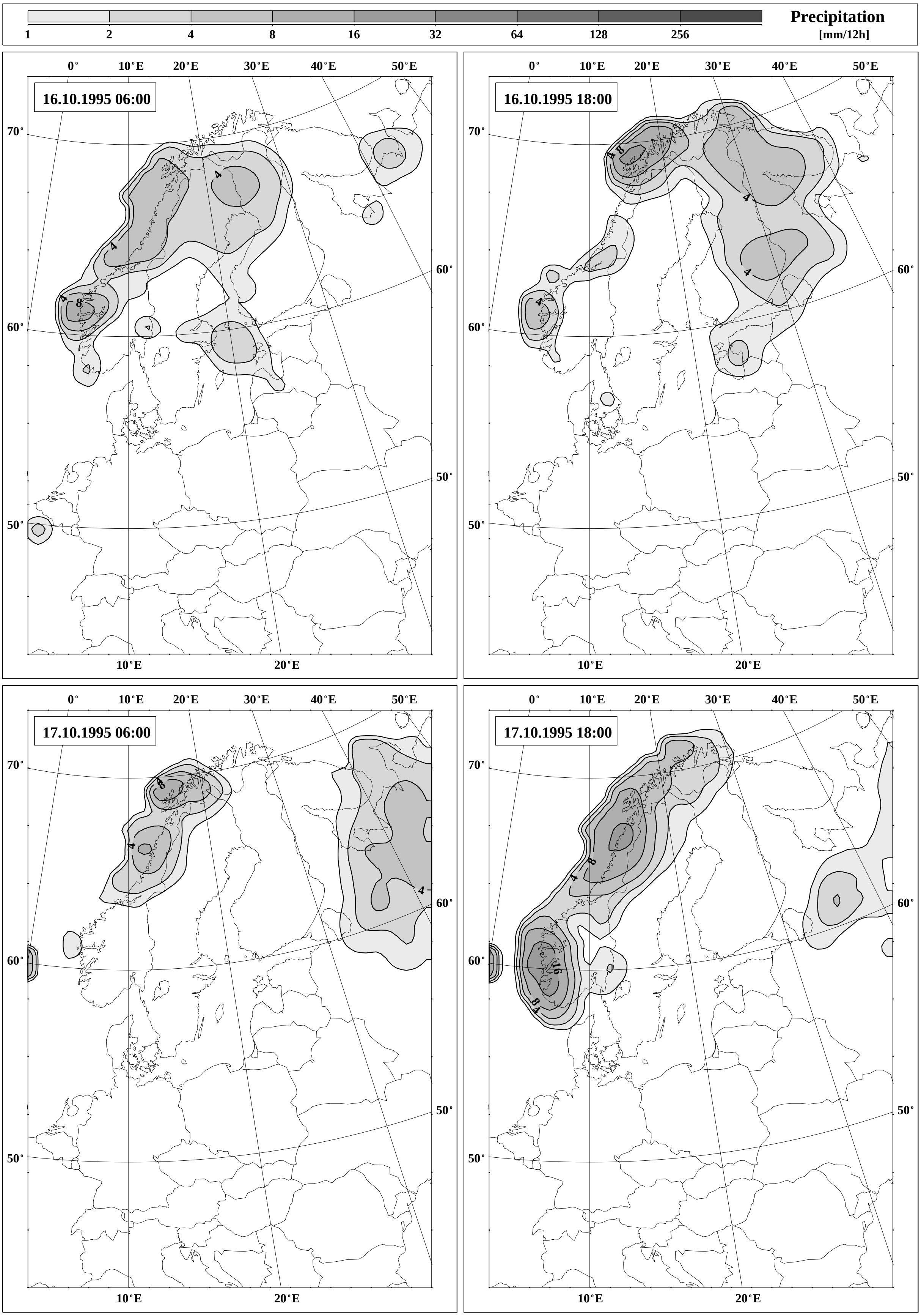
Precipitation
[mm/12h]
1
2
4
8
16
32
64
128
256
16.10.1995 06:00
16.10.1995 18:00
17.10.1995 06:00
17.10.1995 18:00
0°
10°E
20°E
30°E
40°E
50°E
70°
60°
50°

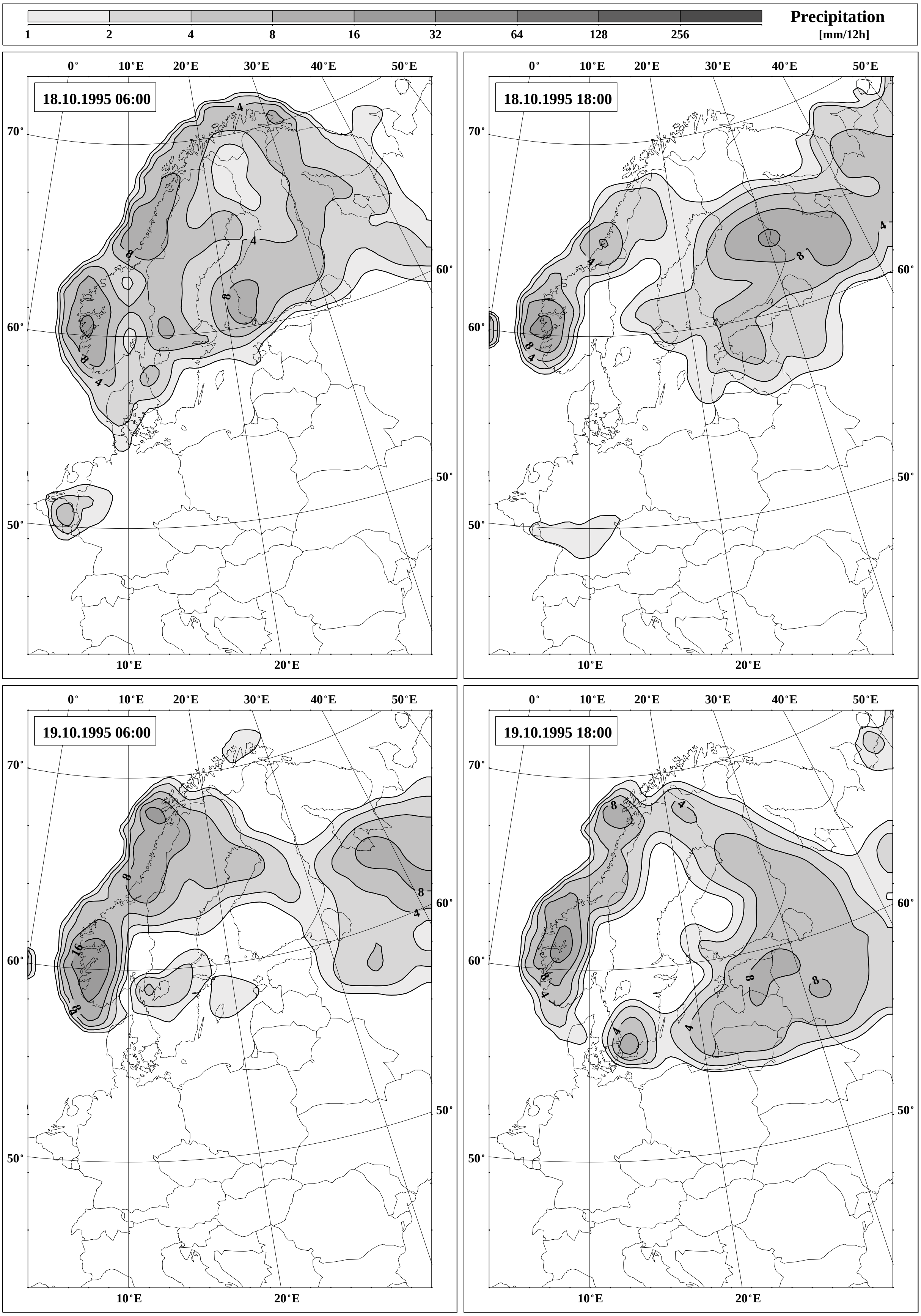
Precipitation
[mm/12h]
1 2 4 8 16 32 64 128 256
18.10.1995 06:00
18.10.1995 18:00
19.10.1995 06:00
19.10.1995 18:00
0° 10°E 20°E 30°E 40°E 50°E
70° 60° 50°
10°E 20°E

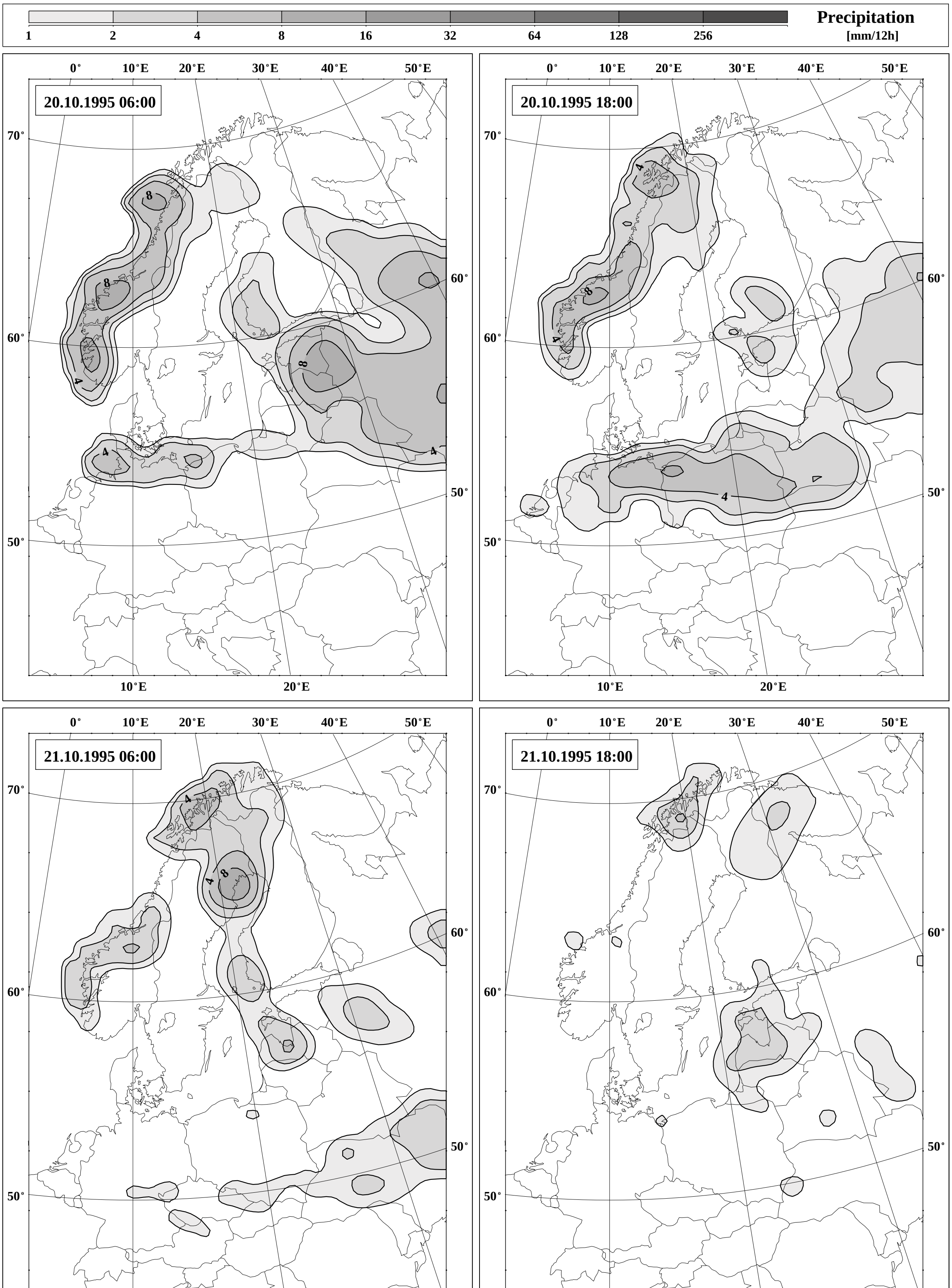
Precipitation
[mm/12h]
1 2 4 8 16 32 64 128 256
20.10.1995 06:00
20.10.1995 18:00
21.10.1995 06:00
21.10.1995 18:00
0° 10°E 20°E 30°E 40°E 50°E
70° 60° 50°
10°E 20°E

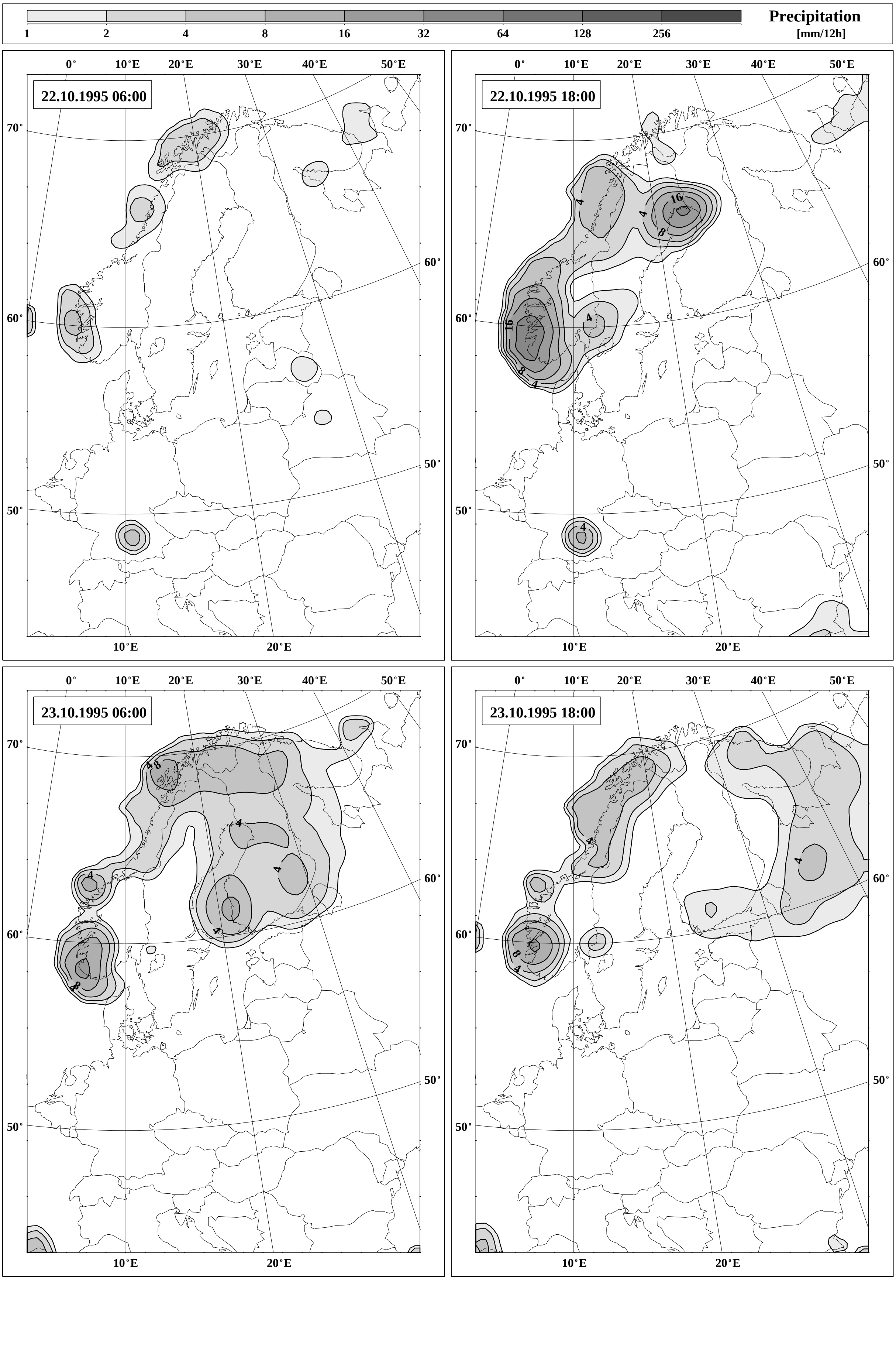
Precipitation
[mm/12h]
1 2 4 8 16 32 64 128 256
22.10.1995 06:00
22.10.1995 18:00
23.10.1995 06:00
23.10.1995 18:00
0° 10°E 20°E 30°E 40°E 50°E
70° 60° 50°
10°E 20°E

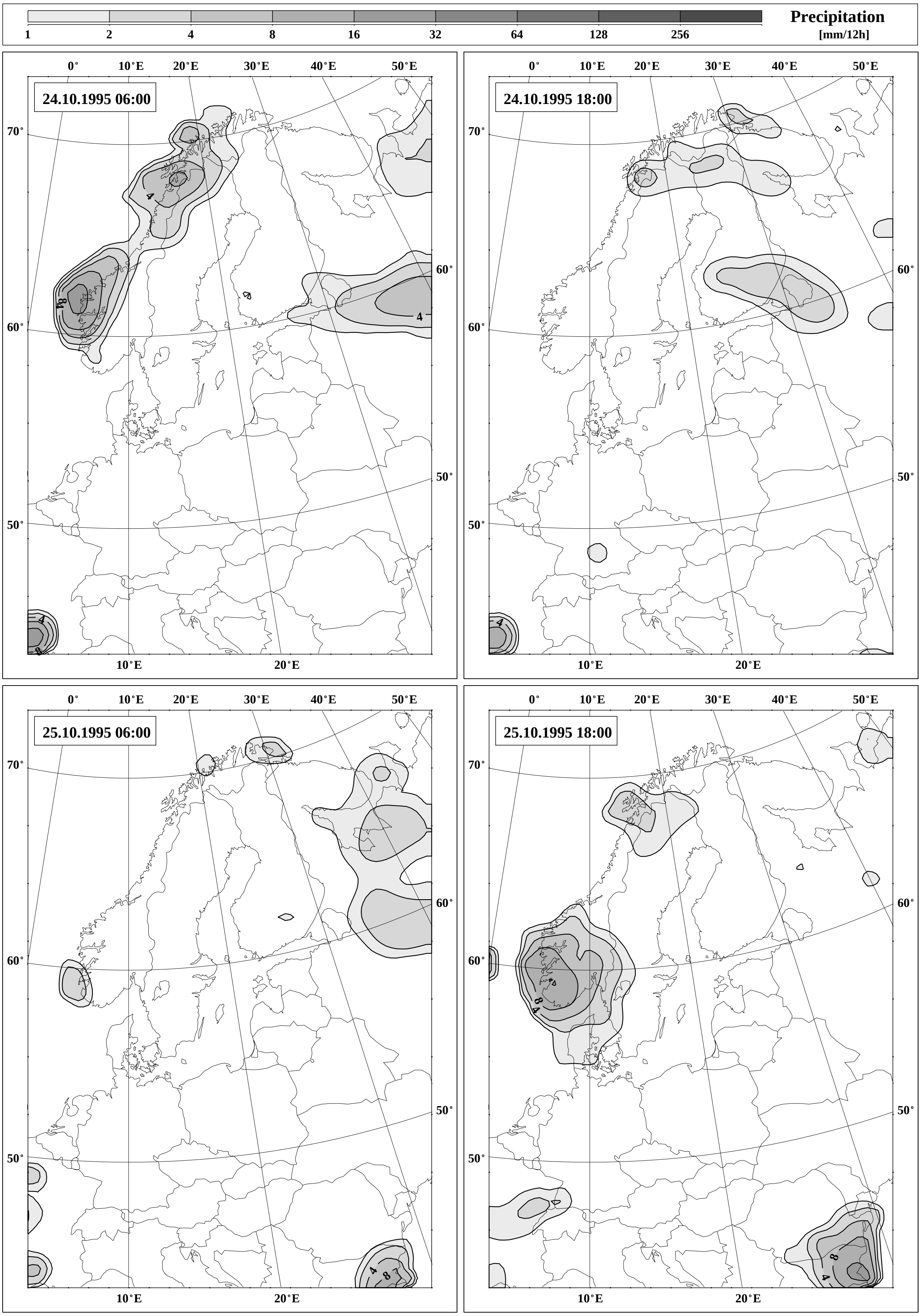
Precipitation
[mm/12h]
1 2 4 8 16 32 64 128 256
24.10.1995 06:00
24.10.1995 18:00
25.10.1995 06:00
25.10.1995 18:00
0° 10°E 20°E 30°E 40°E 50°E
70° 60° 50°
10°E 20°E

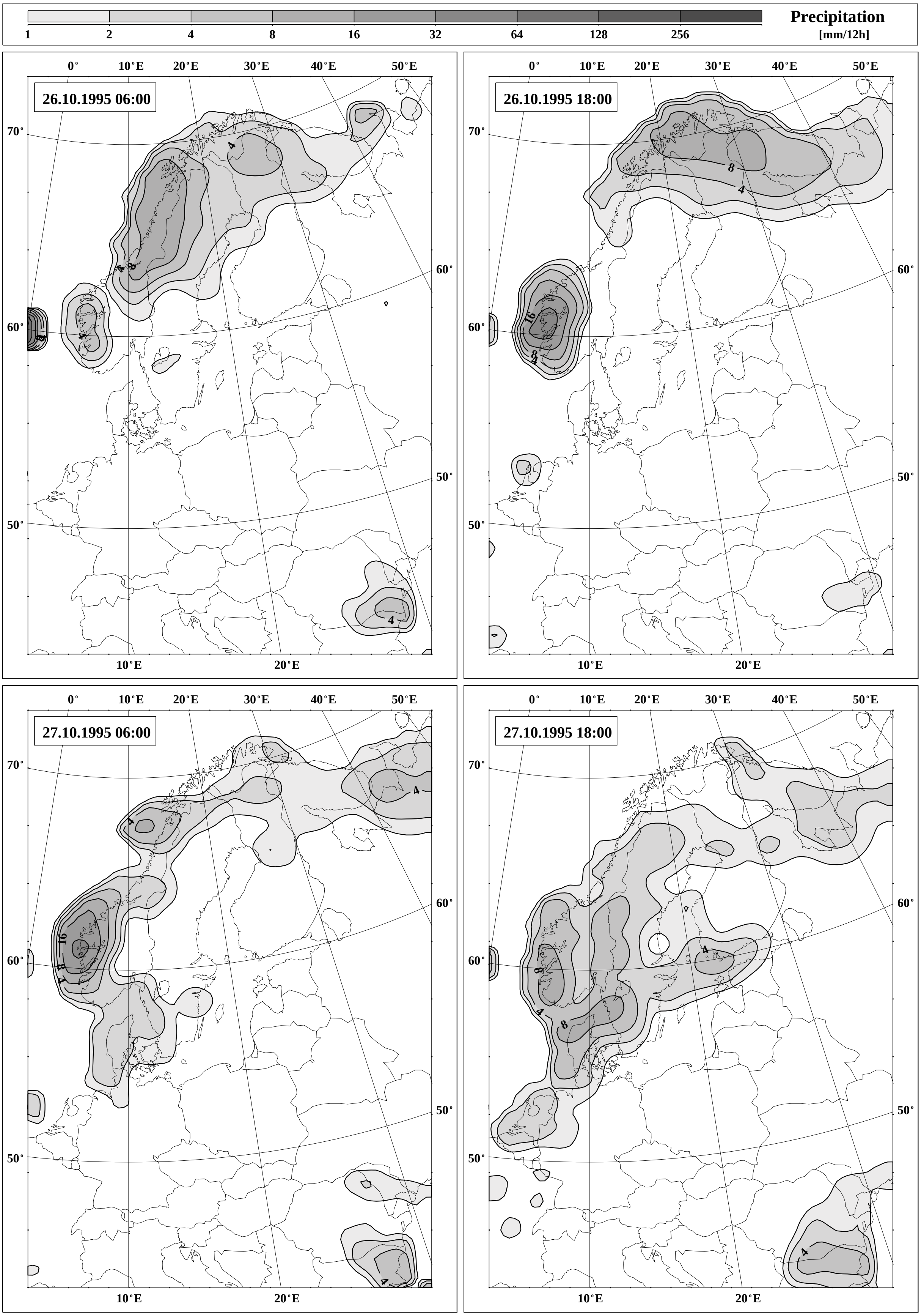
Precipitation
[mm/12h]
1 2 4 8 16 32 64 128 256
26.10.1995 06:00
26.10.1995 18:00
27.10.1995 06:00
27.10.1995 18:00
0° 10°E 20°E 30°E 40°E 50°E
70° 60° 50°
10°E 20°E

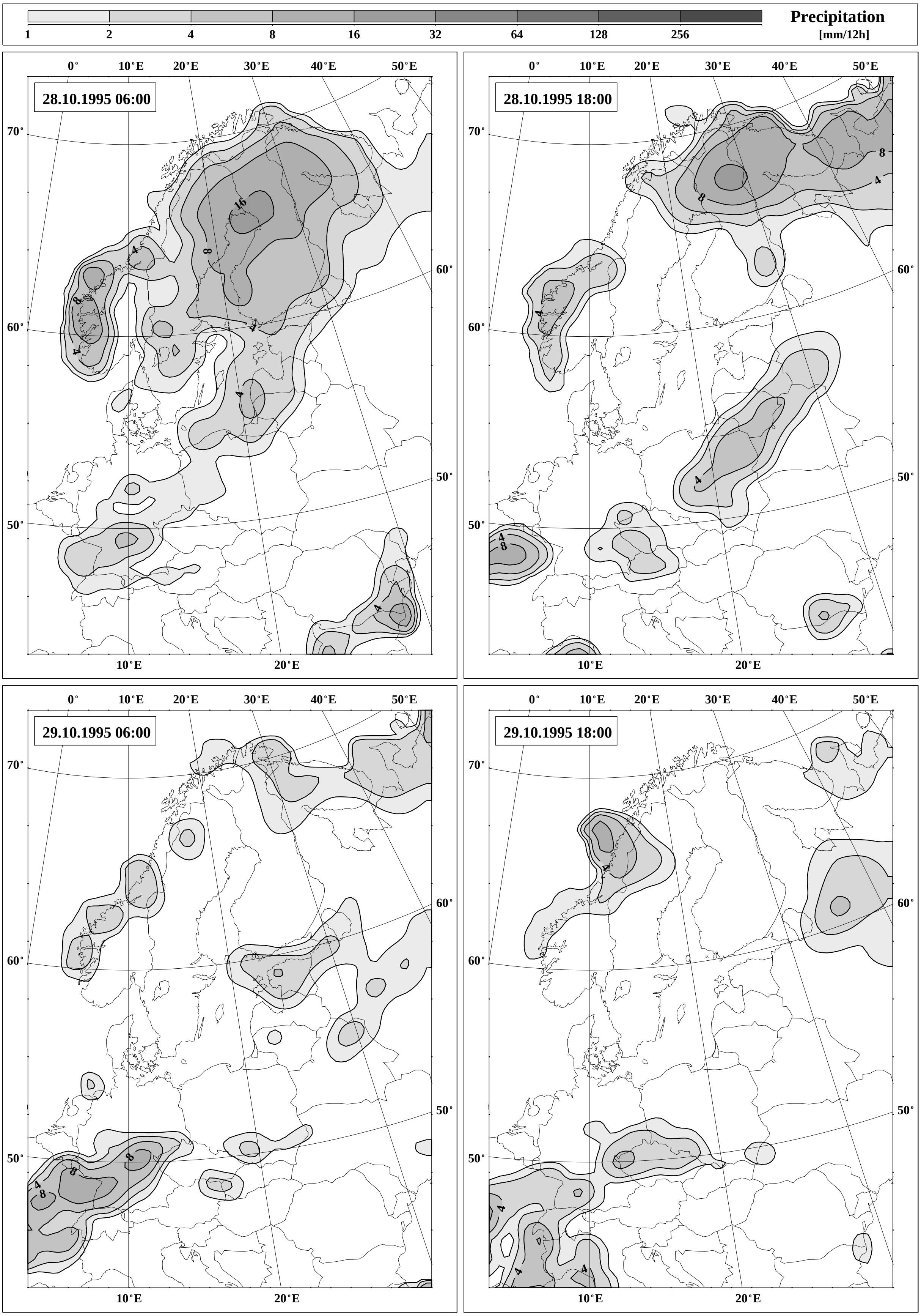
Precipitation
[mm/12h]
1 2 4 8 16 32 64 128 256
28.10.1995 06:00
28.10.1995 18:00
29.10.1995 06:00
29.10.1995 18:00
0° 10°E 20°E 30°E 40°E 50°E
70° 60° 50°
10°E 20°E

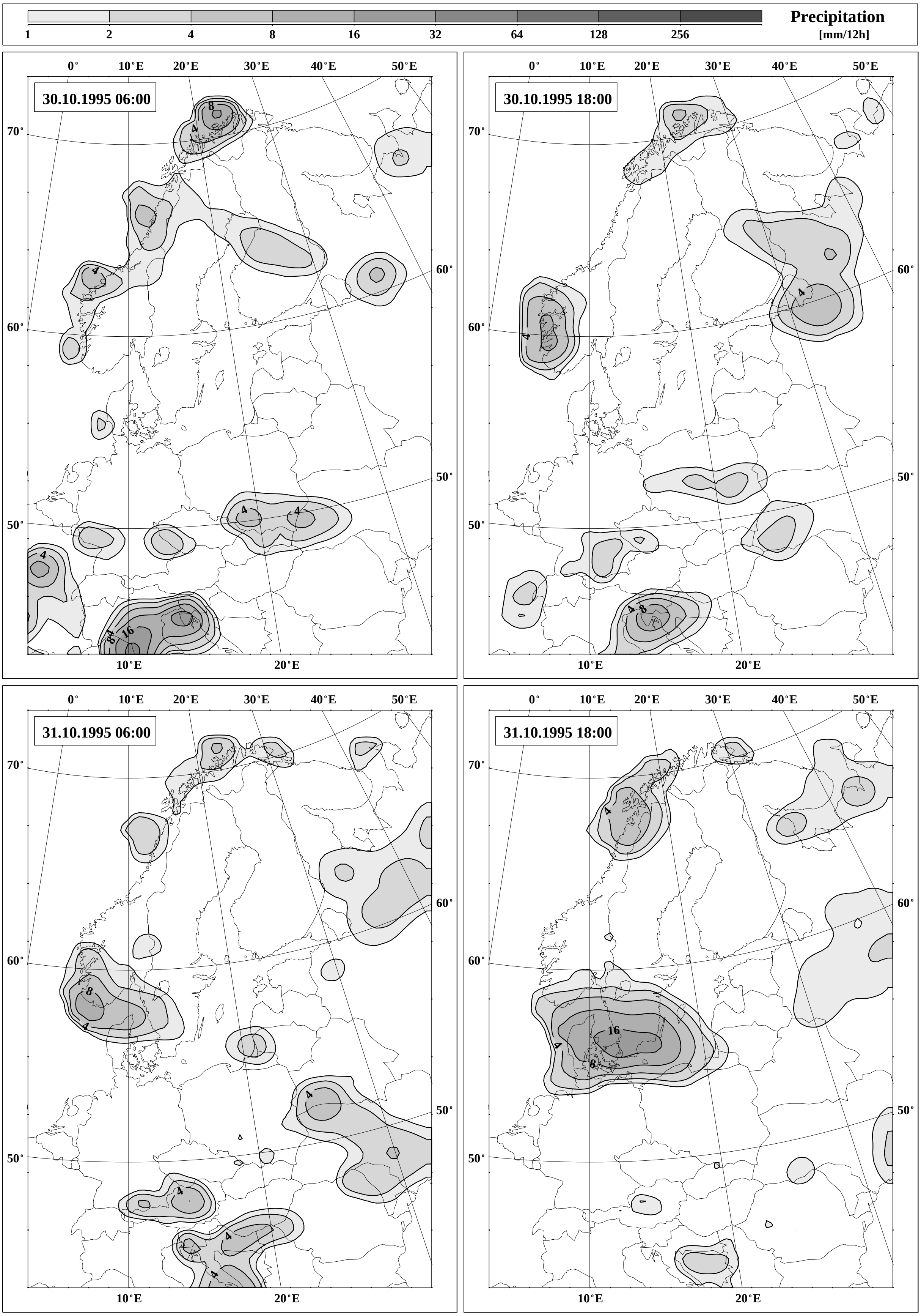
Precipitation
[mm/12h]
1
2
4
8
16
32
64
128
256
30.10.1995 06:00
30.10.1995 18:00
31.10.1995 06:00
31.10.1995 18:00
0°
10°E
20°E
30°E
40°E
50°E
70°
60°
50°

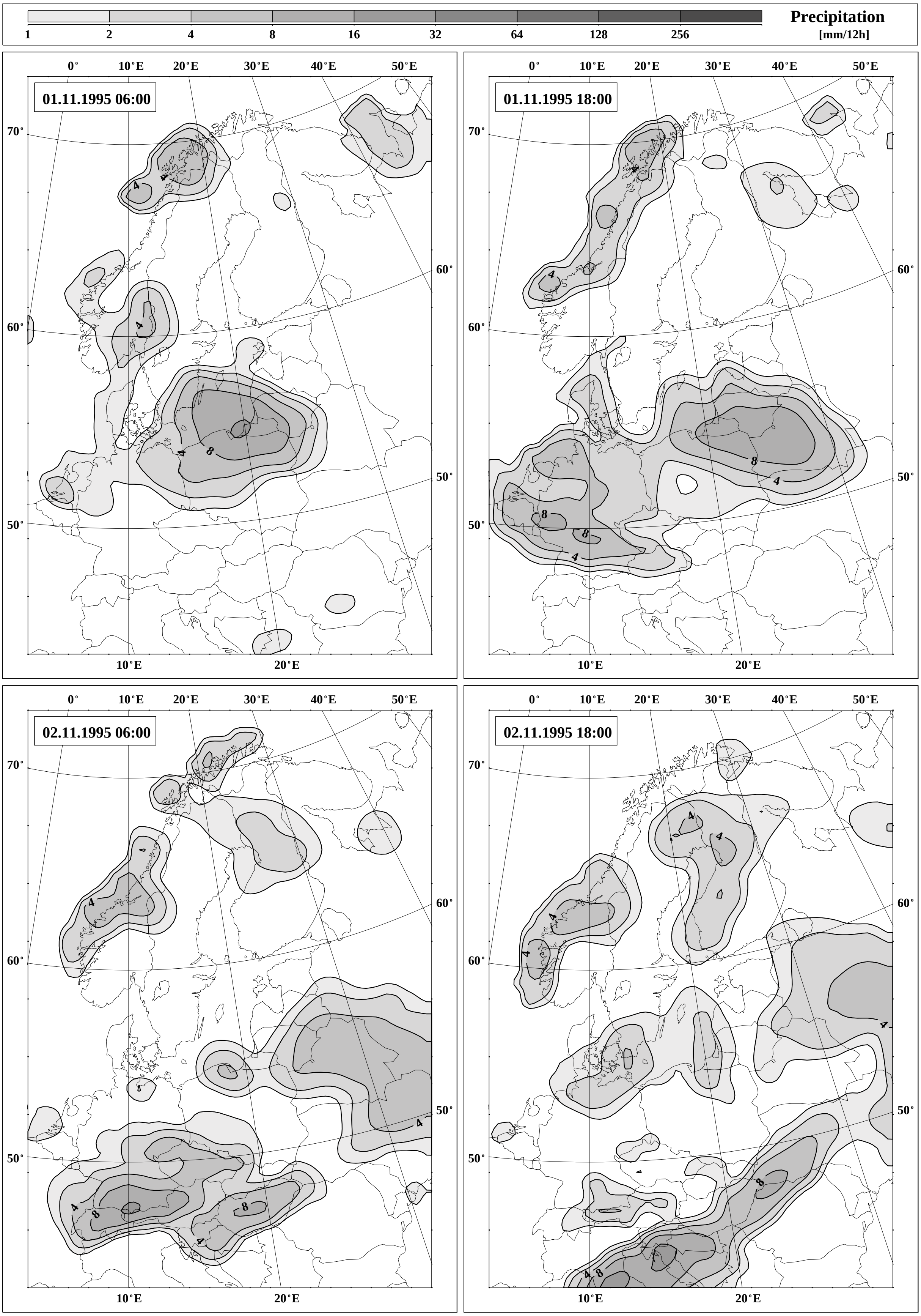

Precipitation
[mm/12h]
1
2
4
8
16
32
64
128
256
01.11.1995 06:00
01.11.1995 18:00
02.11.1995 06:00
02.11.1995 18:00
0°
10°E
20°E
30°E
40°E
50°E
70°
60°
50°

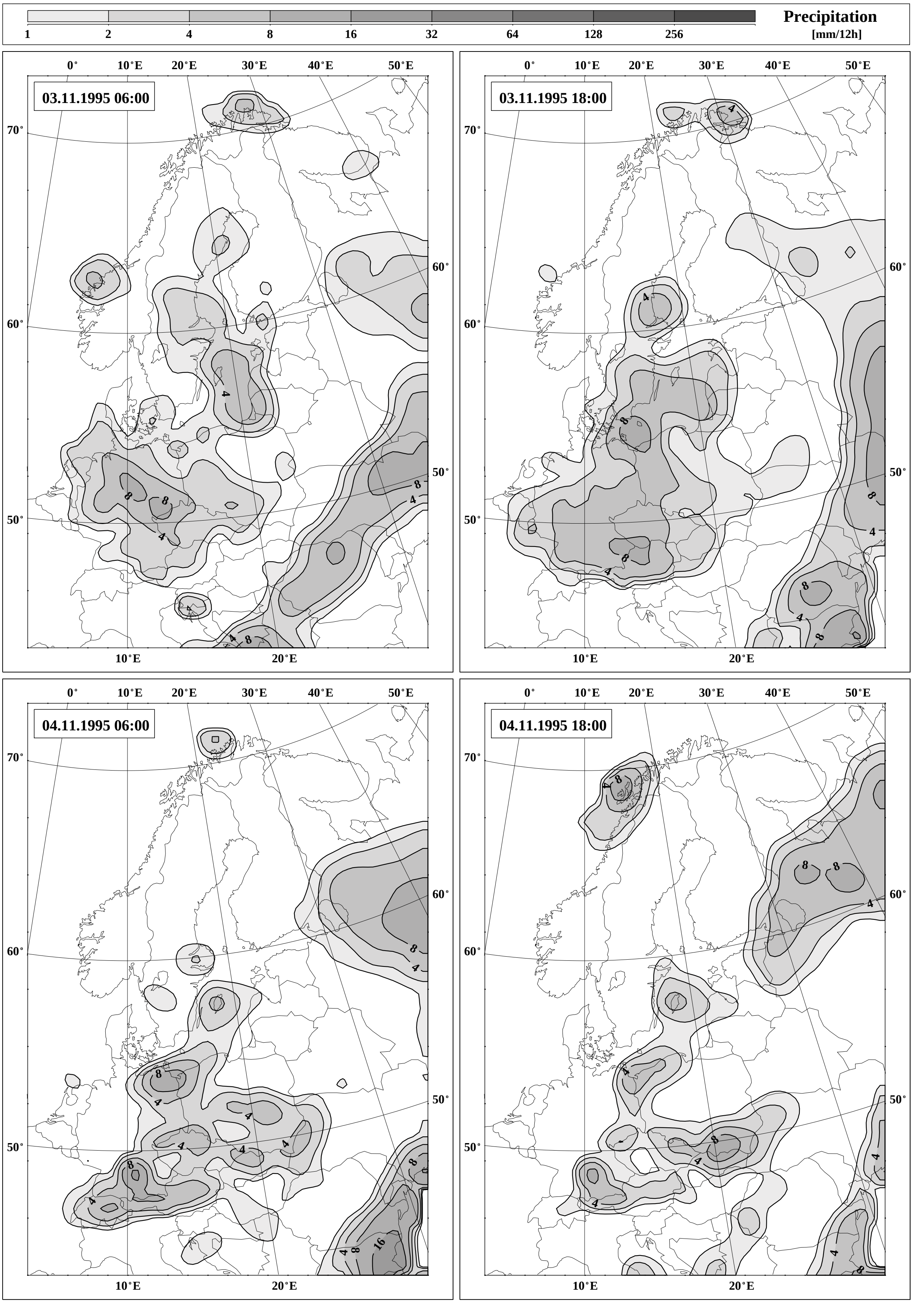
Precipitation
[mm/12h]
1 2 4 8 16 32 64 128 256
03.11.1995 06:00
03.11.1995 18:00
04.11.1995 06:00
04.11.1995 18:00
0° 10°E 20°E 30°E 40°E 50°E
70° 60° 50°
10°E 20°E

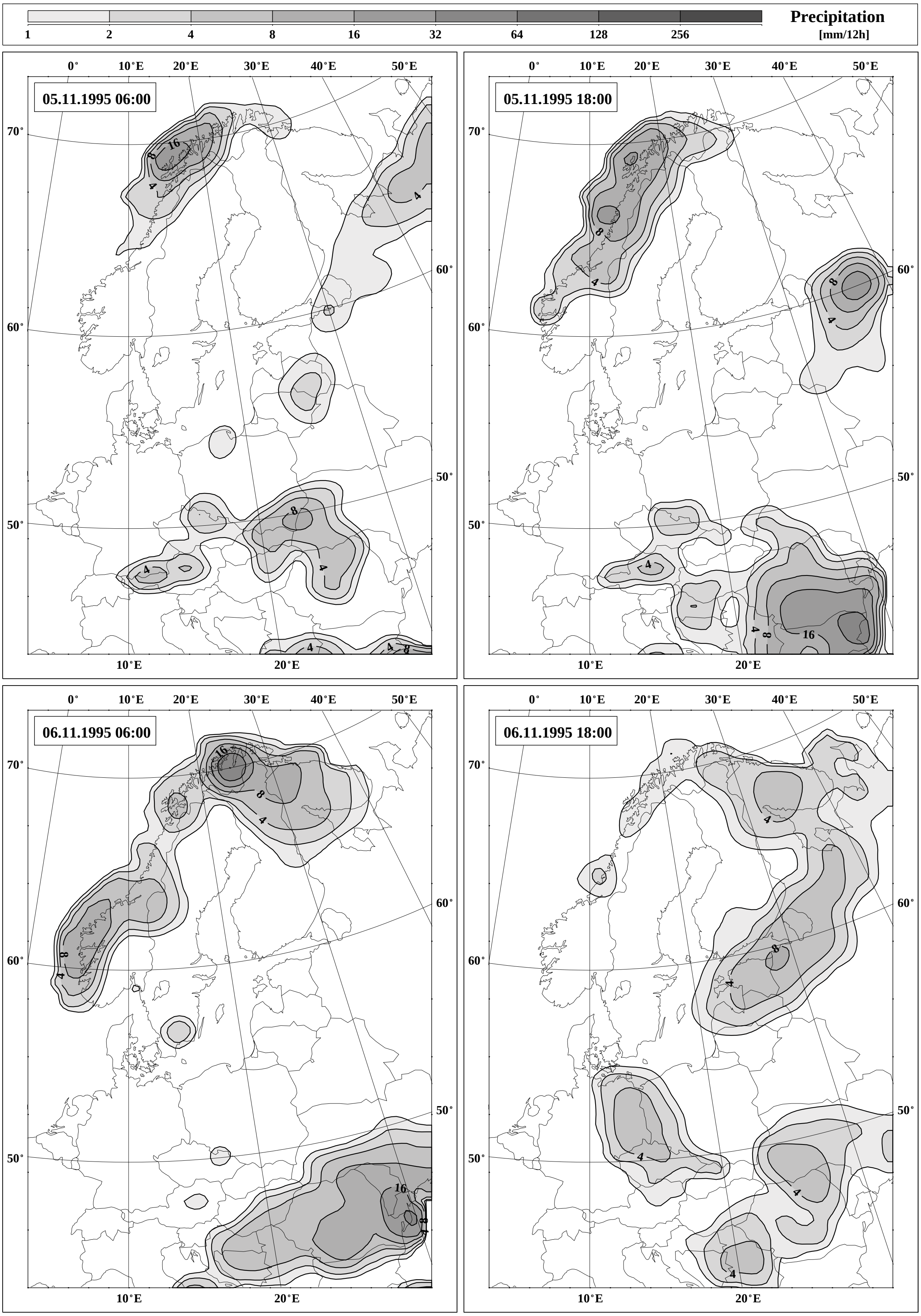

Precipitation
[mm/12h]
1
2
4
8
16
32
64
128
256
05.11.1995 06:00
05.11.1995 18:00
06.11.1995 06:00
06.11.1995 18:00
0°
10°E
20°E
30°E
40°E
50°E
70°
60°
50°

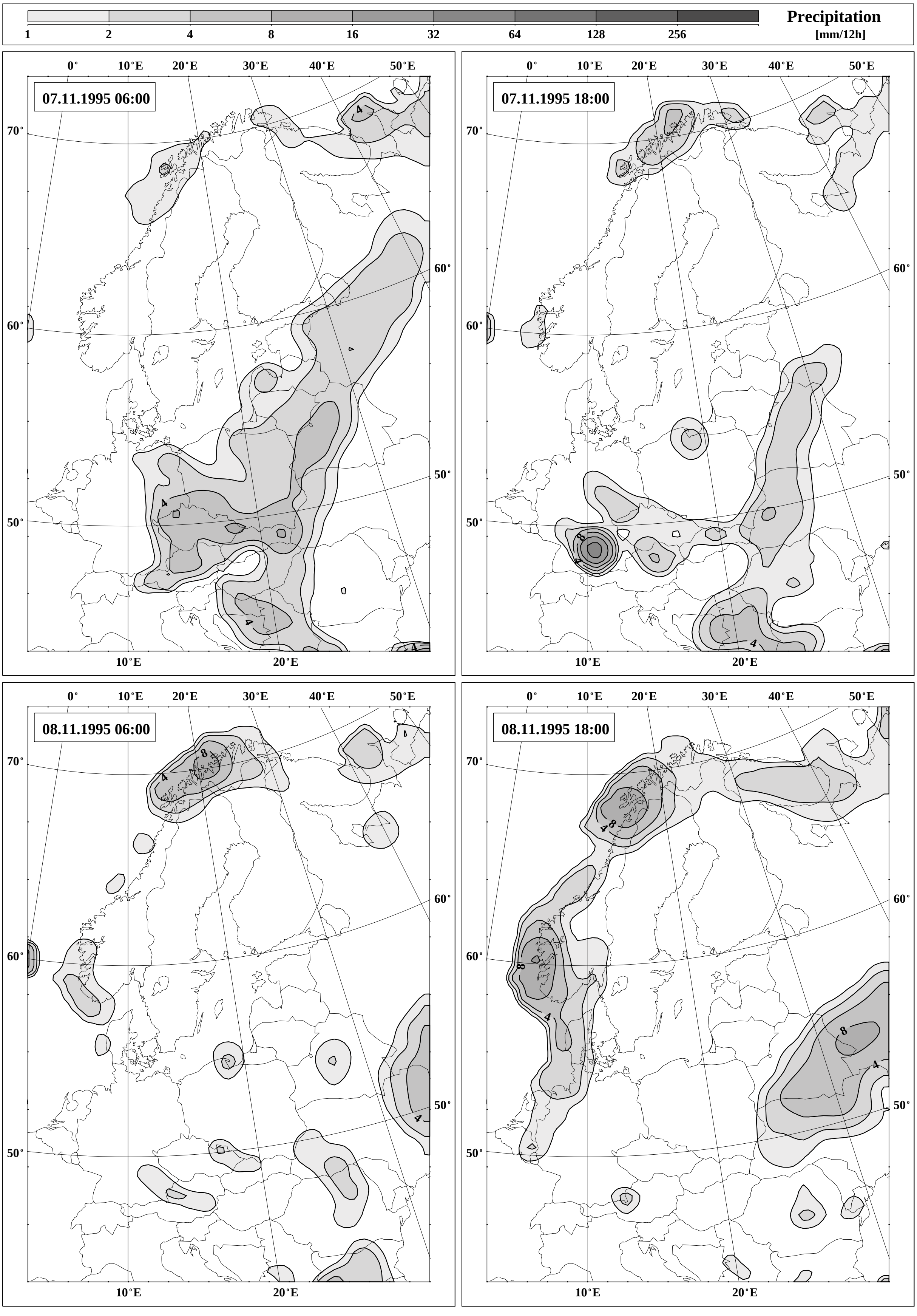
Precipitation
[mm/12h]
1
2
4
8
16
32
64
128
256
07.11.1995 06:00
07.11.1995 18:00
08.11.1995 06:00
08.11.1995 18:00
0°
10°E
20°E
30°E
40°E
50°E
70°
60°
50°

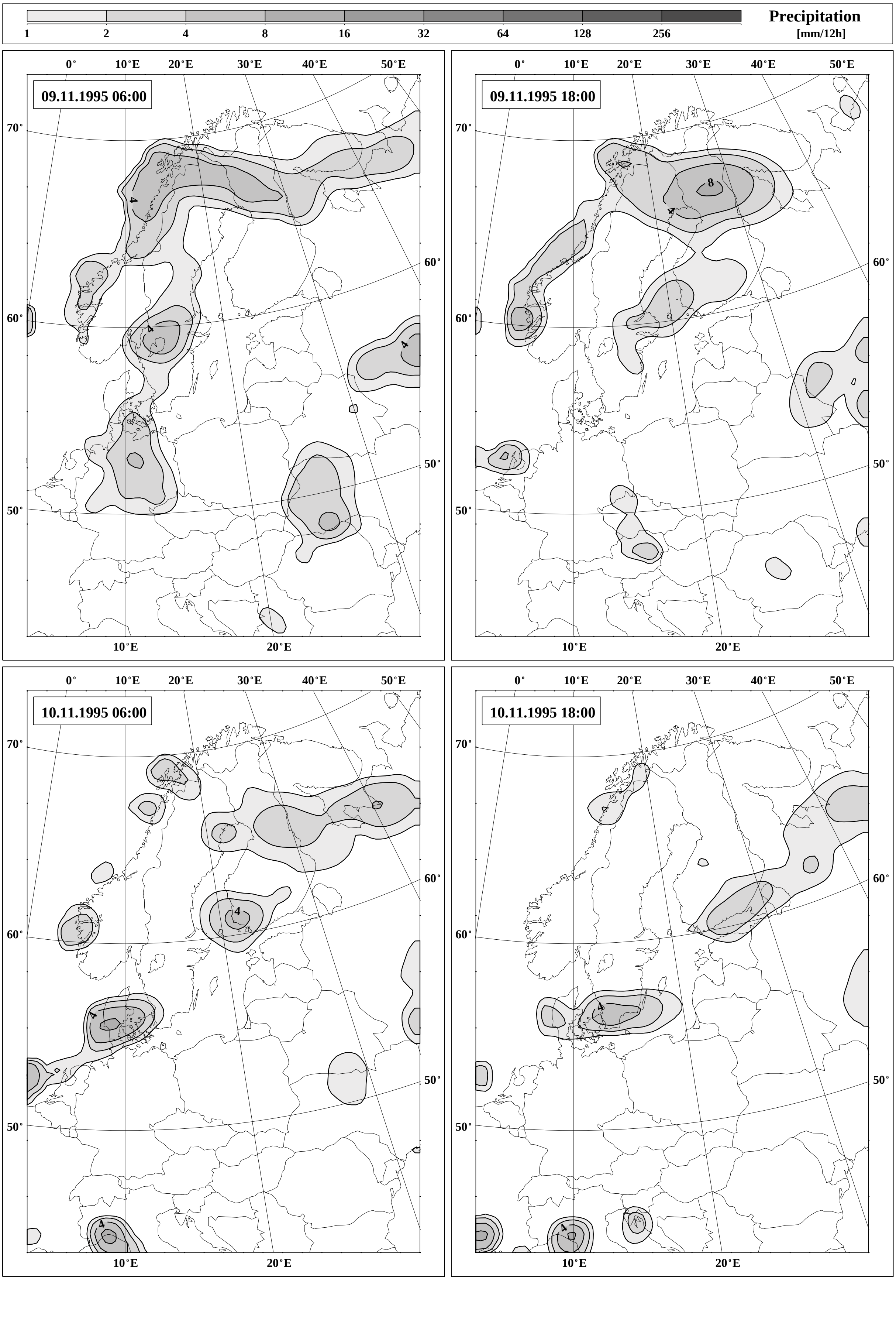

1
2
4
8
16
32
64
128
256
Precipitation
[mm/12h]
09.11.1995 06:00
09.11.1995 18:00
10.11.1995 06:00
10.11.1995 18:00
0°
10°E
20°E
30°E
40°E
50°E
70°
60°
50°

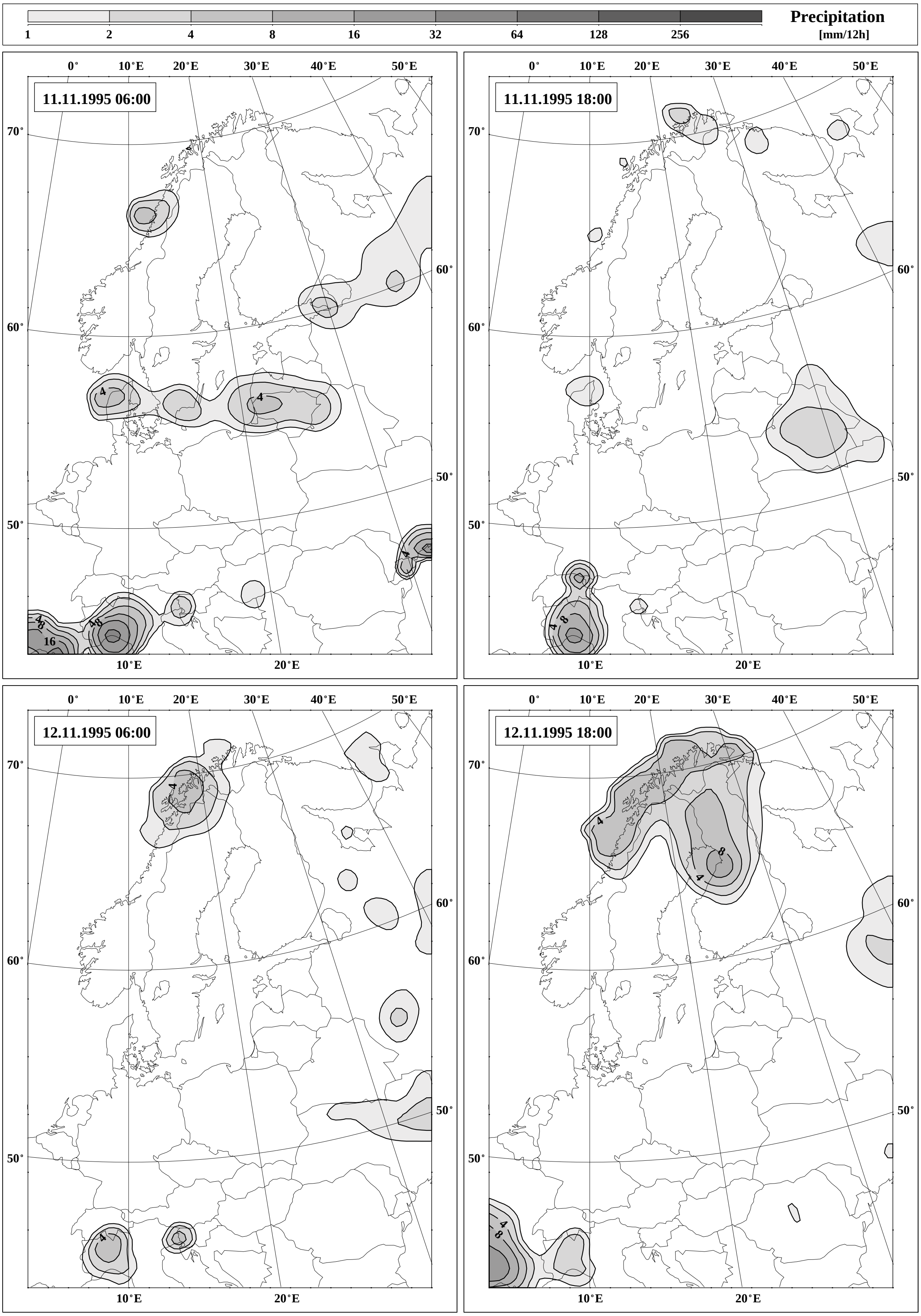
Precipitation
[mm/12h]
1 2 4 8 16 32 64 128 256
11.11.1995 06:00
11.11.1995 18:00
12.11.1995 06:00
12.11.1995 18:00
0° 10°E 20°E 30°E 40°E 50°E
70° 60° 50°
10°E 20°E

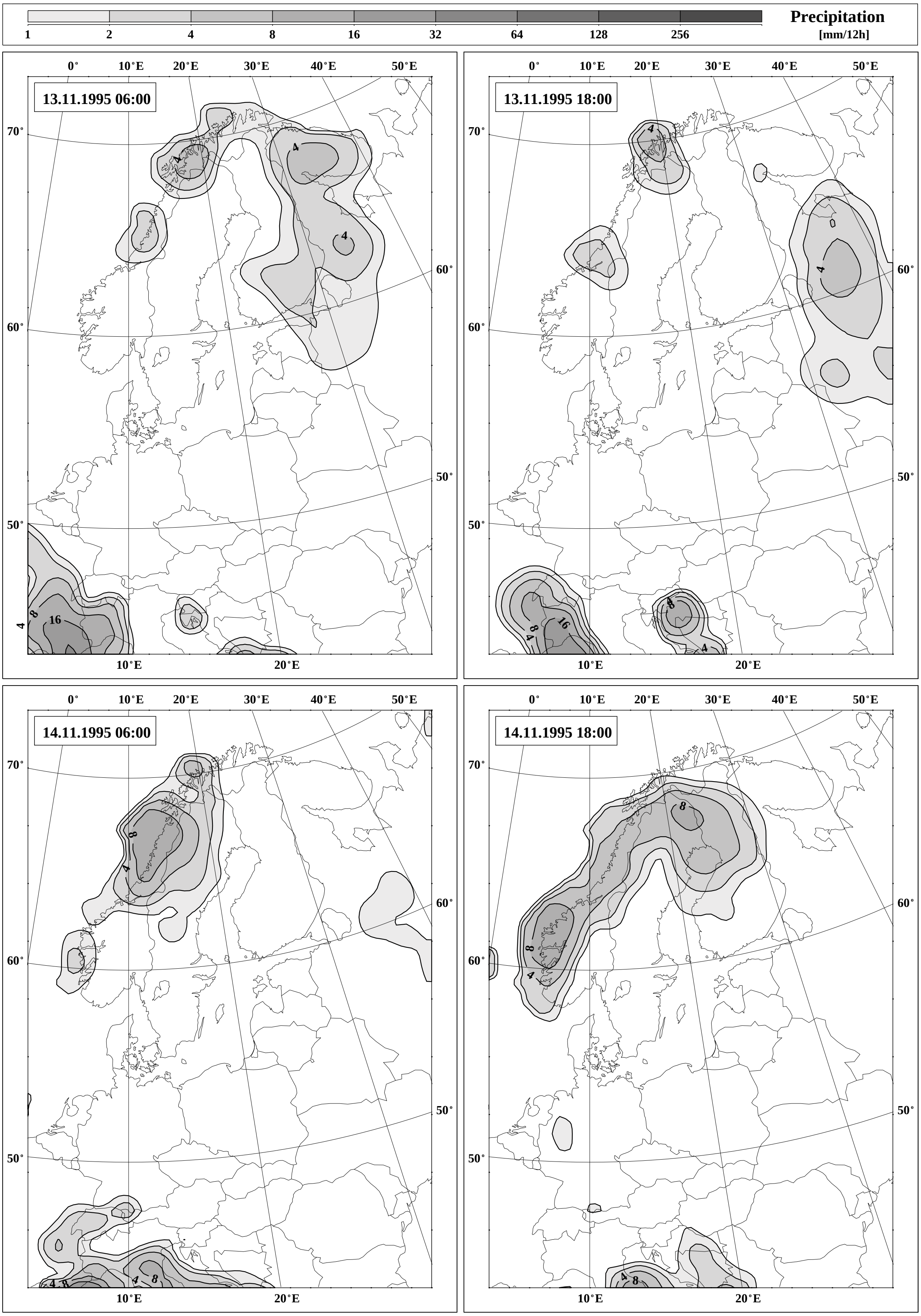
Precipitation
[mm/12h]
1 2 4 8 16 32 64 128 256
13.11.1995 06:00
13.11.1995 18:00
14.11.1995 06:00
14.11.1995 18:00
0° 10°E 20°E 30°E 40°E 50°E
70° 60° 50°
10°E 20°E

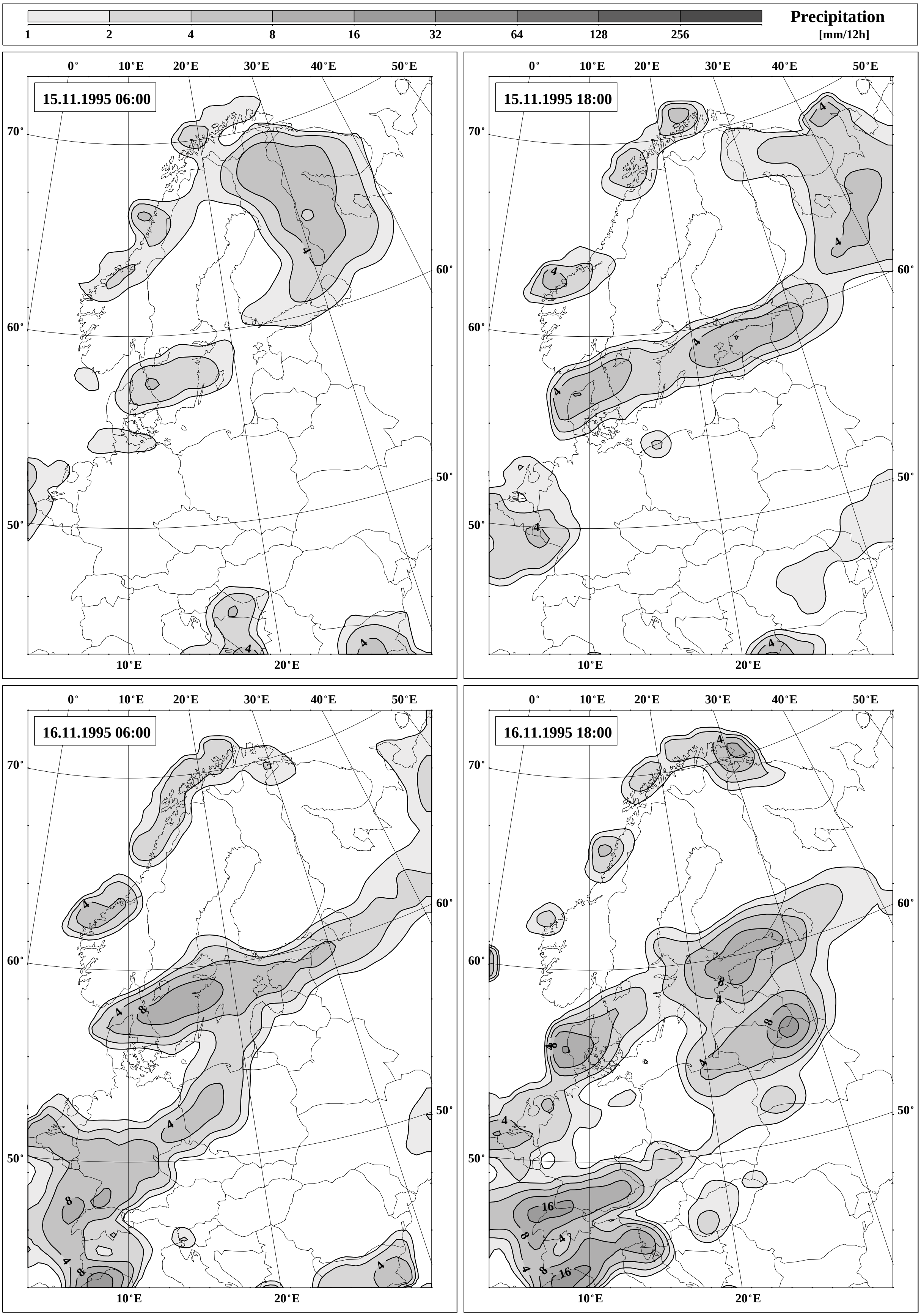
Precipitation
[mm/12h]
1 2 4 8 16 32 64 128 256
15.11.1995 06:00
15.11.1995 18:00
16.11.1995 06:00
16.11.1995 18:00
0° 10°E 20°E 30°E 40°E 50°E
70° 60° 50°
10°E 20°E

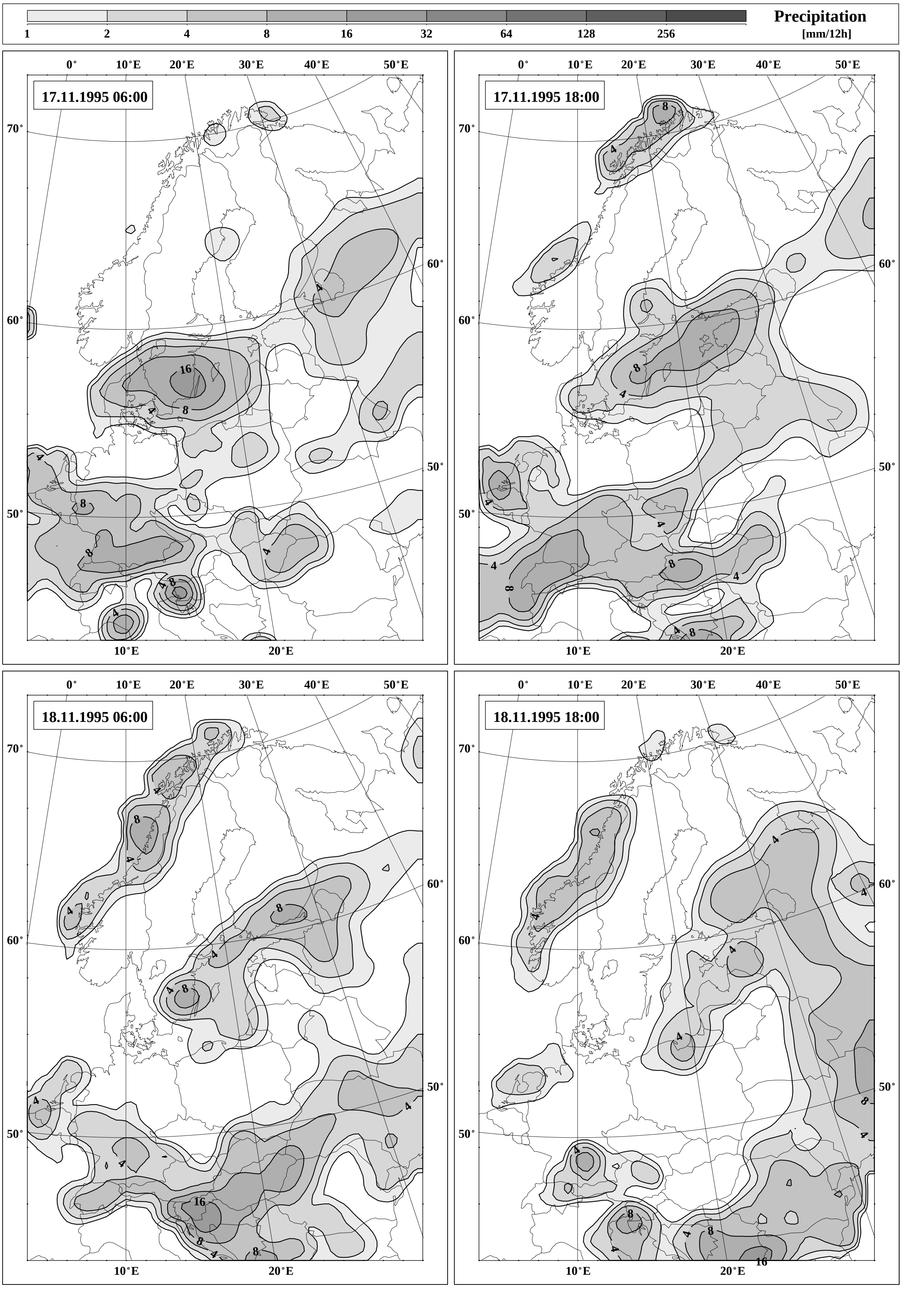
Precipitation
[mm/12h]
1
2
4
8
16
32
64
128
256
17.11.1995 06:00
17.11.1995 18:00
18.11.1995 06:00
18.11.1995 18:00
0°
10°E
20°E
30°E
40°E
50°E
70°
60°
50°

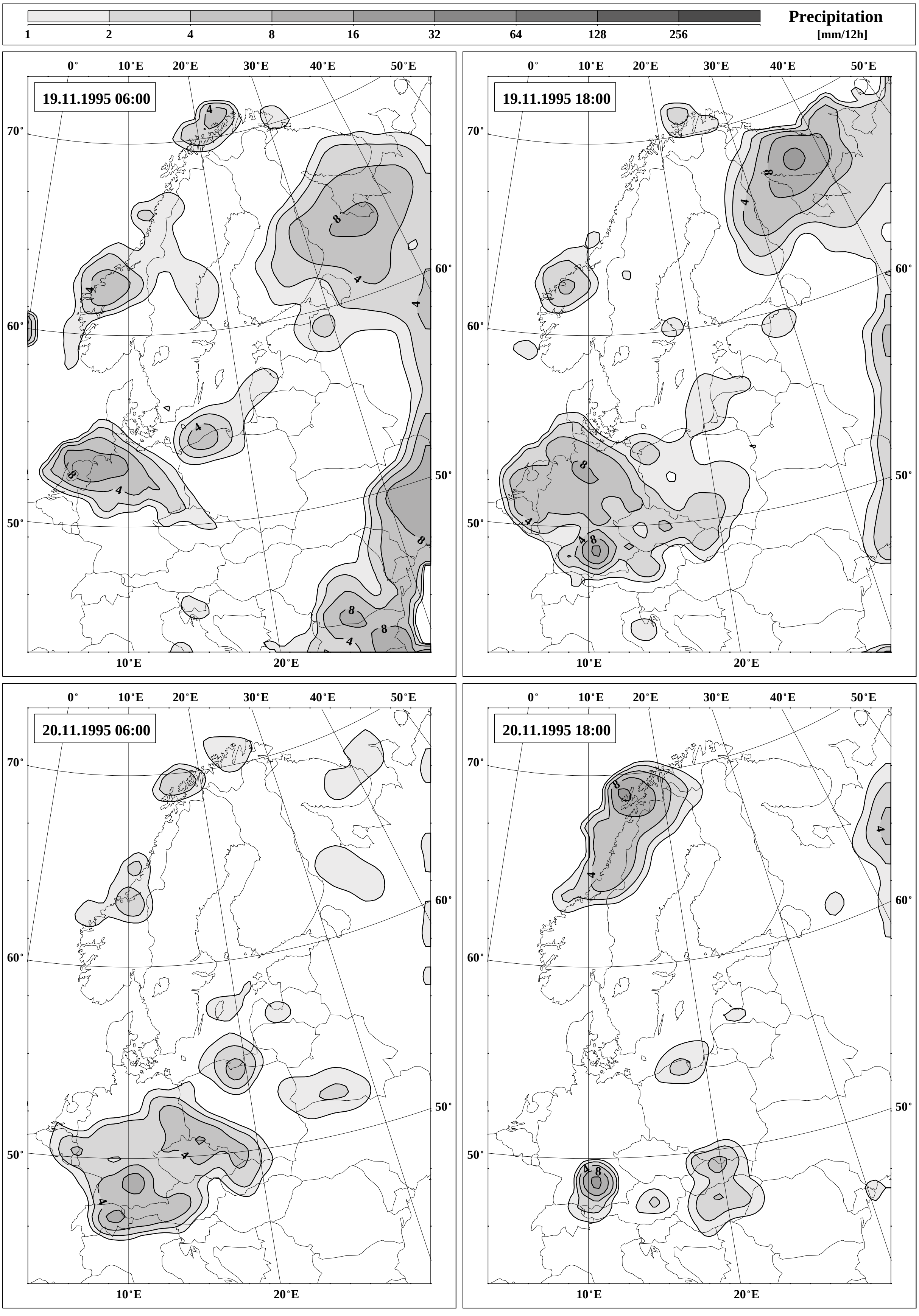
Precipitation
[mm/12h]
1
2
4
8
16
32
64
128
256
19.11.1995 06:00
19.11.1995 18:00
20.11.1995 06:00
20.11.1995 18:00
0°
10°E
20°E
30°E
40°E
50°E
70°
60°
50°

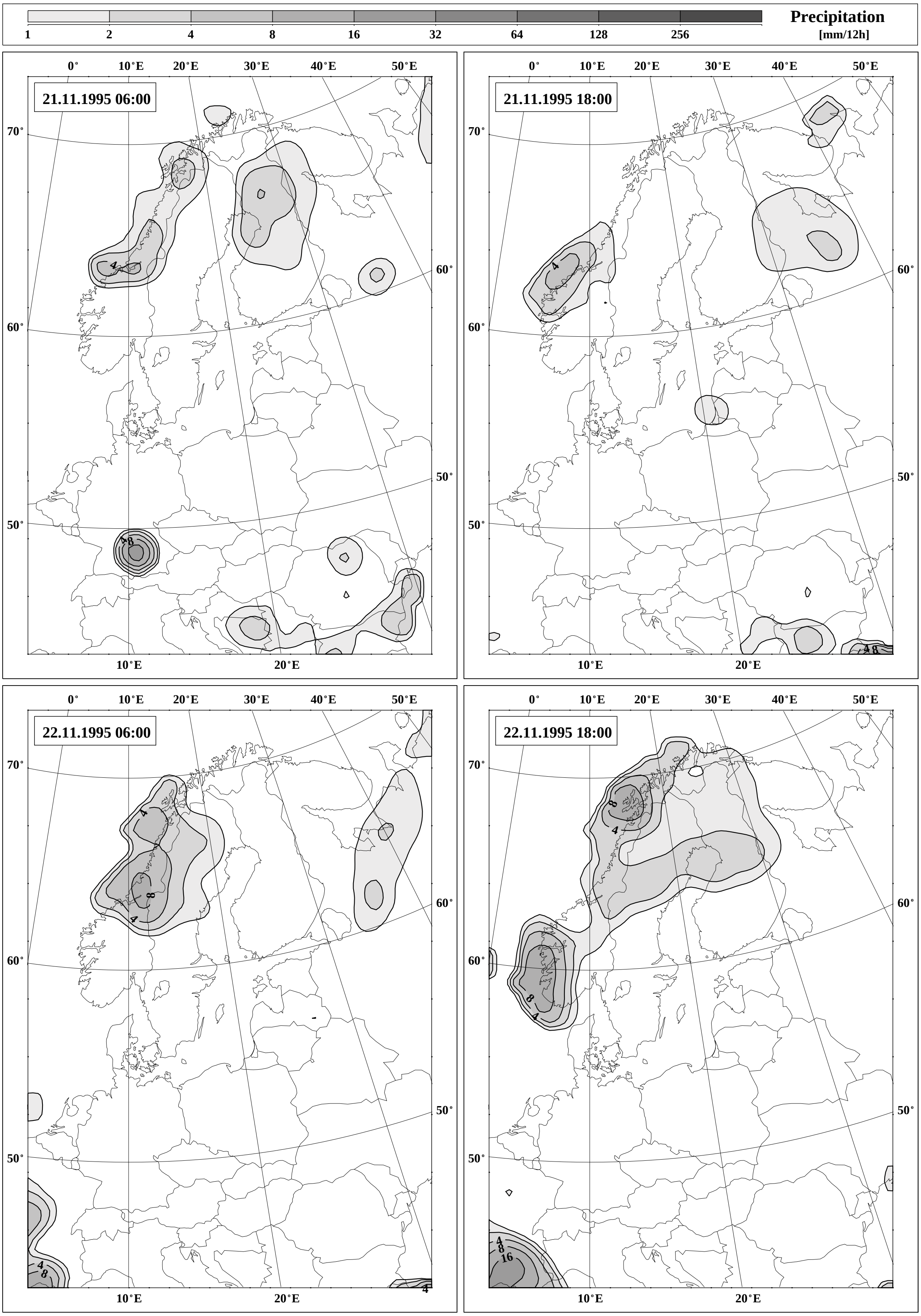
Precipitation
[mm/12h]
1 2 4 8 16 32 64 128 256
21.11.1995 06:00
21.11.1995 18:00
22.11.1995 06:00
22.11.1995 18:00
0° 10°E 20°E 30°E 40°E 50°E
70° 60° 50°
10°E 20°E

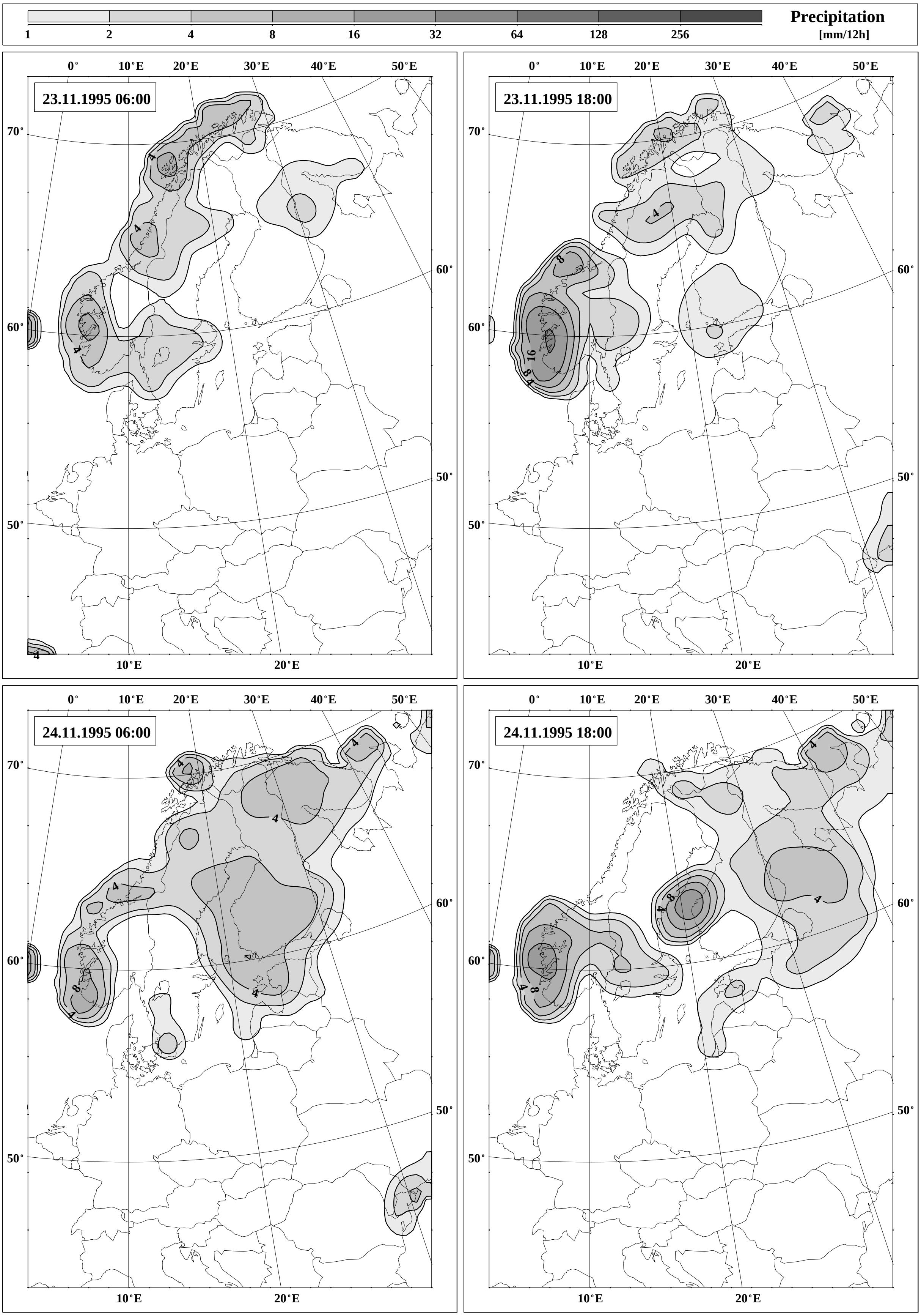
Precipitation
[mm/12h]
1 2 4 8 16 32 64 128 256
23.11.1995 06:00
23.11.1995 18:00
24.11.1995 06:00
24.11.1995 18:00
0° 10°E 20°E 30°E 40°E 50°E
70° 60° 50°
10°E 20°E

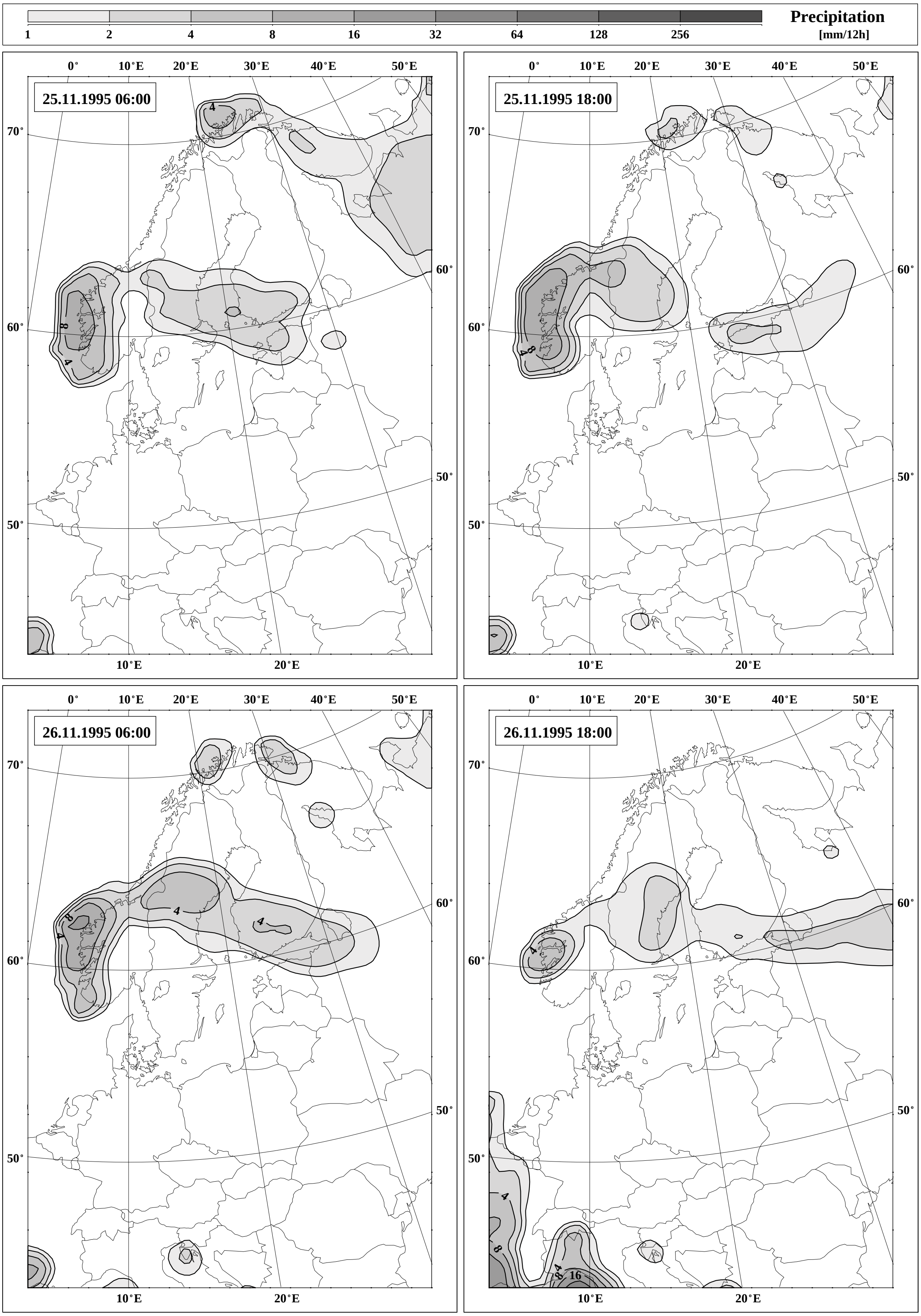

Precipitation
[mm/12h]
1
2
4
8
16
32
64
128
256
25.11.1995 06:00
25.11.1995 18:00
26.11.1995 06:00
26.11.1995 18:00
0°
10°E
20°E
30°E
40°E
50°E
70°
60°
50°

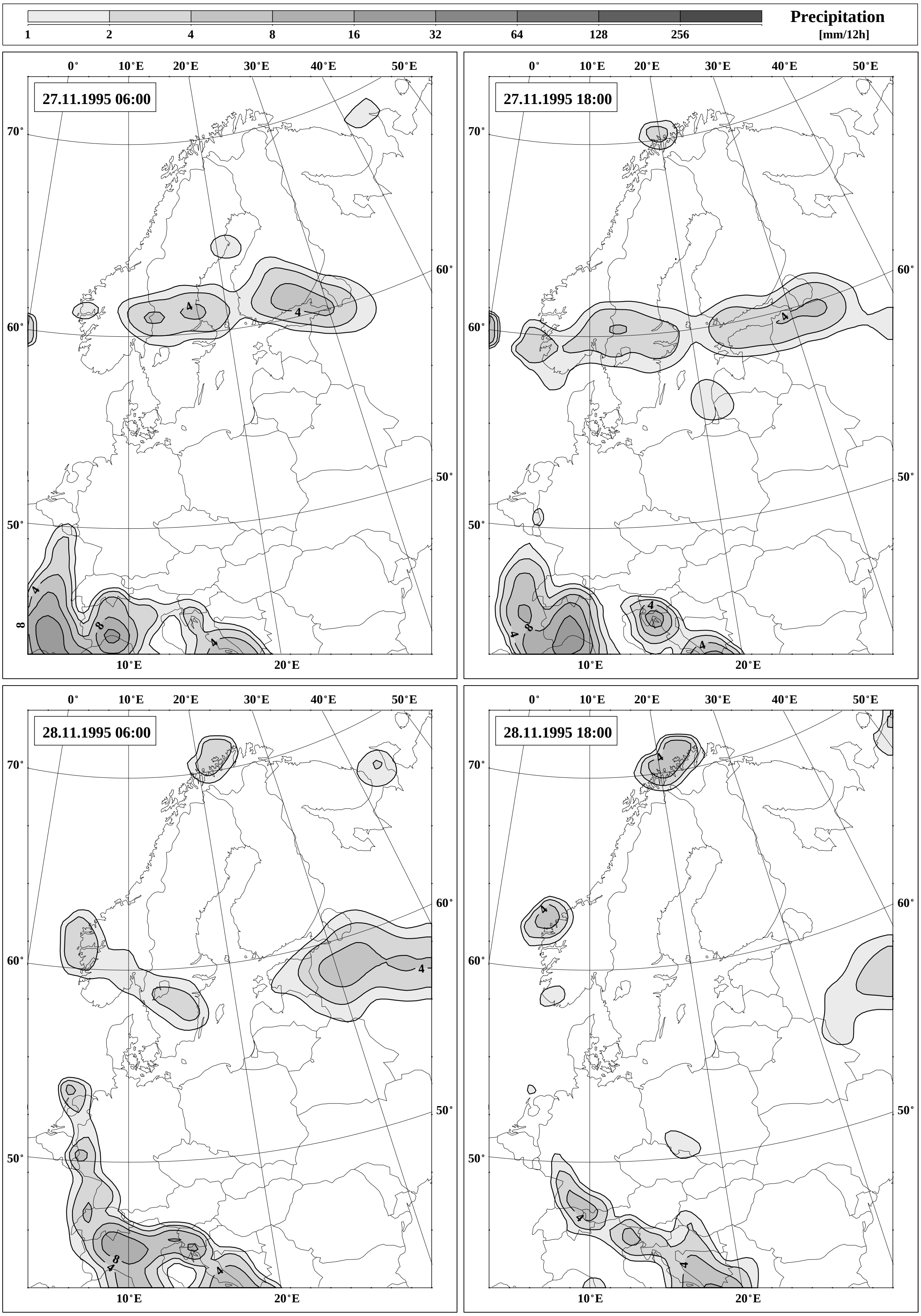
Precipitation
[mm/12h]
1
2
4
8
16
32
64
128
256
27.11.1995 06:00
27.11.1995 18:00
28.11.1995 06:00
28.11.1995 18:00
0°
10°E
20°E
30°E
40°E
50°E
70°
60°
50°

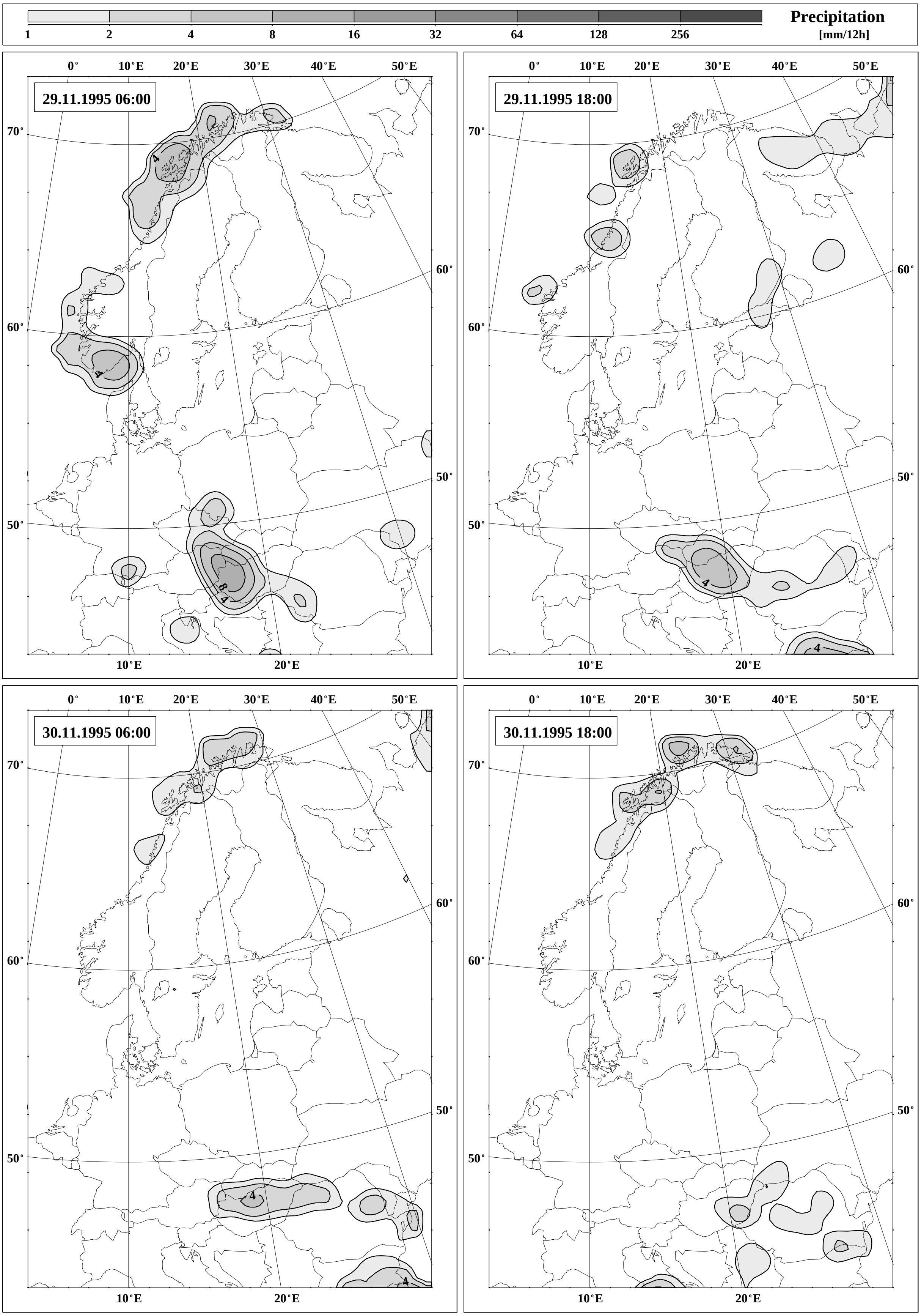
Precipitation
[mm/12h]
1
2
4
8
16
32
64
128
256
29.11.1995 06:00
29.11.1995 18:00
30.11.1995 06:00
30.11.1995 18:00
0°
10°E
20°E
30°E
40°E
50°E
70°
60°
50°
10°E
20°E

8 MONTHLY BALTIC DRAINAGE PRECIPITATION

Beside the 12-hourly accumulated precipitation fields, both the areal distribution and the total amount of the monthly precipitation input into the Baltic drainage basin are of interest. They are both computed from the 12-hourly precipitation fields (fig. 8). The advantage of this as opposed to the use of monthly accumulated precipitation values, is that observations that are not continually measured all month long, are also included in the analysis. Further, the 12-hourly analyses are prepared, and they are easily added. Fig. 9 shows the areal distribution of the monthly precipitation for the four months of the PIDCAP period in the Baltic drainage basin.

In August, the areal precipitation distribution is characterized by values approximately 50 mm higher than the majority of the drainage basin. The maximum is registered in the mountainous North, with values exceeding 128 mm. The minimum, with values lower than 16 mm, is located in southern Sweden. In September the high values are observed at the border between Sweden and Norway, whereas the maximum precipitation has been analyzed in the southern part of the drainage basin. In contrast to this, October is characterized by a marked north-south distribution of precipitation (fig. 9). Again, the highest values exceed 128 mm in the north of the domain, but a pronounced dry region with values lower than 8 mm is observed in the south of Poland. For November, monthly precipitation values ranging from 32 to 64 mm over the whole drainage basin have been analyzed.

If the temporal distribution of the areally averaged precipitation in the Baltic drainage basin (fig. 10) is looked at, the proposed case study periods of heavy rain (chapter 7) are also evident. The monthly areally averaged estimates of precipitation are 53 mm for August, 71 mm for September, 41 mm for October, and 46 mm for November. From the climatological water balance of the Baltic drainage basin (Kuusisto 1995), it can be seen, that there is a strong seasonal dependence on the averaged monthly precipitation input. According to this, the highest amount of precipitation can be expected in August (82 mm), and the lowest values in February (43 mm). This does not correspond with the analyzed monthly averages for the PIDCAP period, which are generally too low when compared to the climatological values. The precipitation deficit is 27 mm for August, 1 mm for September, 23 mm for October, and 19 mm for November 1995. Obviously, the PIDCAP period was too dry, when compared to climatological estimates. The exact quantity of the monthly precipitation has to be regarded as a first estimate, because in the analysis uncorrected observations are used. This may lead to slightly underestimated precipitation values.

Figure 10 Pages 90 - 93: Areal distribution of monthly precipitation for the Baltic drainage basin, obtained from twice daily objectively analyzed precipitation fields. Dates are August, September, October, and November of the PIDCAP year 1995. Units are in mm/month.

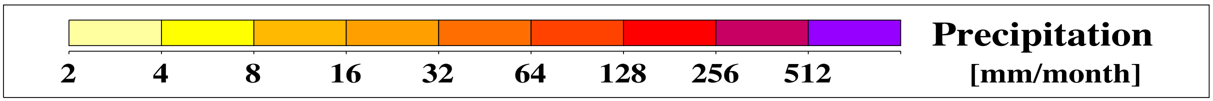
2
4
8
16
32
64
128
256
512
Precipitation
[mm/month]

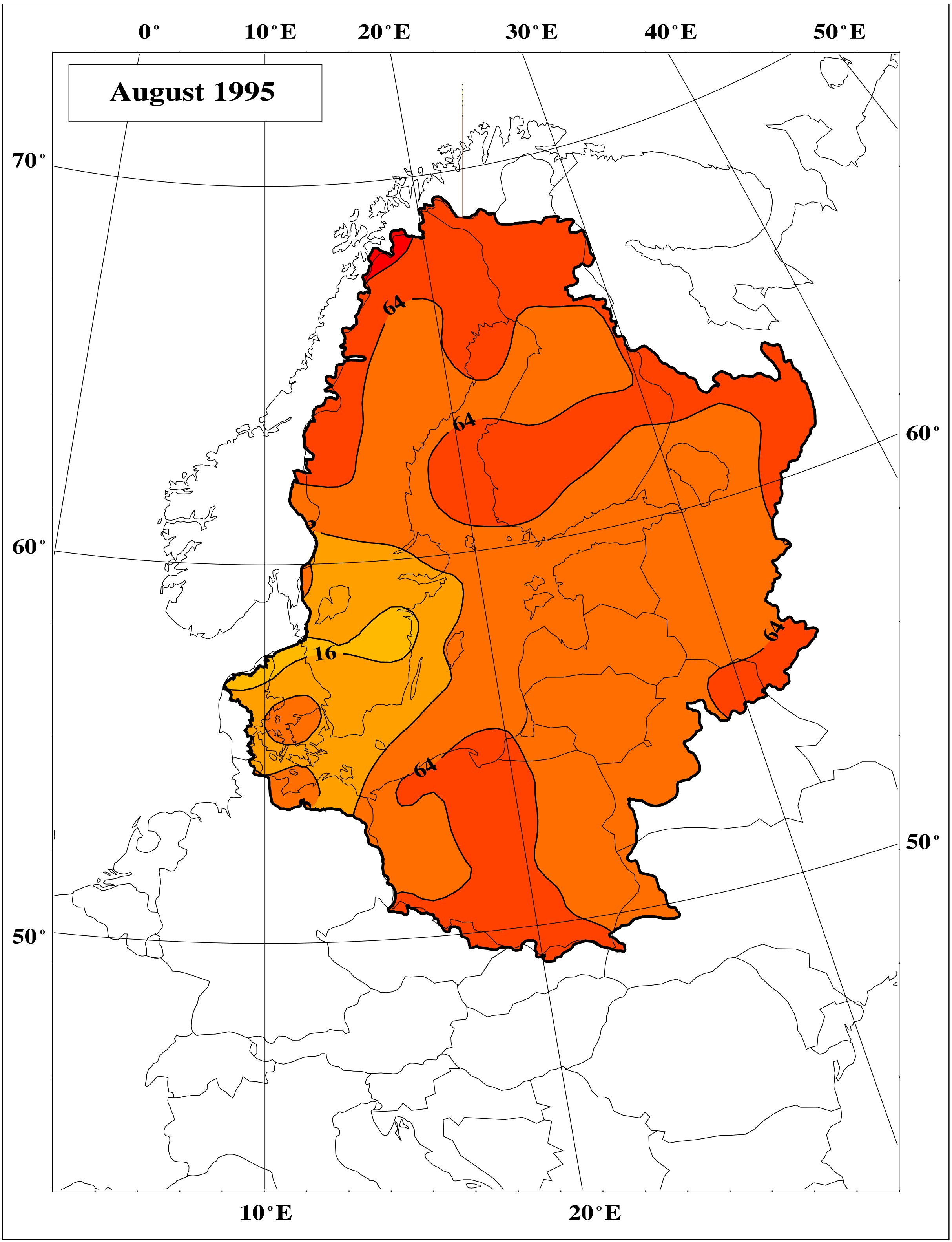
August 1995
0°
10°E
20°E
30°E
40°E
50°E
70°
60°
50°
60°
50°
10°E
20°E
64
64
64
64
16

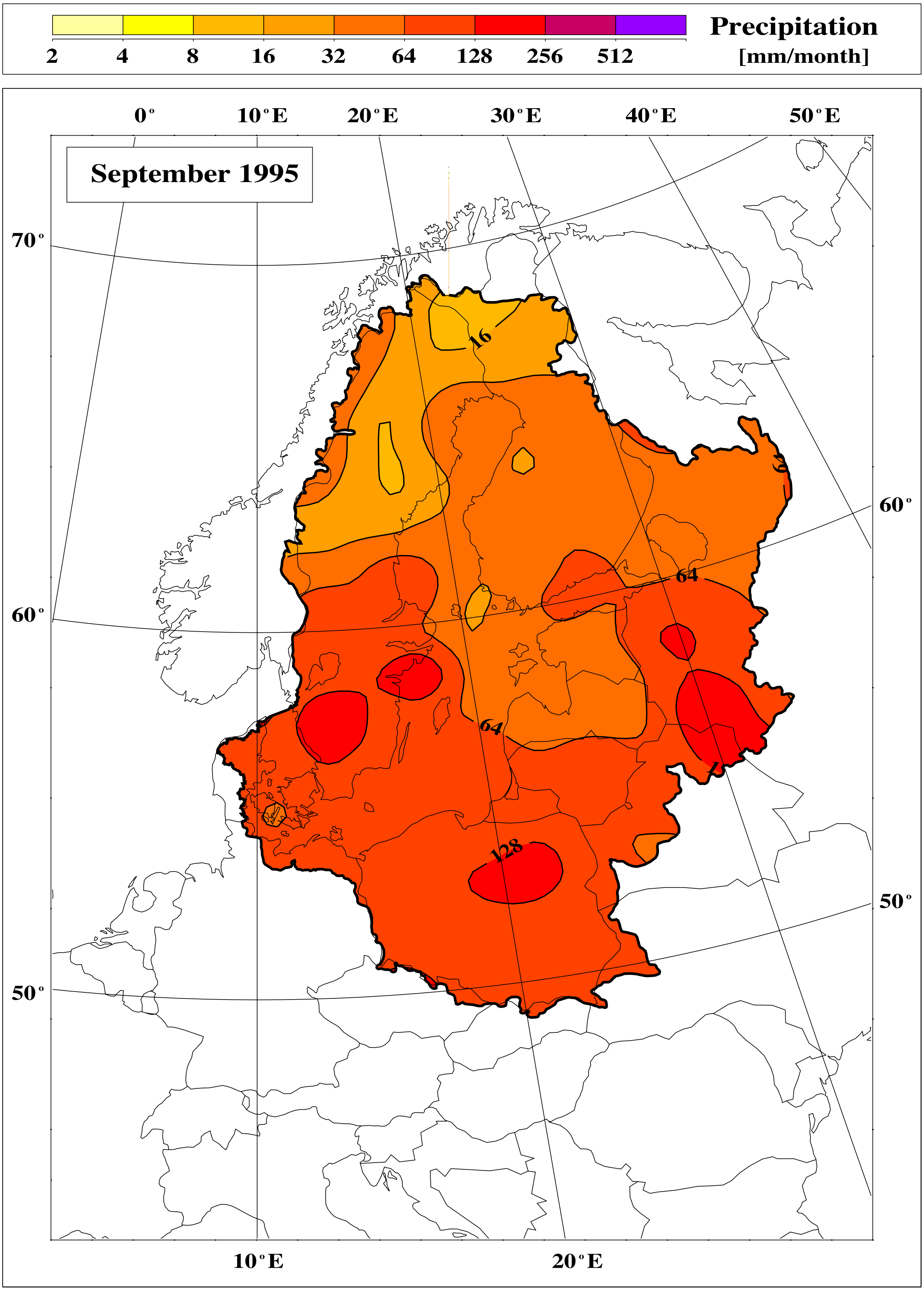
2 4 8 16 32 64 128 256 512
Precipitation
[mm/month]
September 1995
0°
10°E
20°E
30°E
40°E
50°E
70°
60°
50°
16
64
128
10°E
20°E

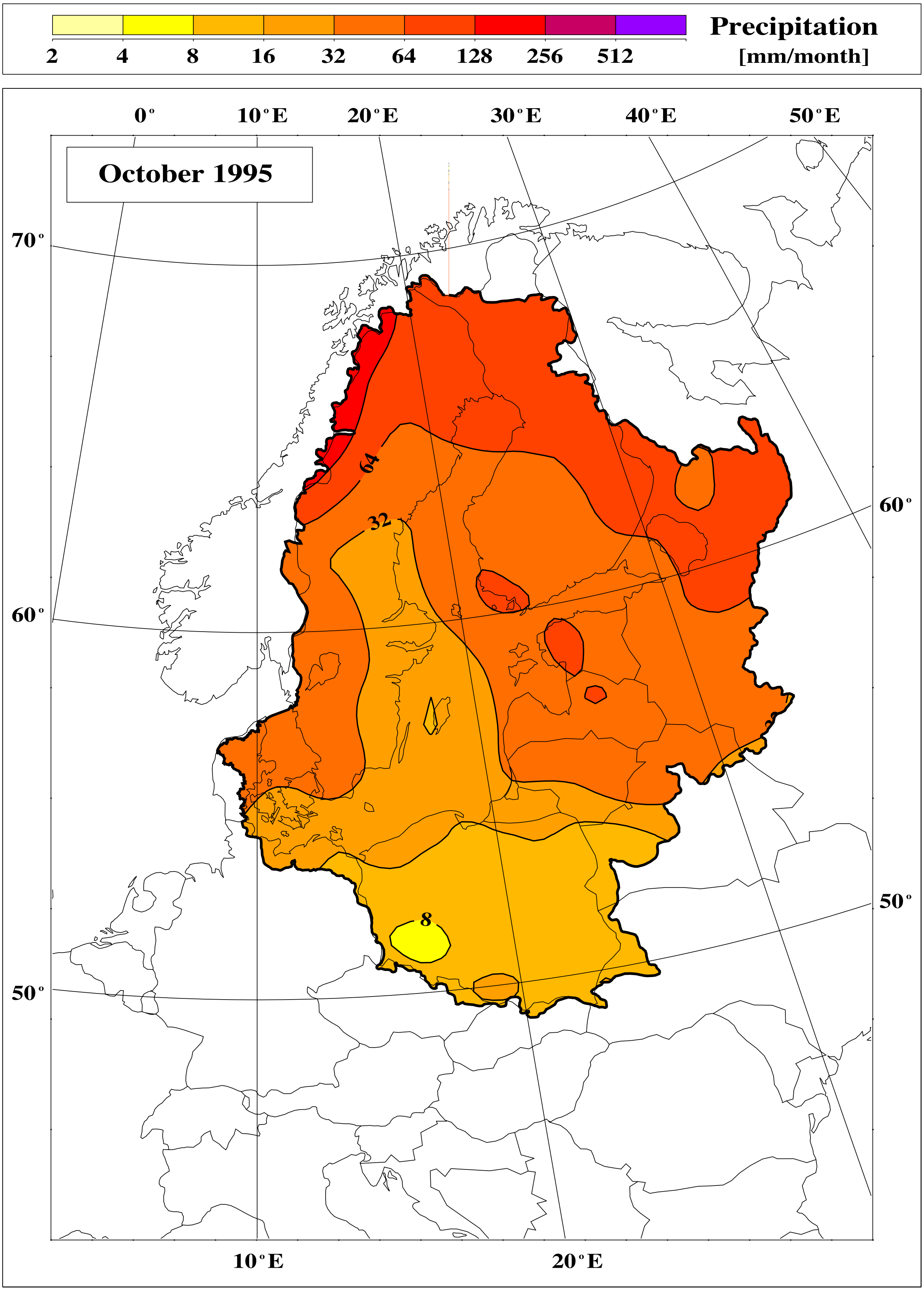
2
4
8
16
32
64
128
256
512
Precipitation
[mm/month]
October 1995
0°
10°E
20°E
30°E
40°E
50°E
70°
60°
50°
64
32
8
10°E
20°E

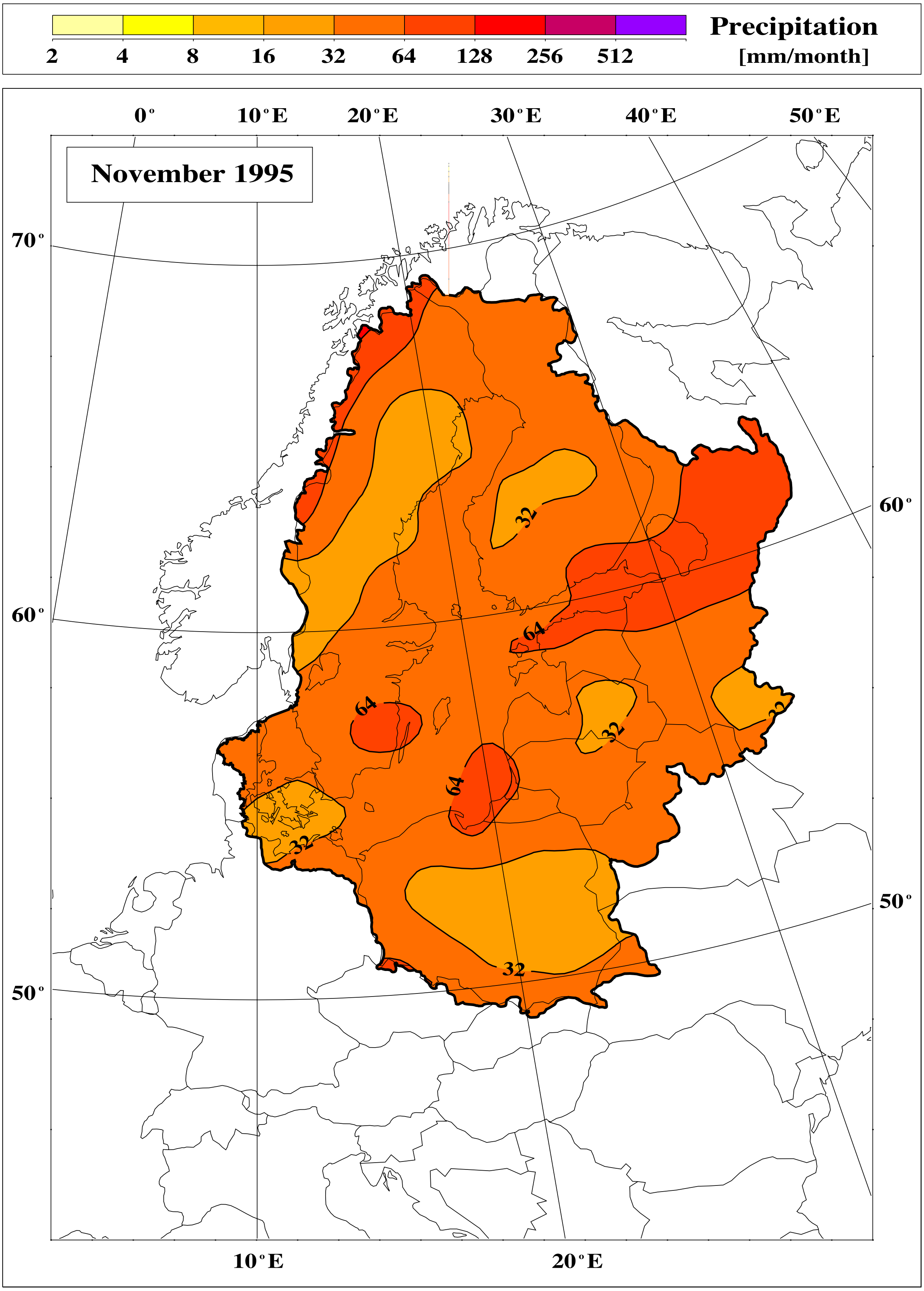
2
4
8
16
32
64
128
256
512
Precipitation
[mm/month]
November 1995
0°
10°E
20°E
30°E
40°E
50°E
70°
60°
50°
60°
50°
32
64
10°E
20°E

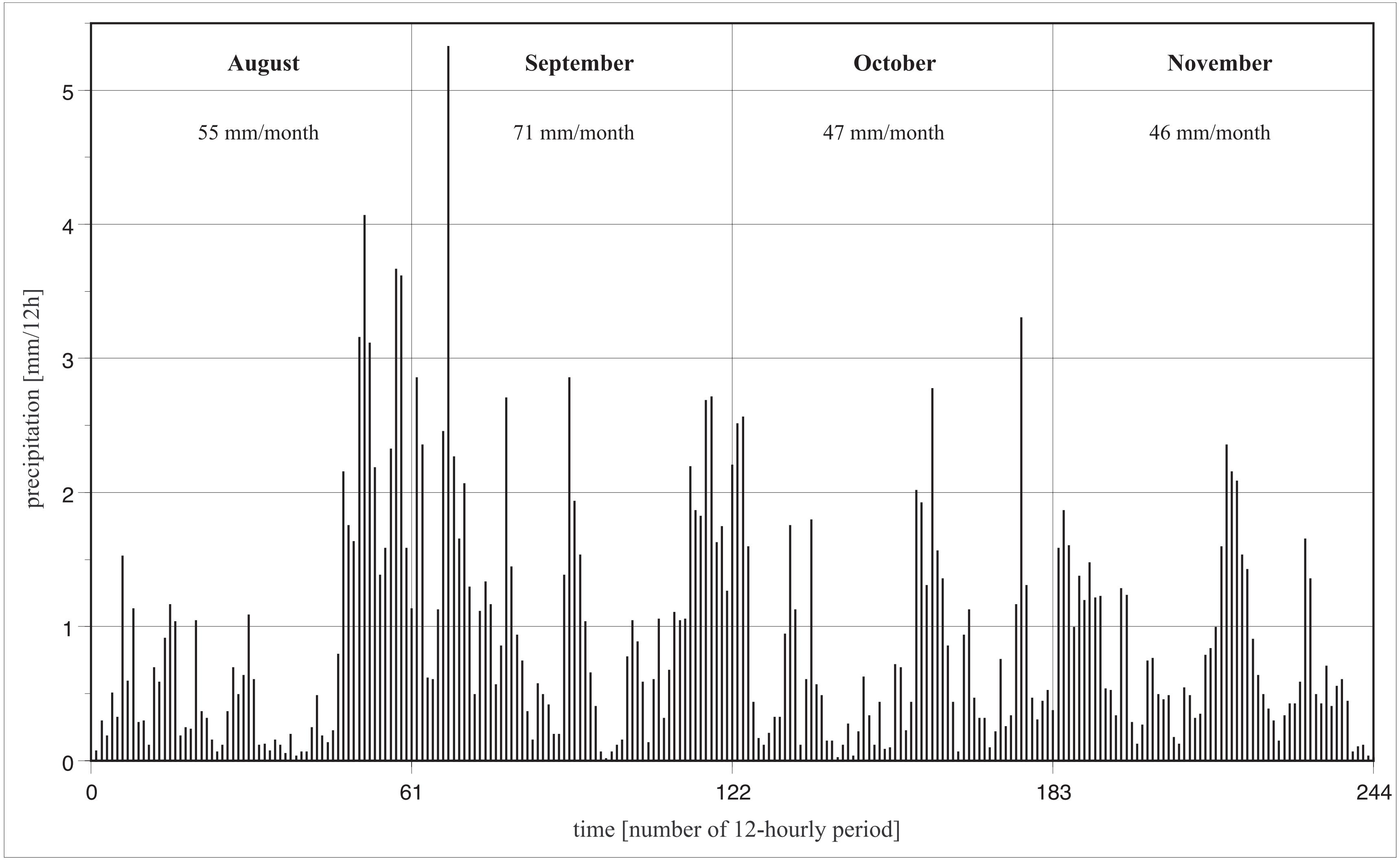

Figure 10 Twice daily precipitation sums of the Baltic drainage calculated from objectively analyzed precipitation fields (fig. 8), for the PIDCAP period of 1 August to 30 November 1995. Units are mm/12h. The monthly precipitation input into the Baltic drainage is 55 mm in August, 71 mm in September, 47 mm in October, and 46 mm in November.

9 CONCLUSIONS

In the presented quick look atlas, observations from the synoptical network, routinely transmitted via GTS, are objectively analyzed. For the analysis, a statistical method well known as *ordinary block kriging* was used. With this method, the areally averaged precipitation is estimated from the irregularly spaced observations, by minimizing the mean square interpolation error. The structure of the precipitation fields was compared with corresponding fields from the ECMWF forecasts. They were found to be in good agreement.

The results are presented in the form of twice daily precipitation maps for the whole BALTEX model domain. Further, the areal distribution of the monthly precipitation input into the Baltic drainage basin was calculated from these twice daily precipitation fields. Averaging over all grid points within the Baltic drainage, gives areally averaged monthly precipitation values for the four months of the PIDCAP period. Additionally, the temporal distribution of the areally averaged precipitation values is presented in the form of a time serie.

The analyzed precipitation fields are routinely used as input fields for the diagnostic model DIAMOD (Dorninger et al. 1995), and can be used for model verifications (Rubel et al. 1993). Further, they give a quick look view of the PIDCAP precipitation events. Despite of the high quality of the analysis, a few improvements will have to be made in the next analysis step, which will be done using a higher resolution analysis grid (18 km grid distance), and additional data from the BALTEX data centre. These are

- Implementation of a correction procedure for the observations, or for the areally averaged precipitation values (Legates 1990).
- Elimination of a small bias in the presented analysis, due to the assumed normal distribution of the precipitation data. It has to be proven wether the observations are really distributed normally, or not. If one assumes that the observed precipitation data are distributed logarithmically, rather than normally, then they have to be transformed to a normal distribution before they are statistical analyzed (Carr 1995). This aspect is well known, but to the knowledge of the author has never been implemented in meteorological applications of statistical precipitation analysis (Creutin and Obled 1982).

Acknowledgments

This research was in part supported by the EC Enviroment and Climate Research Programme (contract: NEWBALTIC, No. ENV4-CT95-0072, Climatology and Natural Hazards) and in part by the Austrian Ministry of Science, Transport and Art. The Central Institute for Meteorology and Geodynamics, Vienna, provided the synoptic data, and the ECMWF, Reading, provided the precipitation forecasts. Sincere appreciation is expressed to Dr. B. Rockel, GKSS, Geesthacht, for providing program code and description of the REMO grid, to Dr. L. Haimberger, IMG, Vienna, for executing the data transfer from ECMWF and for converting the forecast fields onto the REMO grid, to M. Ungersböck, IMG, Vienna, for transferring and archiving the synoptic data, and to O. W. Frauenfeld, Virginia, USA, for reviewing the text. Special thanks is given to Prof. Dr. M. Hantel, IMG, Vienna, for critically commenting and reviewing the manuscript.

References

Bacchi, B., and N. T. Kottegoda, 1995: Identification and calibration of spatial correlation patterns of rainfall. *J. Hydrol.,* **165,** 311-348.

Berndtsson, R., 1987: On the use of cross-correlation analysis in studies of patterns of rainfall variability. *J. Hydrol.,* **93,** 113-134.

Carr, J. R., 1995: Numerical Analysis for the Geological Sciences. *Prentice-Hall,* New Jersey, 592pp.

Creutin, J. D., and Obled, C., 1982: Objective analyses and mapping techniques for rainfall fields: an objective comparison. *Water Resour. Res.,* **18,** 413-431.

Dorninger, M., M. Ehrendorfer, M. Hantel, F. Rubel, and Y. Wang, 1992: A thermodynamic diagnostic model for the atmosphere. Part I: Analysis of the August 1991 rain episode in Austria. *Meteorol. Zeitschrift N. F.,* **1,** 87-121.

Dorninger, M., M. Ehrendorfer, G. Erbes, L. Haimberger, M. Hantel, F. Rubel, and Y. Wang, 1995: The Thermodynamic Diagnostic Model η-DIAMOD: User Manual. *Institut for Meteorology and Geophysics,* Univ. of Vienna, 182pp.

Førland, E. J. (ed.), 1996: Manual for Operational Correction of Nordic Precipitation Data. *Norwegian Meteorological Institut,* Oslo, 66pp.

Gandin, L. S., 1963: Objective Analysis of Meteorological Fields. *Gidrometeor. Izdat.*, Leningrad. [Israel Program for Scientific Translation, Jerusalem 1965, 242pp.].

Gandin, L. S., 1993: Optimal Averaging of Meteorological Fields. *National Meteorological Center,* Office Note 397, 68pp.

Haimberger, L., M. Hantel, and M. Dorninger, 1995: A thermodynamic model for the atmosphere. Part III: DIAMOD with orography and improved error model. *Meteorol. Zeitschrift N. F.,* **4,** 162-182.

Hantel, M., M. Ehrendorfer, and L. Haimberger, 1993: A thermodynamic diagnostic model for the atmosphere. Part II: The general theory and its consequences. *Meteorol. Zeitschrift N. F.,* **1,** 87-121.

Isemer, H.-J., 1996: Weather Patterns and Selected Precipitation Records in the PIDCAP Period, August to November 1995 - A Preliminary Overview. *Int. BALTEX Secr.,* GKSS Research Centre, 94pp.

Krige, D. G., 1981: Lognormal-de Wijsian Geostatistics for Ore Evaluation. *South African Institute of Mining and Metallurgy Monograph Series: Geostatistics 1,* Johannesburg, 51pp.

Krige, D. G., 1962: Statistical applications in mine valuation. *J. Inst. Min. Survey. S. Afr.,* **12(2),** 45-84, 12(3), 95-136.

Kuusisto, E., 1995: Hydrology and hydroenergetics of the Baltic drainage. *First Study Conference on BALTEX - Conference Proceedings,* Int. BALTEX Secr., Publ. No. 3, 18-27.

Legates, D. R., and C. J. Willmott, 1990: Mean seasonal and spatial variability in gauge-corrected, global precipitation. *Internat. J. Climatol.,* **10,** 111-127.

Matheron, G., 1963: Principles of geostatistics. *Economic Geology,* **58,** 1246-1266.

Press, W. H., B. P. Flannery, S. A. Teukolsky, and W. T. Vetterling, 1987: Numerical Recipes. The Art of Scientific Computing. *Cambridge University Press,* Cambridge, 818pp.

Rendu, J. M., 1981: An Introduction to Geostatistical Methods of Mineral Evaluation. *South African Institute of Mining and Metallurgy Monograph Series: Geostatistics 2,* Johannesburg, 84pp.

Rubel, F., Y. Wang, M. Hantel, and M. Ehrendorfer, 1993: Verification of the hydrological cycle in the EURAD model. *The Proceedings of EUROTRAC Symposium '92,* SPB Academic Publishing bv, the Hague, 454-457.

Rubel, F., 1994: Diagnose vertikaler Niederschlagsflüsse. *PhD Theses,* Univ. of Vienna, 175pp.

Rubel, F., 1996: Scale dependent statistical precipitation analysis. *The Proceedings of the International Conference on Water Resources & Environmental Research: Towards the 21st Century,* Kyoto, Japan, 8pp (accepted).

Sevruk, B. (ed.), 1986: Correction of Precipitation Measurements. *Züricher Geographische Schriften,* **23,** 288pp.

Sevruk, B. (ed.), 1992: Snow Cover Measurements and Areal Assessment of Precipitation and Soil Moisture. *WMO-No. 749, Operational Hydrological Report No. 35,* Geneva, Switzerland, 283pp.

Wackernagel, H., 1995: Multivariate Geostatistics - An Introduction with Applications. *Springer,* Berlin, 256pp.

Weber, R. O., and P. Talkner, 1993: Some remarks on spatial correlation function models. *Mon. Wea. Rev.,* **121,** 2611-2617.

Zawadzki, I. I., 1973: Statistical properties of precipitation patterns. *J. Appl. Meteor.,* **12,** 459-472.